Texture Development of High - T$_C$ Superconductors by Application of a High Magnetic Field

by

Hongbao Liu

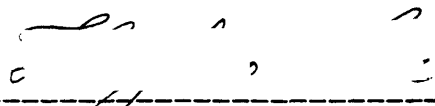M.S., University of Science and Technology of China

Submitted to the Department of Materials Science & Engineering in partial
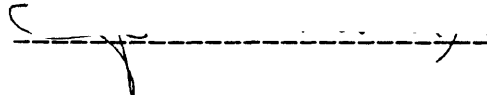fulfillment of the requirement for the Degree of

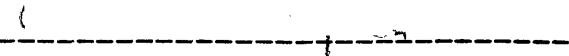DOCTOR OF PHILOSOPHY
in Electronic Materials
at the
Massachusetts Institute of Technology
September, 1995

Signature of Author_____
Department of Materials Science & Engineering
August 11, 1995

Certified by C_____
John B. Vander Sande
Cecil and Ida Green Distinguished Professor of Materials Science
Associate Dean, School of Engineering
Thesis Advisor, Department of Materials Science & Engineering

Accepted by_____
Carl V. Thompson II
Professor of Electronic Materials
Chair, Department Committee on Graduate Students

1

Preface

A theoretical model of texture development under a high magnetic field is developed. Both $RBa_2Cu_3O_7$ and $Bi_2Sr_2(RCa)Cu_2O_8$ superconductors were processed under an elevated magnetic field. The comparison between theory and experimental results is carried out. Finally this new technology was used to produce high critical current density (J_c) tapes.

The sections in chapter 4, 5 and 6 are constructed as manuscripts and classified by processing methods. In each chapter, the materials processed are $RBa_2Cu_3O_7$ and/or $Bi_2Sr_2(RCa)Cu_2O_8$.

The general experimental procedure is described in chapter 2. More detailed processing procedures are described in different sections for different materials and processing methods.

Texture Development of High - T_C Superconductors by Application of a High Magnetic Field

by
Hongbao Liu
Submitted to the Department of Materials Science & Engineering on
August 11, 1995 in partial fulfillment of the requirement for the Degree of
Doctor of Philosophy in Electronic Materials

ABSTRACT

Texture development of high - T_c superconductors by application of a high magnetic field was studied systematically by both theory and experiments. The results are as follows:

A factor describing texture, F, has been expressed as a function of

$$\beta(T, H, V) = \frac{[\Delta\chi VH^2/2 - K(T, x)]}{kT}$$; $\Delta\chi$ is the anisotropic susceptibility, V is grain

volume, H is magnetic field and $K(T, x)$ is the interaction energy. A critical point and a saturation point are defined. From the critical point, we introduce a critical grain size, critical magnetic field, critical anisotropic susceptibility and critical temperature. From the saturation point, we introduce the concept of a saturation grain size, saturation magnetic field, saturation anisotropic susceptibility and saturation temperature. For the interaction energy $K(T, x) = 0$ case, the F factor depends on magnetic field, grain size and temperature. F always increases with increasing magnetic field and grain size, and F decreases with increasing temperature. For the interaction energy $K(T, x) \neq 0$ case, the F factor not only depends on magnetic field, temperature and grain size, but also depends on the interaction constant and liquid phase content, x. For constant magnetic field and grain size, F increases with decreasing interaction constant and increasing liquid phase content. When H -> ∞, F -> 1. These results from the modeling effort are compared to experiments.

Bi - 2212 superconductors were processed under a 10 T magnetic field at 870°C ~ 940°C. It was found that: (a) A high magnetic field can not introduce anisotropic nucleation and anisotropic growth during the early stage of growth. (b) A liquid phase is important for texture development of Bi - 2212 by application of a 10 T magnetic field. (c) Substitution of a small amount of Ca by Ho in Bi - 2212 increases the degree of texture of the Bi - 2212 superconductor by application of a 10 T magnetic field during partial melt - growth.

The mixture $(Bi_2Sr_2Ca_{0.9}Ho_{0.1}Cu_2O_8)_{1-x}(Bi_2Sr_2CaCu_2O_8)_x$ with x = 0, 0.1, 0.2, 0.3 and 0.4 was annealed under an elevated magnetic field. The texture development dependence on temperature T_a, time, magnetic field and liquid phase content were studied systematically. $Bi_2Sr_2Ca_{0.9}Ho_{0.1}Cu_2O_8$ is textured by rotation of the grains under elevated magnetic fields with $Bi_2Sr_2Ca_1Cu_2O_8$ as a liquid phase at high temperatures. Texture development depends on temperature, magnetic field, time and content of the liquid

phase. The degree of texture increases with increasing temperature under a high magnetic field for a fixed time. For a constant liquid phase content x, the degree of texture increases with increasing time and magnetic field. The degree of texture also depends on the liquid phase content for constant magnetic field, temperature and time. The transport critical current density J_c increases with increasing degree of texture.

$Bi_2Sr_2Ca_{0.9}R_{0.1}Cu_2O_8$ (R = Y, Ho and Gd) superconductors were melt - grown under elevated magnetic fields. Texture development in these materials depends upon cooling rate, maximum processing temperature T_m, and magnetic field. A higher T_m is always desirable in obtaining a highly textured structure, and there is a trade off between the cooling rate and the magnetic field strength. Highly textured structures can be introduced either by a faster cooling rate under a stronger magnetic field, or by a lower cooling rate under a weaker magnetic field. The transport critical current density can be increased by improving both texture and connectivity between the grains.

Bulk $R_1Ba_2Cu_3O_7$ superconductors were melt - grown under elevated magnetic fields between 0 ~ 10 T. Highly textured, multi - domained structures were obtained by application of these high magnetic fields. Under a 10 T magnetic field, the degree of texture of $Y_1Ba_2Cu_3O_7$ increases with increasing maximum processing temperature, T_m. The domain alignment depends upon the cooling rate and applied magnetic field. There is a trade off between cooling rate and magnetic field, i.e. to obtain the same degree of texture, either a higher magnetic field and higher cooling rate, or lower magnetic field and lower cooling rate must be combined. During melt - growth under a high magnetic field, the domain orientation of $RBa_2Cu_3O_7$ (R = Ho, Gd and Er) is determined by the ionic moment orientation of the rare earth element in the superconductor.

The grain orientation of Bi - 2212 / Ag thick films can be controlled by application of a 10 T magnetic field during high temperature processing. With a liquid phase present, the grains can be rotated by a 10 T magnetic field. The c - axis of the grains produced are parallel to the applied magnetic field H_α, i.e. the c - axis of the grains can be perpendicular or parallel to the silver substrate depending upon the magnetic field orientation. A 10 T magnetic field can overcome the Bi - 2212 / Ag interface effect and dominate the Bi - 2212 grain orientation and texture development when a liquid phase is present. Thick films and tapes with different thickness were melt - grown under an elevated magnetic field. The degree of texture and transport critical current, J_c, of thick films with different thickness were enhanced by application of the magnetic fields. J_c increases with increasing magnetic field and a new thermal sequence was introduced to produce high J_c tape, i.e. $J_c = 8.3 \times 10^4$ A/cm^2 and $I_c = 45$ A.

Thesis Supervisor: John B. Vander Sande
                       Professor of Materials Science
                       Associate Dean, School of Engineering
                       Department of Materials Science & Engineering

Table of Contents

7

8

List of Figures

Chapter 1.

Chapter 2.

Chapter 3.

Chapter 4.

14

16

Chapter 6.

Chapter 7.

Acknowledgments

I would like to thank my thesis advisor, Prof. John B. Vander Sande, for his guidance, advice, support and encouragement throughout this work. I thank the members of my thesis committee, Prof. Harry L. Tuller and Prof. Yet-Ming Chiang, for their advice and encouragement, particularly with respect to the writing of this document. I would also like to thank staff members in Francis Bitter National Magnetic Lab. for their kind help, including Larry Rubin, Bill Fietz, David Lynch, Z. H. Wang and Nancy Tucker. I also would like to thank many staff members for the help which made this endeavor possible. This list includes, but is not limited to, Fred Wilson, Jean Dimauro, Marj Joss, Pat Gavagan.

Most of all, I would like to thank my wife, Haiyan, for her unending support, encouragement and understanding. I also would like to thank Dr. James C. Ho and Dr. Donald E. Morris for their support and encouragement throughout my years in the U.S.A. I would like to thank the members in our research group who made my stay at MIT a pleasant experience, including Dr. Wei Gao, Dr. Monica Kaforey and Dr. Norimitsu Murayama. I also like thank Dr. A. Otto in American Superconductor Corporation for his kind help.

Chapter 1. Introduction

Section 1.1. The key factor for high - T_C superconductor application: Texture

The recent discovery of high - T_C superconductors [1] [2] [3] has led to an explosion of research in the field because of their potential for technological applications. The materials can be fabricated basically in four configurations: (a) thin films for Josephson junctions, SQUIDs, infrared sensors or voltage standards, etc, (b) thick films for circuit interconnections and current switches [4], (c) bulk materials for levitation and magnetic bearings [5], and (d) wire or tape for magnets, motors, generators and power transmission [5]. Thin film fabrication is a subject beyond this thesis and will not be discussed in the following sections.

The feature common to the structure of high - T_C superconductors is an oxygen - deficient multiple perovskite with some Cu - O planes, which leads to the strong anisotropy of superconductivity. The crystal structure of two typical high - T_C superconductors are shown in Fig. 1-1 and Fig. 1-2. The resistivity and diamagnetic moment M along the c - axis direction is much larger than that along the ab - plane; the critical current density J_c in the ab - plane is much larger than that in the c - axis direction. Thus, the diamagnetic moment and critical current density will be reduced by mis - orientation of the grains in the material, even if there are no weak links between the grain boundaries. It is clear that texturing the grains in these types of materials is key to improving the properties and moving toward applications for high - T_C superconductors.

For bulk applications such as permanent magnets (levitation application), it is necessary to maximize the diamagnetic moment to increase

22
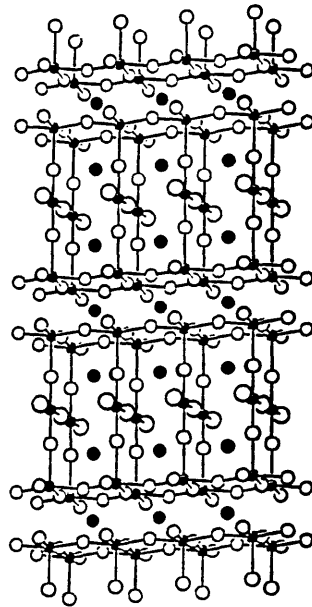
Fig. 1-1.   Crystal structure of $Y_1Ba_2Cu_3O_y$.
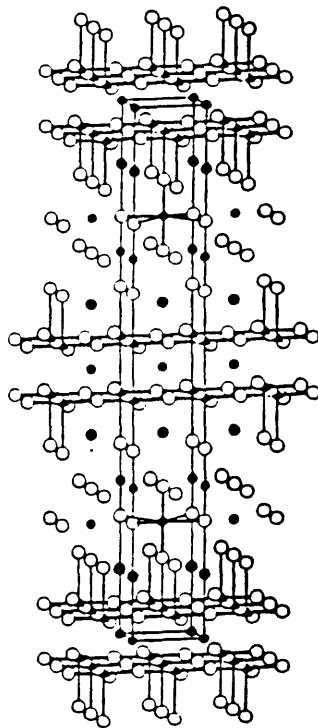
Fig. 1-2.   Crystal structure of $Bi_2Sr_2CaCu_2O_8$.

the levitation force. To achieve the maximum diamagnetic moment, first we need to texture the superconductors and increase the diamagnetic moment in the c - axis direction and, second, to introduce pinning centers inside the grains and increase the moment. Combining these two steps, the resulting permanent magnet will yield the maximum levitation force.

For thick films and tapes applications [6] [7], the high T_c superconductors require critical current densities of 10^4 - 10^5 A / cm^2 in a magnetic field of several tesla over long lengths. The key microstructural requirements to achieve high critical currents in these materials are known to be the improvement of crystallographic texture and the elimination of weak links between the grains. If we assume there were no weak links between the grains and the grains were misoriented, the transport critical current density would still be very low because of the anisotropy of the critical current density. Thus control's texture of the grains is necessary to satisfy requirements for materials applications.

Section 1.2. Methods of texturing high - T_c superconductors

It is known that a promising approach to enhance J_c, therefore, is to prepare grain - oriented or c - axis textured superconductors. YBCO materials with large aligned grains, high density and clean grain boundaries obtained by melt - textured growth [8] demonstrate a sharp gain in J_c with increasing texture [9]. The highly textured YBCO domains produced by the melt - growth method are usually very small and far from useful dimensions and each domain is randomly oriented with respect to other domains. A similar way to produce highly textured high - T_c superconductors is through directional solidification [5]. Both YBCO and BSCCO have been fabricated by this method.

24

Unfortunately this method requires an unacceptably long time to produce a textured structure over a long length and it is impossible to produce long wires for transport applications.

Bi - 2212 superconductor tapes and thick films with high J_c have been produced by a partial melting method. The microstructure of the oxide zone formed under partial melting heat treatment has been investigated. It was observed [10] [11] [12] that when the oxide thickness is less than 20 μm, a well - aligned microstructure with plate - like grains is formed. When the oxide layer is thicker than 20 μm, two zones with differing microstructure are observed: a highly textured microstructure near the oxide / Ag interface, and a weakly textured region in the middle of the tape. It was reported that the critical current density increases when the thickness decreases [10]. During the growth of the tape, Ag sheets provided the flat shape of the melt volume that gives rise to an extended texture because of the growth features of a 2212 phase crystallite [12]. The thinner the tape, the more quickly unfavorably oriented crystallites come into contact with the Ag sheet and the higher the degree of texture. Consequently, the higher the critical current density will be. Thus the oxide layer thickness will have to be less than 20 μm, which is inconvenient for technological applications, because of the concomitant low critical current I_c.

Another way of aligning ceramic grains is to align the grains under a high magnetic field while curing in epoxy at room temperature. If a grain has an anisotropic paramagnetic susceptibility in its normal state, then being placed in a magnetic field, the magnetic energy is minimized when the axis of maximum susceptibility is aligned parallel to the field. Thus, the magnetic field will tend to rotate the grain to an angle minimizing its energy. For high

25

- T_c superconductors, the difference in the normal state magnetic susceptibility is $\Delta\chi \sim 10^{-4} - 10^{-6}$ [13] [14], and the normal anisotropic magnetic energy is given by $\Delta E = \Delta\chi H^2 V / 2$ [15], where V is the volume of a grain (cm^3) and H is magnetic field (in Oe). The energy associated with this rotation was large enough [16] to align YBCO grains under 9.4 T while curing in epoxy at room temperature. The partial alignment of YBCO powders has also been achieved in isopropanol in a 2 T magnetic field [17]. For $Bi_2Sr_2Ca_1Cu_2O_8$ and $Y_1Ba_2Cu_3O_7$, there are no magnetic elements in the compounds. The magnetic alignment of $Bi_2Sr_2Ca_1Cu_2O_8$ and $Y_1Ba_2Cu_3O_7$ should result from anisotropy in the paramagnetic susceptibility associated with the Cu - O conducting planes [15]. Since the susceptibility parallel to the c - axis is higher than that perpendicular to the c - axis, these compounds should align with the c - axis parallel to the applied field. For $Bi_2Sr_2(Ca,R)_1Cu_2O_8$ and $R_1Ba_2Cu_3O_7$ with R = rare earth elements, the paramagnetic susceptibility is dominated by the R^{3+} ion, and the source of anisotropy is single - ion anisotropy associated with crystal fields at the rare - earth site [15]. For $Bi_2Sr_2(Ca, R)_1Cu_2O_8$, when R = Ho the particles always align with c // H, when R = Er the particles align with c $\perp$ H [18]. For $R_1Ba_2Cu_3O_7$ it was observed that for R = Gd and Ho the particles align with c $\parallel$ H but the opposite way (c $\perp$ H) for R = Er [18]. However, so far only a limited increase in J_c has been obtained through a room temperature alignment method, since during heat treatment the organic species reacted with the superconducting phase and produced secondary phases at the grain boundaries.

Section 1.3. Applying a high magnetic field during processing

Recently it was reported that anisotropic grain growth in a Ho-Ba-Cu-O superconductor was introduced under a 1.6 T magnetic field during sintering

above 900°C [19]. It has been observed that the degree of alignment increases as the magnitude of the magnetic field increases between 0 and 1.6 T for a fixed temperature and processing time. Sarkar et al [20] also reported that the magnetic field (i.e. 1 T) influences the grain orientation of a YBCO thick film during sintering at 890°C. It also has been demonstrated that it is possible to prepare textured $YBa_2Cu_3O_7$ ceramic materials by solidification in a 5 T magnetic field [21].

It is clear that processing HTSC in a high magnetic field at high temperature during phase formation is a potential way to improve the degree of texture and minimize weak links between the grains. We have introduced a critical volume of a grain, V_c, which corresponds to $\Delta\chi H^2 V_c / 2 = kT$, i.e. the magnetic anisotropy energy is equal to the thermal disorder energy. Thus,

$$V_c = 2kT / H^2 \Delta\chi .$$

When $V < V_c$, the magnetic field can not overcome thermal disorder and introduce grain alignment. This implies that the application of a high magnetic field can not introduce anisotropic nucleation, or anisotropic growth at an early stage of grain growth. When $V > V_c$, the magnetic field will tend to rotate the grains by mechanical interaction between the grains. This effect is unlikely to happen in the solid state at lower temperature. If there are liquid phases between the grains, the grains will be more easily rotated by the magnetic field.

In this work, the texture development of Bi - 2212 and R - 123 materials were systematically studied by application of a high magnetic field in four parts: (1) grain rotation by a high magnetic field when there exists a liquid phase, (2) melt - growth of Bi - 2212 and R - 123 material under an elevated

magnetic field, (3) production of high quality Bi - 2212 thick films and tapes by application of a high magnetic field, and (4) modeling texture development under a high magnetic field during high temperature processing.

Chapter 2. A Theoretical Model of Texture Development Under A High Magnetic Field

A factor describing texture, F, has been expressed as a function of $\beta(T, H, V) = \dfrac{[\Delta\chi VH^2/2 - K(T, x)]}{kT}$, $\Delta\chi$ is anisotropic susceptibility, V is grain volume, H is magnetic field and $K(T, x)$ is interaction energy. A critical point and a saturation point are defined. From the critical point, we introduce a critical grain size, critical magnetic field, critical anisotropic susceptibility and critical temperature. From the saturation point, we introduce the concept of a saturation grain size, saturation magnetic field, saturation anisotropic susceptibility and saturation temperature. For the interaction energy $K(T, x) = 0$ case, the F factor depends on magnetic field, grain size and temperature. F always increases with increasing magnetic field and grain size, and F decreases with increasing temperature. For the interaction energy $K(T, x) \neq 0$ case, the F factor not only depends on magnetic field, temperature and grain size, but also depends on the interaction constant and liquid phase content, x. For constant magnetic field and grain size, F increases with decreasing interaction constant and increasing liquid phase content. When H -> ∞, F -> 1. These results from the modeling effort are compared to experiment and are found to be consistent with them.

Section 2. 1: The Relationship between the F factor and processing parameters

2. 1. 1: Magnetic energy of a grain under a high magnetic field

Assuming that an anisotropic grain with a volume V is placed in a high magnetic field H, the angle between $\overset{\perp}{H}$ and $\overset{\perp}{c}$ is θ (see Fig. 2-1-1). The magnetic energy of the grain can be written as
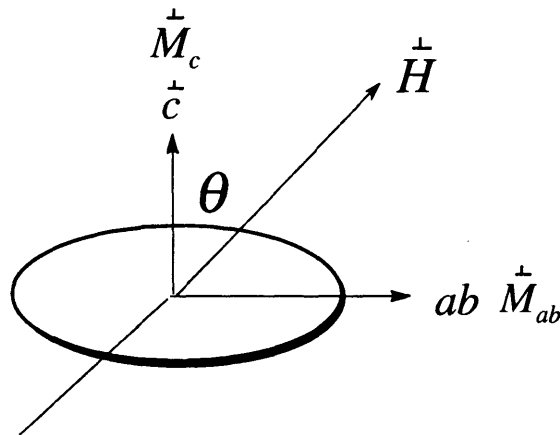
Fig. 2-1-1: An anisotropic grain in a magnetic field.

$$dE_m = -\overset{\perp}{M} \cdot d\overset{\perp}{H} = -(M_c \cos\theta + M_{ab}\sin\theta)dH \qquad (1)$$

For high - T_C superconductors in their normal state, the magnetic moment M_c and M_{ab} are paramagnetic moment. We can then write the magnetic moment as

$$M_c = V\chi_c H \cos\theta \qquad\qquad (2a)$$

$$M_{ab} = V\chi_{ab} H \sin\theta \qquad\qquad (2b)$$

V is the volume of the grain, χ_c is the paramagnetic susceptibility along the $\bar{c}$ direction and χ_{ab} is the paramagnetic susceptibility along the ab plane. Substituting (2a) and (2b) into (1), the magnetic energy can be written as

$$dE_m = -(\chi_c \cos^2\theta + \chi_{ab} \sin^2\theta)VHdH \qquad\qquad (3)$$

Integrating (3) and we can obtain the magnetic energy of a grain as

$$E_m = \int_0^{\frac{\pi}{2}} dE_m = -(\chi_c \cos^2\theta + \chi_{ab}\sin^2\theta)VH^2 / 2 \qquad\qquad (4)$$

Substituting

$$\sin^2\theta = 1 - \cos^2\theta \qquad\qquad (5)$$

into (4) the magnetic energy can be written as

$$E_m(\theta, H) = -(\chi_{ab} + \Delta\chi \cos^2\theta)VH^2 / 2 \qquad\qquad (6)$$

where $\Delta\chi = \chi_c - \chi_{ab}$ is the difference in the susceptibilities of the grain.

When $\theta \to 0$, $\qquad E_m(0,H) \to -V\chi_c H^2 / 2 \qquad\qquad (7)$

When $\theta \to \pi/2$, $\qquad E_m(\frac{\pi}{2},H) \to -V\chi_{ab}H^2 / 2 \qquad\qquad (8)$

For an un-doped material, such as pure Bi - 2212 and Y-123, the paramagnetic susceptibility comes from the conducting Cu - O plane and always has $\chi_c >> \chi_{ab}$. We have $E_m(0,H) << E_m(\frac{\pi}{2},H)$, this means that the magnetic field will tend to rotate the grain to $\theta \to 0$, the lowest energy state.

For a rare earth doped material, such as Er - 123, the paramagnetic susceptibility is dominated by the atomic magnetic moment of Er^{+3}, and we have $\chi_c << \chi_{ab}$ and $E_m(0,H) >> E_m(\frac{\pi}{2},H)$. In this case the magnetic field will tend to rotate the grain to $\theta \rightarrow \pi/2$, the lowest energy state.

In summary, under a high magnetic field an anisotropic grain will be rotated by the magnetic field to its lowest energy state. The driving force is given by the anisotropy magnetic energy of the grain. The direction of the grain rotation will be determined by the paramagnetic susceptibilities χ_c and χ_{ab}.

2. 1. 2: Interaction energy of the grains.

If two grains contact each other, there is an interaction between the grains. This interaction will interfere with the grain rotation by the magnetic field. The interaction energy of grain i and j, ε_{ij}, can be written as

$$\varepsilon_{ij} = k_{ij}\vec{c}_i \cdot \vec{c}_j \tag{9}$$

$\vec{c}_i$ and $\vec{c}_j$ are unit vectors of c - axis direction. k_{ij} is grain to grain interaction constant. Actually, there are many grains which interact with grain i, such that the total interaction energy of grain i can be written as

$$E_{Ii}(T,\theta_i) = \sum_j k_{ij}\vec{c}_i \cdot \vec{c}_j = \vec{c}_i \cdot \sum_j k_{ij}\vec{c}_j \tag{10}$$

If we introduce an interaction field to grain i as

$$\vec{W}(T,\theta_i) = \sum_j k_{ij}\vec{c}_j \tag{11}$$

and the interaction energy on any grain can be written as

$$E_I(T,\theta) = \vec{c} \cdot \vec{W}(T,\theta) \tag{12}$$

This interaction can be expanded as a series of terms

$$E_I(T,\theta) = E_0 + E_1 \cos\theta + E_2 \cos^2\theta \tag{13}$$

From Fig. 2-1-1, it is clear that the interaction energy will not change when we reverse the magnetic field from $\vec{H}$ to - $\vec{H}$. This means that

$$E_I(T,\theta) = E_I(T, \pi - \theta) \tag{14}$$

This requires that $E_1 = 0$ and we can also drop the constant E_0. Finally, the interaction energy can be written as

$$E_I(T,\theta) = K(T,x)\cos^2\theta \tag{15}$$

K(T, x) is the interaction energy constant, which depends on temperature and liquid phase content x. It is an adjustable parameter.

2. 1. 3: F factor as a function of processing parameters.

The total energy of a grain under a magnetic field can be written as

$$U(T,H,\theta) = E_m(H,\theta) + E_I(T,\theta) \tag{16}$$

and substituting (6) and (15) into (16), the total energy can be written as

$$U(T,H,\theta) = -V\chi_{ab}H^2 / 2 - [\Delta\chi VH^2/2 - K(T,x)]\cos^2\theta \tag{17}$$

if we write

$$\alpha = V\chi_{ab}H^2 / 2 \tag{18a}$$

$$\gamma = \Delta\chi VH^2 / 2 - K(T,x) \tag{18b}$$

The total energy of a grain in the bulk material can be written as

$$U(T,H,\theta) = -\alpha - \gamma \cos^2 \theta \qquad (19)$$

For a bulk material, there are many small grains in the material and each grain has an anisotropic susceptibility. Under a high magnetic field, each grain will be rotated by the magnetic field and the rotation process will be obstructed by the interaction between the grains. We can treat the small grains as small particles by classical statistical mechanics. The measurable physics parameters of the bulk material are the average values of the contribution from a large number of small grains.

First let us calculate the average paramagnetic moment of the material under a high magnetic field at high temperature. As seen in Fig. 2-1-1, according to classic Boltzman statistics, the probability $f(\theta)$ that a grain has an orientation with angle θ can be written as

$$f(\theta)d\theta = \frac{\sin\theta e^{-U(T,H,\theta)/kT}d\theta}{\int_0^{\frac{\pi}{2}} \sin\theta e^{-U(T,H,\theta)/kT}d\theta} \qquad (20)$$

The average paramagnetic moment of the material can be written

$$\overline{M} = \int_0^{\frac{\pi}{2}} (M_c\cos\theta + M_{ab}\sin\theta)f(\theta)d\theta \qquad (21)$$

Substituting (2a),(2b) and (20) into (21), we obtain

$$\overline{M} = V\chi_{ab}H + \Delta\chi VH\frac{\int_0^{\frac{\pi}{2}}\cos^2\theta\sin\theta e^{-U(T,H,\theta)/kT}d\theta}{\int_0^{\frac{\pi}{2}}\sin\theta e^{-U(T,H,\theta)/kT}d\theta} \qquad (22)$$

Now define the integration as

$$I = \frac{\int_0^{\frac{\pi}{2}} \cos^2 \theta \sin \theta e^{-U(T,H,\theta)/kT} d\theta}{\int_0^{\frac{\pi}{2}} \sin \theta e^{-U(T,H,\theta)/kT} d\theta} \tag{23}$$

Substituting (19) into (23), we obtain for the integration

$$I = \frac{\int_0^{\frac{\pi}{2}} \cos^2 \theta \sin \theta e^{(\alpha + \gamma \cos^2 \theta)/kT} d\theta}{\int_0^{\frac{\pi}{2}} \sin \theta e^{(\alpha + \gamma \cos^2 \theta)/kT} d\theta} \tag{24}$$

We define

$$\beta(T, H, V) = \frac{\gamma}{kT} = \frac{[\Delta \chi V H^2 / 2 - K(T, x)]}{kT} \tag{25}$$

then let $x = \cos \theta$, thus

$$I = \frac{\int_0^1 x^2 e^{\beta x^2} dx}{\int_0^1 e^{\beta x^2} dx} \tag{26}$$

Finally, the average of the paramagnetic moment can be written as

$$\overline{M} = V \chi_{ab} H + \Delta \chi V H \frac{\int_0^1 x^2 e^{\beta x^2} dx}{\int_0^1 e^{\beta x^2} dx} \tag{27}$$

If the magnetic field H -> 0, all grains in the bulk material will be randomly oriented and $\overline{M}_{min} \to 0$. If the magnetic field H -> ∞, all grains in the bulk material will be rotated to θ -> 0, i.e. perfectly textured, and the magnetic moment will be maximum with $\overline{M}_{max} \to V \chi_c H$.

Now let us re-examine the meaning of Lotgering factor F. The F was calculated to quantify the degree of c - axis orientation in the polycrystalline phase as

35

$$F = (P - P_0)/(1 - P_0)$$

where $P = \Sigma\,I_{(00l)}/\Sigma\,I_{(hkl)}$, is the sum of integrated intensities for all (00l) reflections divided by the sum of all intensities (hkl) in the textured specimen. P_0 is an equivalent parameter for a random specimen where the intensities were obtained from a powder diffraction pattern. The factor F varies from 0 (unoriented) to 1 (completely oriented).

If the grains are randomly distributed in the bulk material, F = 0. If the grains are perfectly textured, F = 1. Thus it is reasonable to assume

$$F = \frac{\overline{M}}{\overline{M}_{max}} = \frac{\chi_{ab}}{\chi_c} + \frac{\Delta\chi}{\chi_c}\frac{\int_0^1 x^2 e^{\beta x^2}\,dx}{\int_0^1 e^{\beta x^2}\,dx} \tag{28}$$

For high-T_C superconducting oxides, $\chi_c >> \chi_{ab}$, so that

$$\frac{\chi_{ab}}{\chi_c} \to 0 \quad \text{and} \quad \frac{\Delta\chi}{\chi_c} = \frac{\chi_c - \chi_{ab}}{\chi_c} \to 1$$

Finally, the factor F as a function of β can be written as

$$F = \frac{\int_0^1 x^2 e^{\beta x^2}\,dx}{\int_0^1 e^{\beta x^2}\,dx} \tag{29a}$$

where

$$\beta(T, H, V) = \frac{[\Delta\chi V H^2/2 - K(T, x)]}{kT} \tag{29b}$$

It is clear that the F factor is a function of the magnetic field H, temperature T, grain size V, anisotropic susceptibility $\Delta\chi$ and grain interaction energy constant $K(T, x)$. Based on equations (29a) and (29b), we can directly compare the theoretical value with experimental results and thereby determine the texture development dependence on processing parameters.

Section 2-2: Texture development under a high magnetic field without interaction between the grains: the case where K(T,x) = 0.

In this section, we assume K(T,x) = 0 and study texture development under a high magnetic field with the influence of the thermal disorder effect. This case can be applied to small grains which are textured in a liquid or organic solvent.

When K(T,x) = 0, from equation (29b) we know that $\beta = \dfrac{V\Delta\chi H^2}{2kT}$, because $\chi_c >> \chi_{ab}$, so that we always have $\beta > 0$. Then we integrate equation (29a) to yield

$$F = \frac{\dfrac{e^\beta}{2\beta} - \dfrac{\sqrt{\pi}Erfi(\sqrt{\beta})}{4\beta^{\frac{3}{2}}}}{\dfrac{\sqrt{\pi}Erfi(\sqrt{\beta})}{2\sqrt{\beta}}} = -\frac{1}{2\beta} + \frac{e^\beta}{\sqrt{\pi\beta}Erfi(\sqrt{\beta})} \tag{30}$$

so that

$$F = -\frac{1}{2\beta} + \frac{e^\beta}{\sqrt{\pi\beta}Erfi(\sqrt{\beta})} \tag{31a}$$

where

$$\beta = \frac{V\Delta\chi H^2}{2kT} \tag{31b}$$

2. 2. 1: Critical point and saturation point.

(a) Definition of critical point and saturation point

F is plotted as a function of β in Fig. 2-2-1. It is clear that the F factor increases with increasing β and approaches 1 when $\beta \to \infty$. We define the critical point as $\beta_c = 1$. When β reaches the critical point β_c, the F factor

reaches F = 0.4. If β is below 1, the F factor will always be below 0.4 and the degree of texture is low.

From the definition of the critical point $\beta_c = \dfrac{V\Delta\chi H^2}{2kT} = 1$, we can introduce the concept of a critical grain size V_c, critical magnetic field H_c, critical anisotropic susceptibility of the material $\Delta\chi_c$ and critical temperature T_c as follows:

$$V_c = \frac{2kT}{\Delta\chi H^2} \tag{32a}$$

$$H_c = \sqrt{\frac{2kT}{\Delta\chi V}} \tag{32b}$$

$$\Delta\chi_c = \frac{2kT}{VH^2} \tag{32c}$$

$$T_c = \frac{V\Delta\chi H^2}{2k} \tag{32d}$$
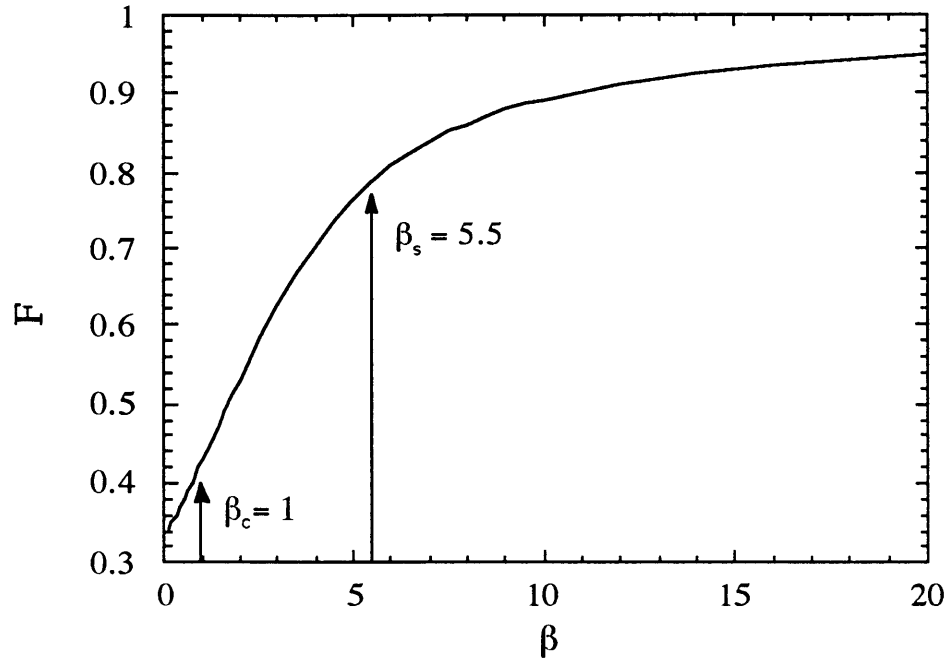
Fig. 2-2-1: F factor as a function of β.

The saturation point is defined when the F factor reaches 0.8, such that β$_s$ = 5.5. This means that if β has a value beyond the saturation point, the F factor will be larger than 0.8. In a similar fashion, the saturation grain size V$_s$, saturation magnetic field H$_s$, saturation anisotropic susceptibility of the materials $\Delta\chi_s$ and saturation temperature T$_s$ can be defined as follows:

$$V_s = \frac{11kT}{\Delta\chi H^2}$$ (33a)

$$H_s = \sqrt{\frac{11kT}{\Delta\chi V}}$$ (33b)

$$\Delta\chi_s = \frac{11kT}{VH^2}$$ (33c)

$$T_s = \frac{V\Delta\chi H^2}{11k}$$ (33d)

From the definition, if only three of the four parameters satisfy the critical value, a high degree of texture processes is possible. In other words, if we want to texture a material under a weaker magnetic field, the grain size has to be increased or the anisotropic susceptibility has to be larger. If a material has a weaker anisotropic susceptibility, the magnetic field or the grain size has to be increased to texture the material, and so on.

(b)   Critical and saturation grain size dependence of field, temperature and susceptibility.

Because the critical grain size and saturation grain size share the same relationship with magnetic field, temperature and susceptibility, the only difference is a constant. Thus it is only necessary to discuss one of these parameters and we will chose the critical size for discussion.

If we assume $V_c = d_c^3$ and $\Delta\chi = C / T$ (Curie Law), and using (32a) we plot d_c as a function of magnetic field for different temperatures in Fig. 2-2-2. It is clear that the critical size decreases with increasing magnetic field and decreasing temperature. Thus, we can use a strong magnetic field to texture very small grains. In Fig. 2-2-3, d_c as a function of magnetic field is plotted for different Curie constants, C. If a material has a strong paramagnetic anisotropy susceptibility, the material can be textured by a weaker magnetic field even at a high temperature. A three dimensional plot of d_c as a function of magnetic field H and Curie constant C at 1200 K is shown in Fig. 2-2-4.
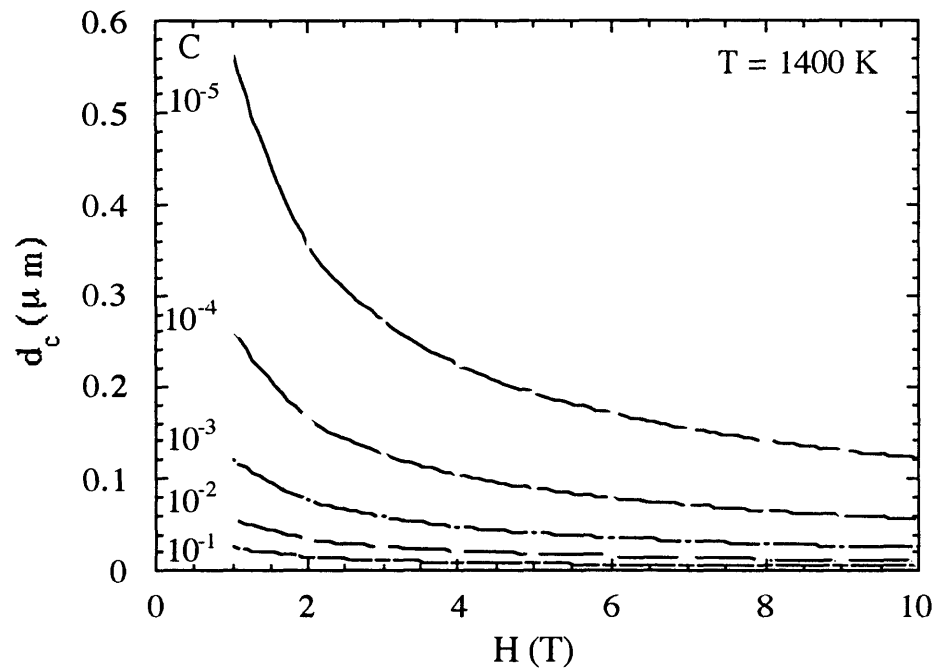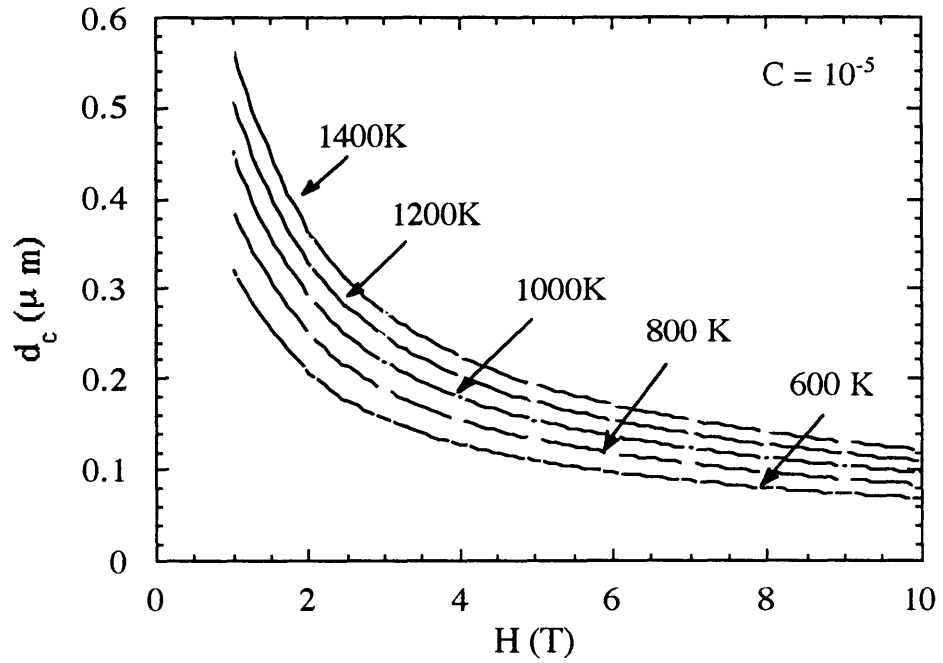
Fig. 2-2-2: d_c as a function of magnetic field for various temperature.

Fig. 2-2-3: d_c as a function of magnetic field for different C.
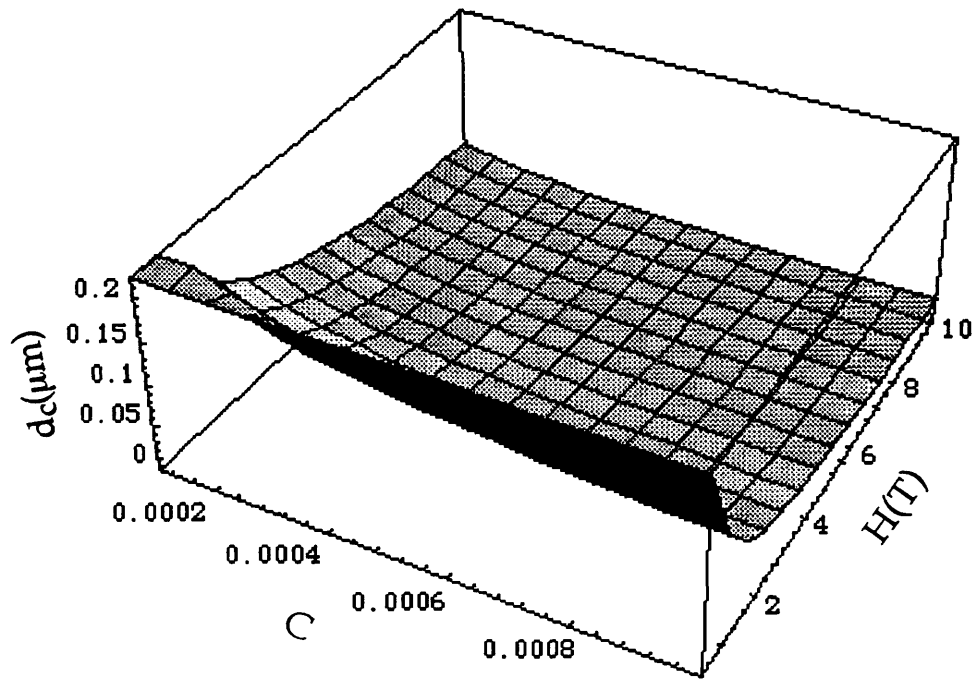
Fig. 2-2-4: d_c as a function of magnetic field and Curie constant C.
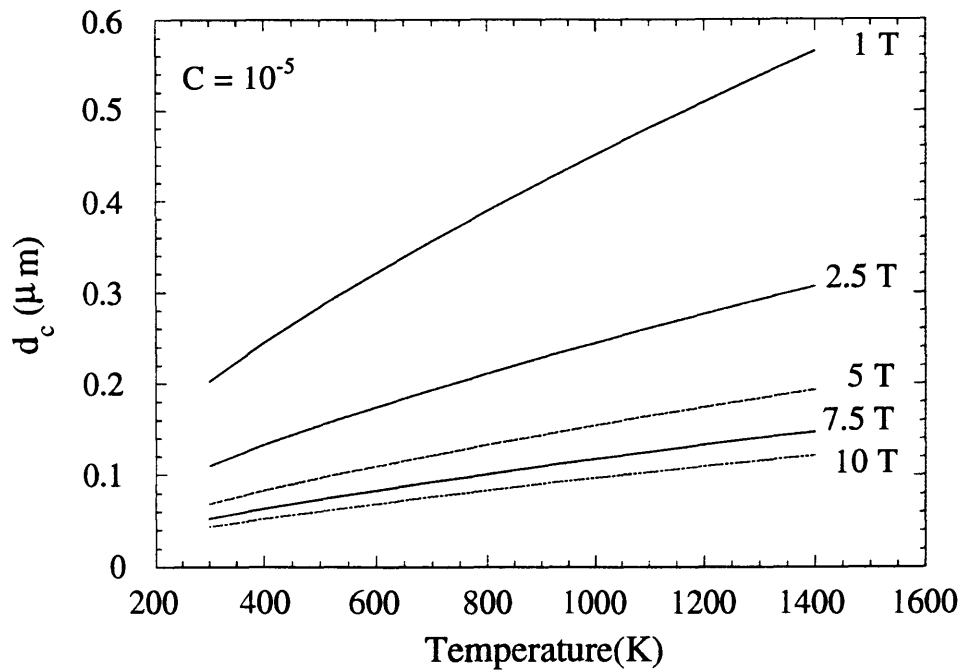
Fig. 2-2-5: d_c as a function of temperature for different magnetic fields.

The temperature dependence of the critical grain size, d_c, for different magnetic fields is plotted in Fig. 2-2-5. d_c always increases with increasing temperature for a constant magnetic field. For a higher temperature, the thermal disorder energy is larger. In order to develop a well textured structure, the grain size and the magnetic field must be large.

The temperature dependence of the critical grain size for different values of C is plotted in Fig. 2-2-6. d_c increases with increasing temperature and can be reduced by increasing the paramagnetic anisotropy susceptibility. A three dimensional plot of d_c vs magnetic field and temperature is shown in Fig. 2-2-7. The relationships between the important variables can be clearly seen.

(c)   Temperature and grain size dependence of the critical and saturation magnetic field H_c and H_s.

In this section, we will only discuss the critical magnetic field. The saturation magnetic field will have a similar behavior except for a constant shift. Critical susceptibility and critical temperature can be discussed in a similar way, and we will not repeat these discussions here.

First let us plot H_c as a function of temperature T and grain size d for C = 10^{-4} in Fig. 2-2-8. It is clear that if the grain size is very small, the critical magnetic field can reach 30 T. If the grain size is 0.2 - 0.5 μm, the critical magnetic field will be reduced to several Tesla. We know that $H_c \propto d^{-\frac{3}{2}}$ and $H_c \propto T$, but the processing temperature T can not be reduced much. Thus the critical magnetic field H_c can only be dramatically reduced by increasing the grain size. In other words, if a higher magnetic field is not available we still can texture the material by increasing the grain size·d.
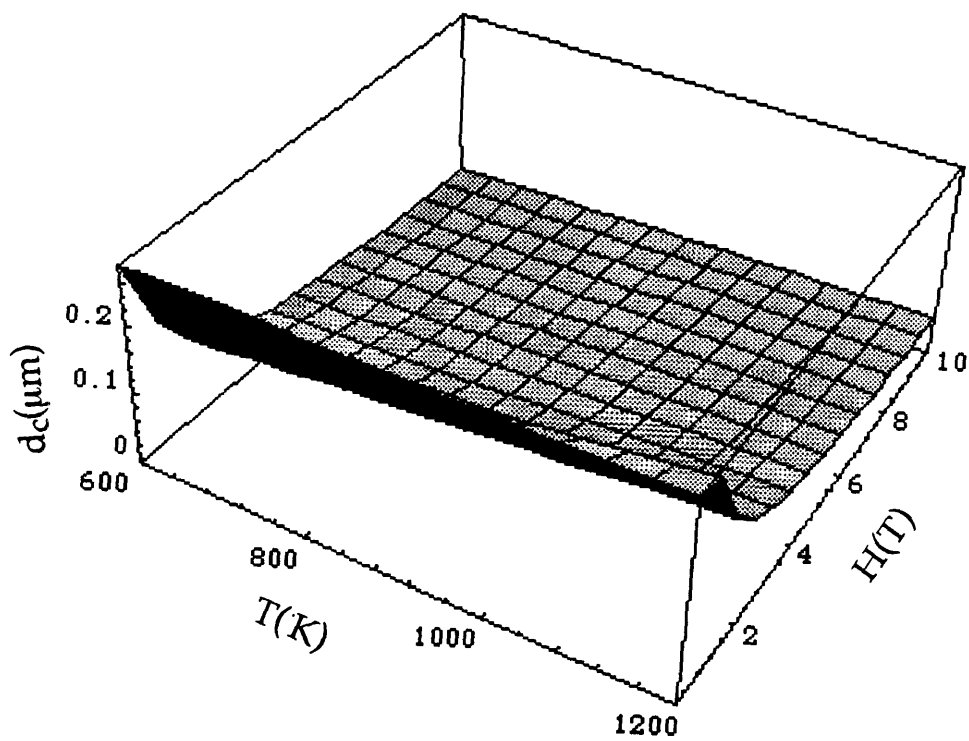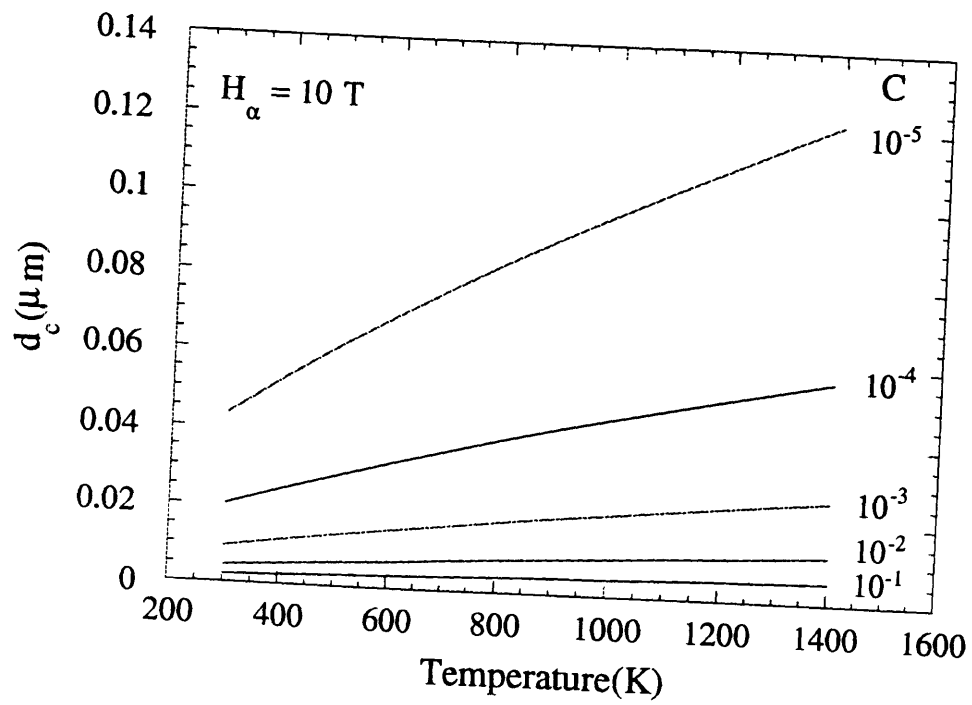
Fig. 2-2-6: d_c as a function of temperature for different C.

Fig. 2-2-7: d_c as a function of temperature T and magnetic field H.
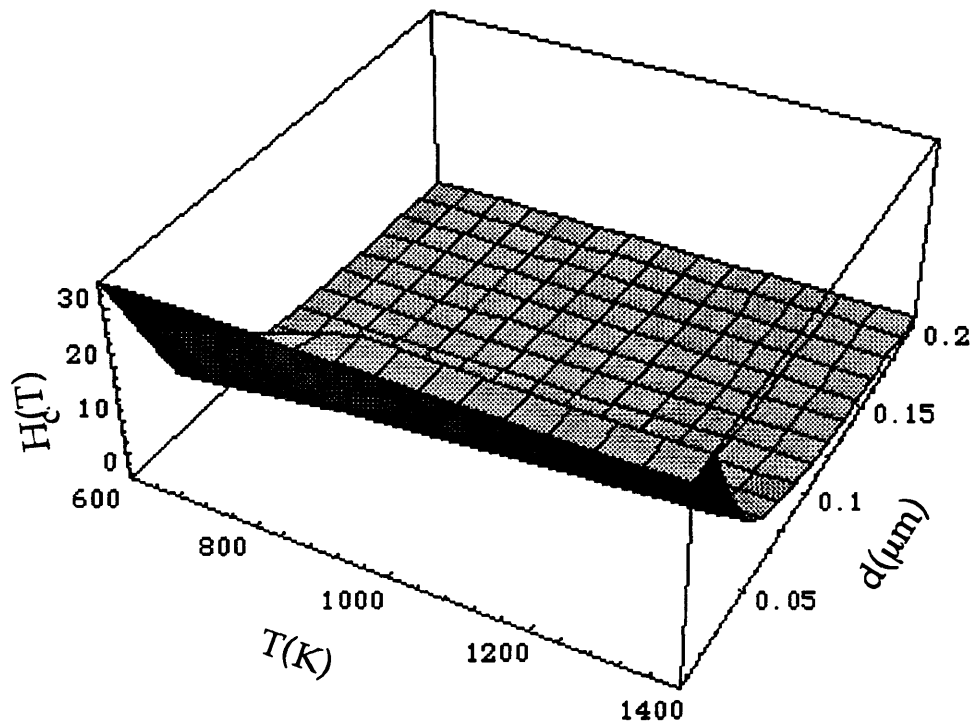
Fig. 2-2-8: H_c as a function of temperature T and grain size d.

2. 2. 2: F factor as a function of the processing parameters

(a)   F factor as a function of temperature T and magnetic field H.

We plot F factor as a function of magnetic field H for different temperature T in Fig. 2-2-9. In this case we choose d = 0.1µm and C = 10^{-4} as fixed values. When the magnetic field increases, the F factor increases and saturates at a higher magnetic field. When H -> ∞, F -> 1. Therefore a perfectly textured structure can always be obtained by increasing H to very large values. However, ones H goes beyond the saturation magnetic field, the F factor increases with increasing H very slowly. A very efficiency way to use

the high magnetic field to texture the material, therefore, is to choose a magnetic field just several Tesla above the saturation magnetic field H_s. When the processing temperature decreases, the saturation magnetic field shifts to lower values and the textured structure can be obtained at a lower magnetic field.
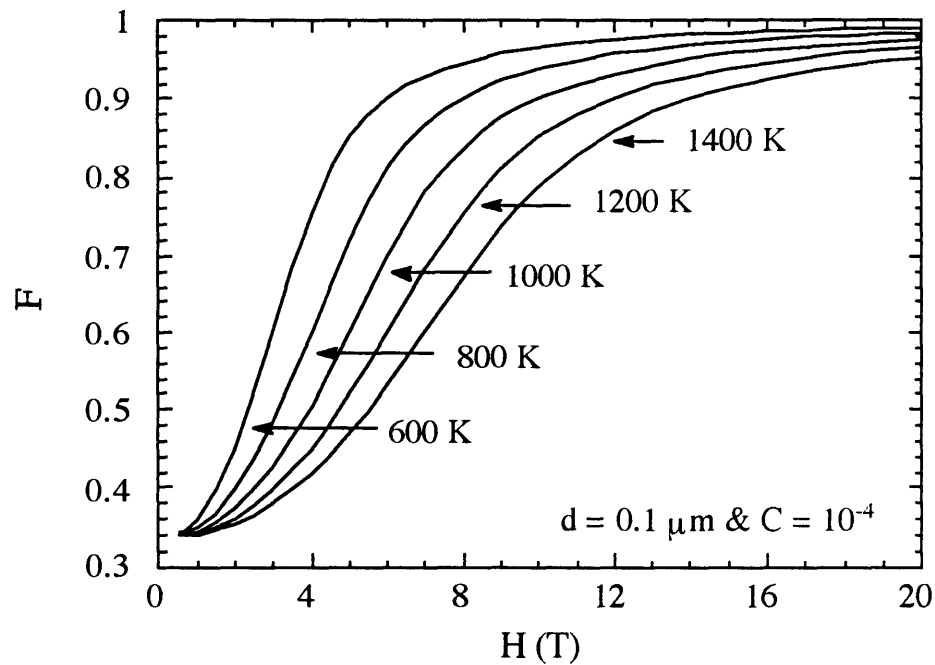
Fig. 2-2-9: F as a function of magnetic field for different Ts.

The F factor as a function of temperature T for different magnetic fields H is shown in Fig. 2-2-10. We still choose d = 0.1μm and C = 10^{-4} as fixed values. The F factor always decreases with increasing temperature. For different magnetic fields, the temperature dependence of F difference. For a low magnetic field (2 T), the temperature effect is less important. For a

46

medium value of magnetic field (4 - 6 T), the F factor decreases sharply with increasing temperature. For a high magnetic field, i.e. above 10 T, the F factor depends less on the temperature. When we process materials, we should choose the temperature and magnetic field properly to yield the desired degree of texture.

In order to see the temperature and magnetic field dependence of the F factor more clearly, a three dimensional plot of F vs T and H is shown in Fig. 2-2-11. From this we can choose the processing parameter correctly.
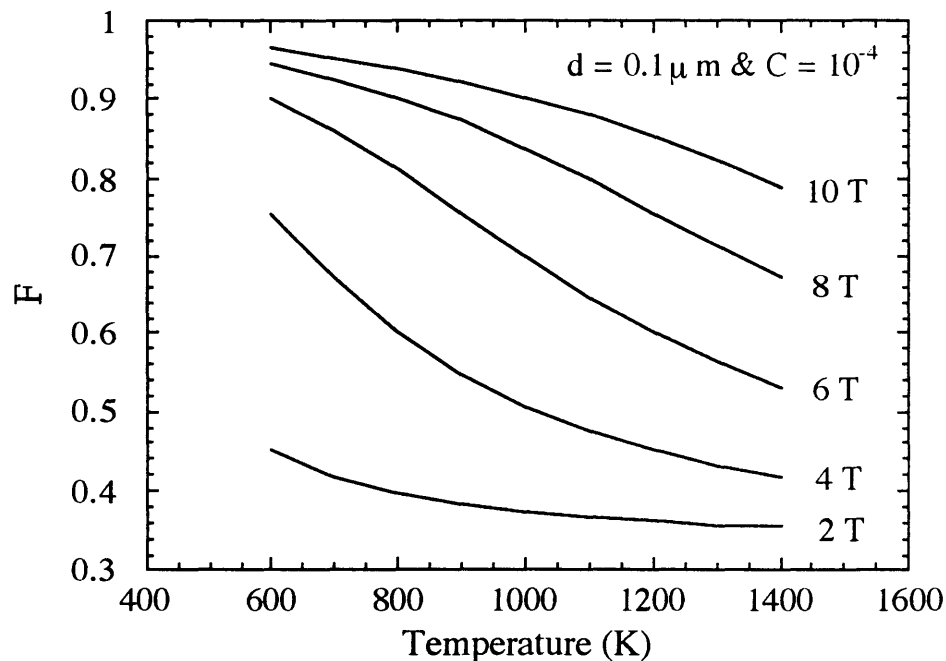
Fig. 2-2-10: F as a function of temperature T for different H.
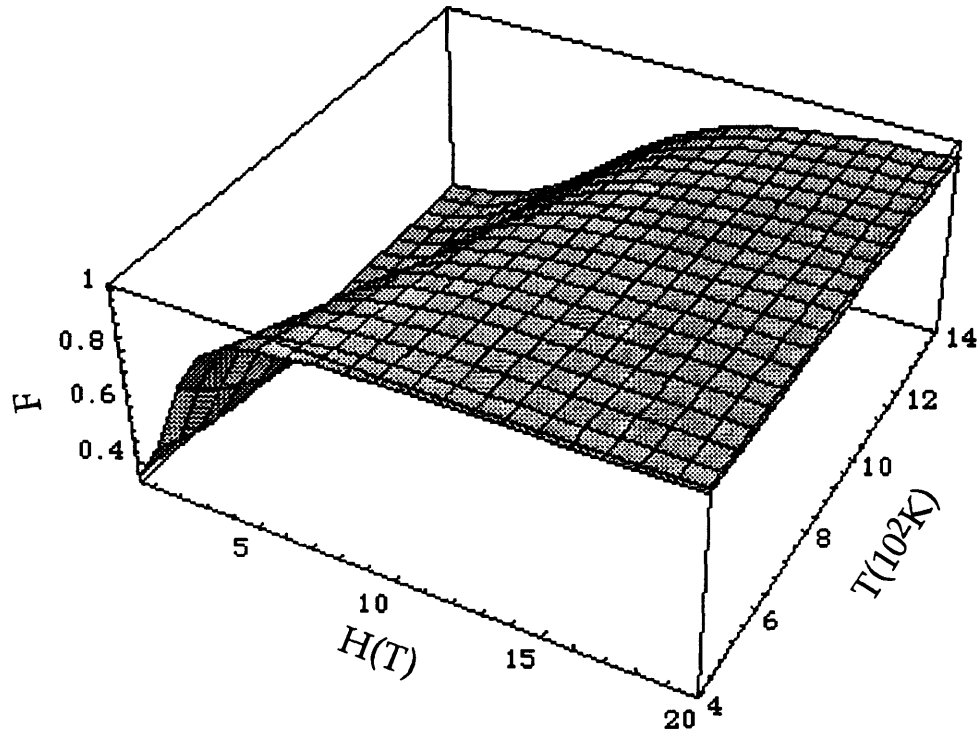
Fig. 2-2-11: F as a function of magnetic field H and temperature T.

(b)   F factor as a function of magnetic field and grain size.

We plot F factor as a function of magnetic field H for different grain sizes, d, in Fig. 2-2-12. The temperature T and Curie constant C are fixed at 1200 K and 10^{-4}. As discussed above, the F factor always increases with increasing magnetic field H and saturates for very large magnetic fields. When the grain size increases, the curve shifts to lower magnetic fields. This means that we need high magnetic fields to texture materials with small grains. If the high magnetic field is not available, higher degrees of texture can be obtained by using larger grain sizes.

In Fig. 2-2-13, the F factor as a function of grain size for varying magnetic fields is plotted. For larger grain sizes, the saturation magnetic field is lower than that for a smaller grain size. A three dimensional plot of F vs H and d is shown in Fig. 2-2-14. The relationships can be clearly seen.

(c)   The F factor as a function of temperature and grain size.

We plot F as a function of temperature for different grain sizes in Fig. 2-2-15, and a three dimension plot is shown in Fig. 2-2-16. The results are similar to the discussion above, and will not be repeated here.
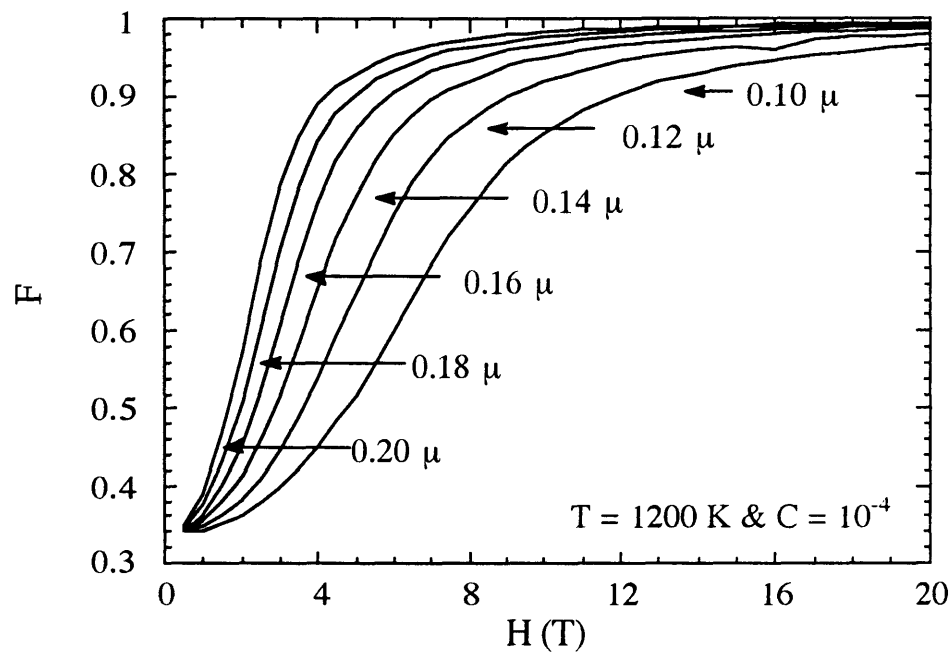
Fig. 2-2-12: F as a function of magnetic field for different grain sizes.
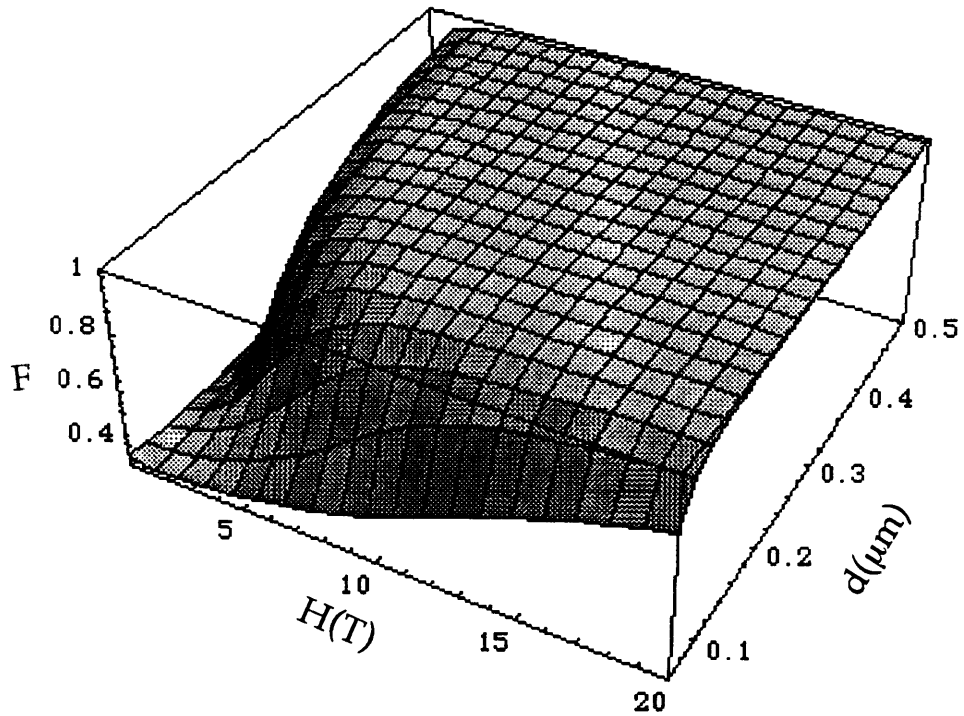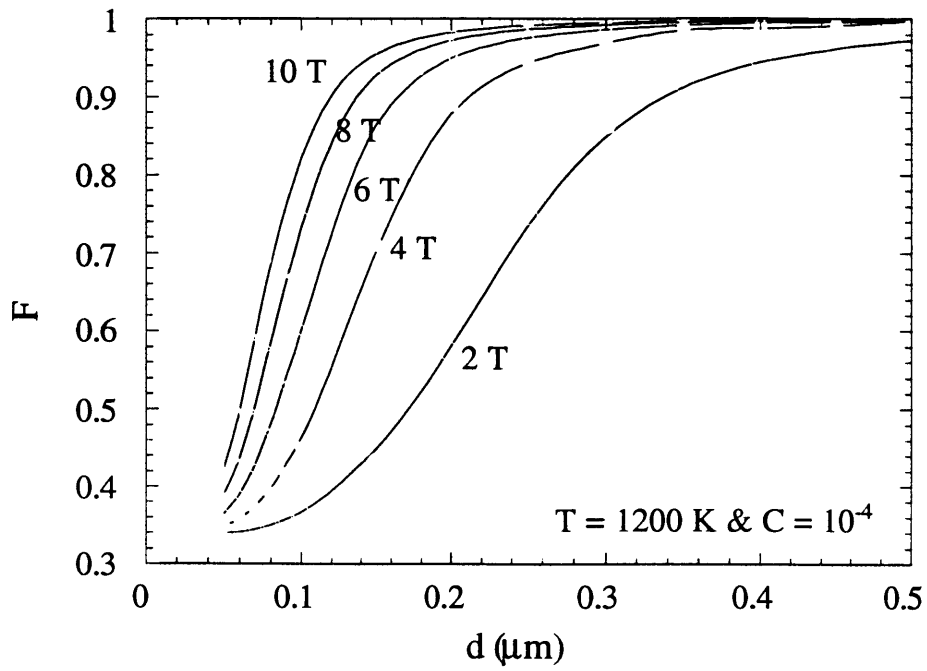
Fig. 2-2-13: F as a function of grain size for different magnetic fields.

Fig. 2-2-14: F as a function of magnetic field H and grain size d.

5 0
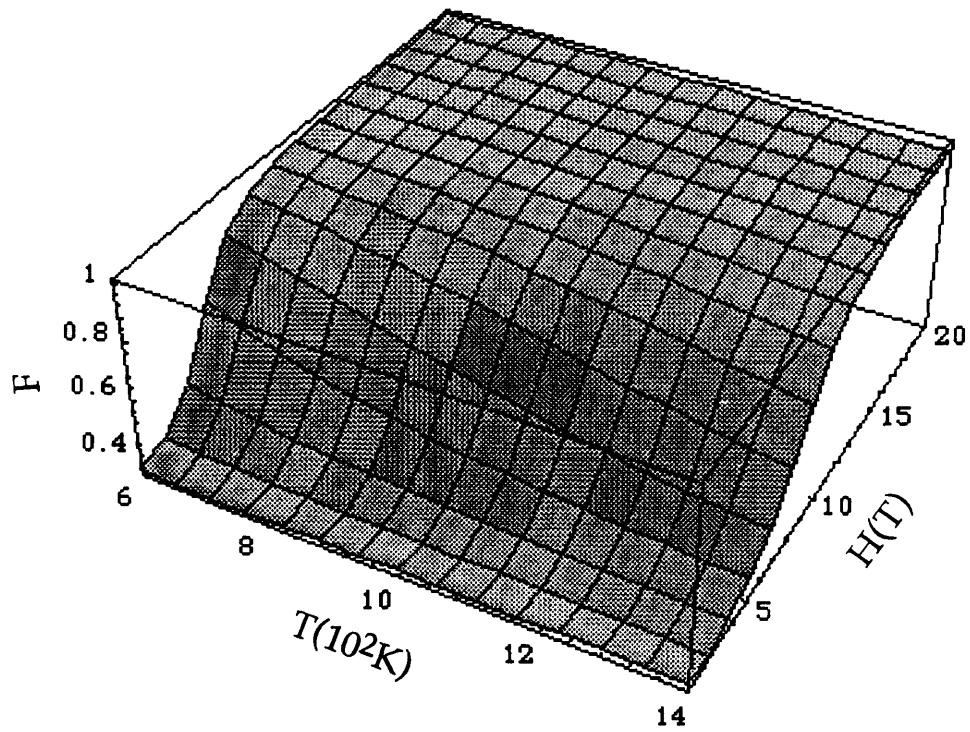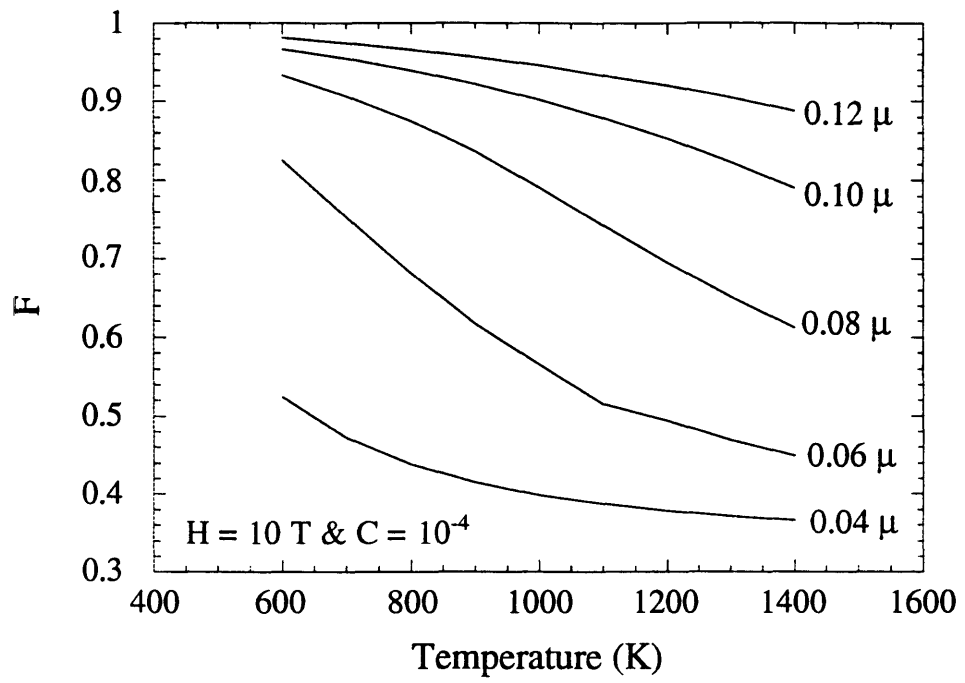
Fig. 2-2-15: F as a function of temperature for different grain sizes.

Fig. 2-2-16: A three dimensional plot of F as a function of H and T.

Section 2. 3: Texture development under a high magnetic field with interaction between grains: $K(T, x) \neq 0$

In this section, we assume $K(T, x) \neq 0$ and investigate texture development under a high magnetic field with the influence of the interaction between the grains in the materials. This case can be applied to small grains being textured in a solid or semisolid under a high magnetic field.

We know that

$$\beta = \frac{\dfrac{V\Delta\chi H^2}{2} - K(T,x)}{kT}$$

and that $\beta > 0$ if the magnetic energy is larger than the interaction energy; and that $\beta < 0$ if the magnetic energy is smaller than the interaction energy. For these two cases, we can integrate (29a) to yield

$$F = -\frac{1}{2\beta} + \frac{e^\beta}{\sqrt{\pi\beta}\,Erfi(\sqrt{\beta})} \qquad \beta > 0 \qquad (34a)$$

$$F = \frac{1}{2|\beta|} - \frac{1}{\sqrt{\pi|\beta|}\,e^{|\beta|}Erf(\sqrt{|\beta|})} \qquad \beta < 0 \qquad (34b)$$

2. 3. 1: Critical point and saturation point.

Let us first plot the F factor as a function of β in Fig. 2-3-1. When $\beta < 0$, i.e. there is a strong interaction between the grains in the material, the F factor decreases with β going to more negative values, i.e. more interaction between the grains. This is the case for a material in the high density solid state, where the magnetic field cannot rotate the grains in the material and introduce the textured structure. If the material has a low density or has a liquid phase

present, the values of the interaction energy and the magnetic energy will be close to one another and β will be in the middle region. As such, a low degree of texture can be introduced. If the magnetic field is very strong and the interaction constant is small, β is on the right side of the curve and a well textured structure can be introduced by the magnetic field. This is the case where there is significant liquid phase in the material or the melt -growth case.

According to the definition of the critical point and the saturation point, $\beta_c = 1$ and $\beta_s = 5.5$, which corresponds to F = 0.4 and 0.8, we can re-examine the critical grain size d_c and critical magnetic field H_c for the case where there is interaction between the grains. For this case,

$$\beta = \frac{\dfrac{V\Delta\chi H^2}{2} - K(T,x)}{kT}$$

Thus, the critical volume and critical magnetic field are

$$V_c = \frac{2(kT + K(T,x))}{\Delta\chi H^2} \tag{35a}$$

$$H_c = \sqrt{\frac{2(kT + K(T,x))}{V\Delta\chi}} \tag{35b}$$

The saturation volume and saturation magnetic field should be

$$V_s = \frac{11(kT + K(T,x))}{\Delta\chi H^2} \tag{36a}$$

$$H_s = \sqrt{\frac{11(kT + K(T,x))}{V\Delta\chi}} \tag{36b}$$

It is clear that taking into account the interaction energy $K(T,x)$, the critical volume and critical magnetic field shift to larger values. It is necessary to

53

increase the magnetic energy to overcome the interaction between the grains, thus the critical grain size and critical magnetic field increase.
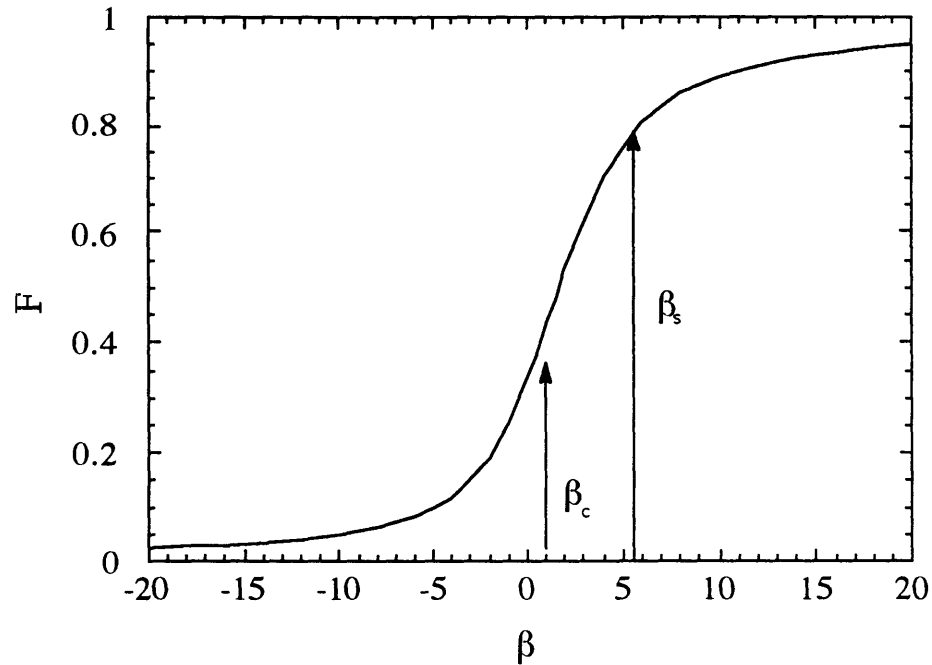
Fig. 2-3-1: F as a function of β.

2. 3. 2: F factor dependence on the magnetic field.

Now let us begin to discuss how the interaction energy influences the magnetic field dependence of the F factor. In a simple way we assume

$$K(T, x) = \frac{\alpha \times 10^4}{Tx} \tag{37}$$

When the temperature increases, the viscosity of the liquid decreases and the interaction energy decreases. When the liquid phase content x increases, the interaction energy decreases. α is an interaction constant. Substituting (37) into (35a) and (35b), we plot F as a function of magnetic field

for different interaction constants α in Fig. 2-3-2. In this plot we choose grain size d = 0.2μm, C = 10^{-4}, liquid content x = 0.1 and temperature T = 1200 K.

When the interaction constant α is small, the saturation magnetic field is low, i.e. we can use a low magnetic field to texture the material. This is the case when there is a significant liquid phase in the material and the interaction between the grains is weak and the grains can be more easily rotated by a high magnetic field. When the interaction constant increases from 10 to 100, the saturation magnetic field shifts to a higher value, i.e. if there is a strong interaction between the grains and a larger magnetic field is required to overcome the interaction between the grains to texture the material.
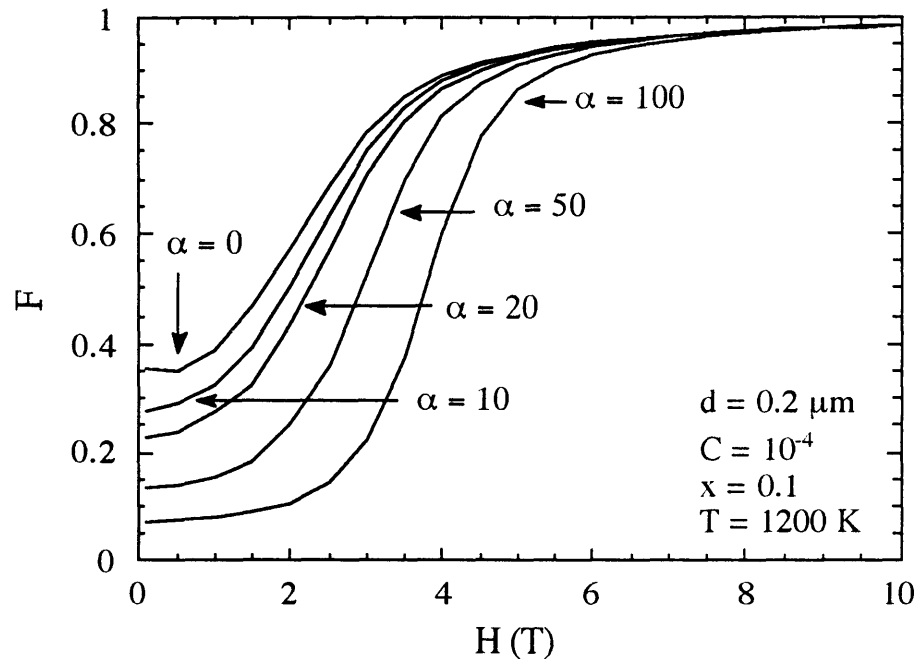
Fig. 2-3-2: F as a function of magnetic field for different α.

In Fig. 2-3-3 we plot F factor as a function of magnetic field for different liquid phase content. In this plot we choose a grain size of d = 0.2μm,C = 10^{-4}, α = 100 and temperature T = 1200 K. When the liquid phase content x increases, the saturation magnetic field shifts to a lower value. If there is more liquid phase present between the grains, the interaction between the grains will be reduced and the grains are more easily rotated by the magnetic field. For the $K(T, x) \neq 0$ case, the temperature and grain size dependence of F will be similar to the K(T,x) = 0 case. The only difference between these cases is that the magnetic effect will be compensated by the interaction effect between the grains, thus H_c and H_s will shift to higher values.
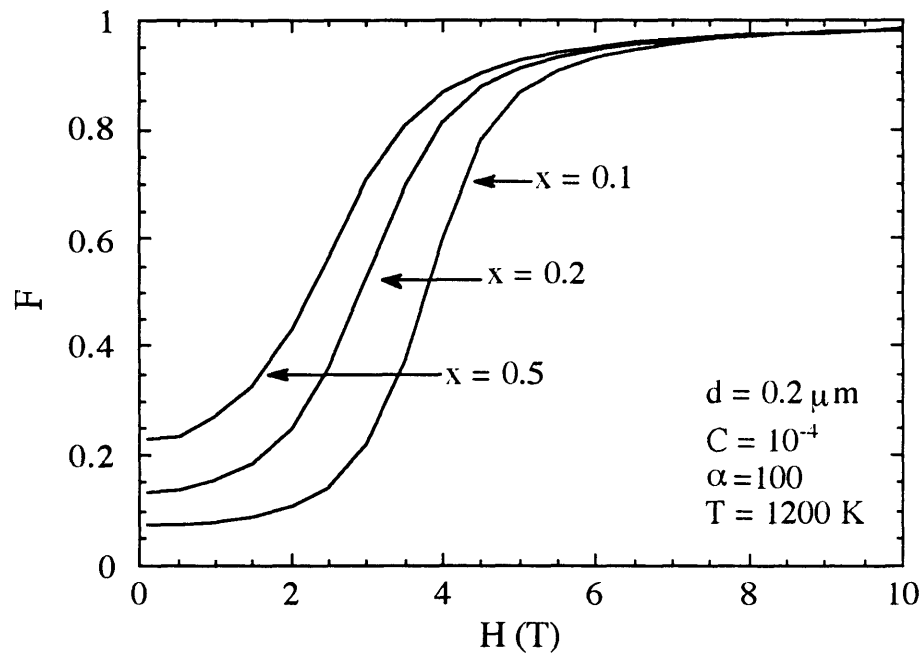
Fig. 2-3-3: F as a function of magnetic field for different liquid phase content.

In all of the discussion, thus for, we have assumed that the grain size is a constant during the rotation process. Actually, during high temperature

56

processing, grain growth should be considered. If we assume that during slow grain growth that thermal equilibrium is always established at any time t, we can easily substitute grain size d as a function of kinetic parameters in the classic grain growth theory. All our theoretical treatments will be valid.

Section 2. 4: Conclusion.

The F factor has been expressed as a function of β, and a critical point and a saturation point are defined. From the critical point, we introduce critical grain size d_c, critical magnetic field H_c, critical anisotropic susceptibility $\Delta\chi_c$ and critical temperature T_c. From the saturation point, we introduce saturation grain size d_s, saturation magnetic field H_s, saturation anisotropy susceptibility $\Delta\chi_s$ and saturation temperature T_s.

For the interaction energy $K(T, x) = 0$ case, the F factor depends on the magnetic field, grain size and temperature. F always increases with increasing magnetic field and grain size and F decreases with increasing temperature. For the interaction energy $K(T, x) \neq 0$ case, the F factor not only depends on magnetic field, temperature and grain size, but also depends on the interaction constant and liquid phase content x. For constant magnetic field and grain size, F increases with decreasing interaction constant and increasing liquid phase content. When $H \rightarrow \infty$, $F \rightarrow 1$. These results are consistent with the experimental results as shown in the following sections.

Chapter 3. Experimental Procedure

Section 3.1. Processing of high - T_c superconductors under a high magnetic field

A small tubular furnace was constructed, 4 cm diameter and 25 cm long with a water cooled jacket. The furnace is placed in the room temperature bore of a superconducting magnet at the FBNML at MIT (see Fig. 3-1). Samples are synthesized in an Al_2O_3 crucible under an atmosphere of air in a magnetic field at high temperature (800 - 1100°C). Magnetic fields of up to 10 T can be applied parallel to the long axis of the furnace throughout the high temperature cycle. The field was increased from 0 T to 10 T, then the temperature was raised. After processing, the temperature was decreased to room temperature, then the magnetic field was reduced to zero.

Section 3.2. Scanning electron microscopy and microprobe analysis

After the high temperature processing in a high magnetic field, the samples were prepared for scanning electron microscopy (SEM) and microprobe analysis by mounting in epoxy and polishing with a 0.05 micron alumina solution and examining from polished longitudinal cross sections of the specimens. Microstructural observation and microanalysis were performed in a JEOL Superprobe 733 microanalyzer with Tracor Northern 5500-5600 wavelength - dispersive spectroscopy (WDS) and energy - dispersive spectroscopy systems. Back - scattered electron images were used to produce contrast from the different phases consisting of different elements. Microanalysis was accomplished through SEM micrographs from the surface and polished longitudinal cross sections of the specimens.
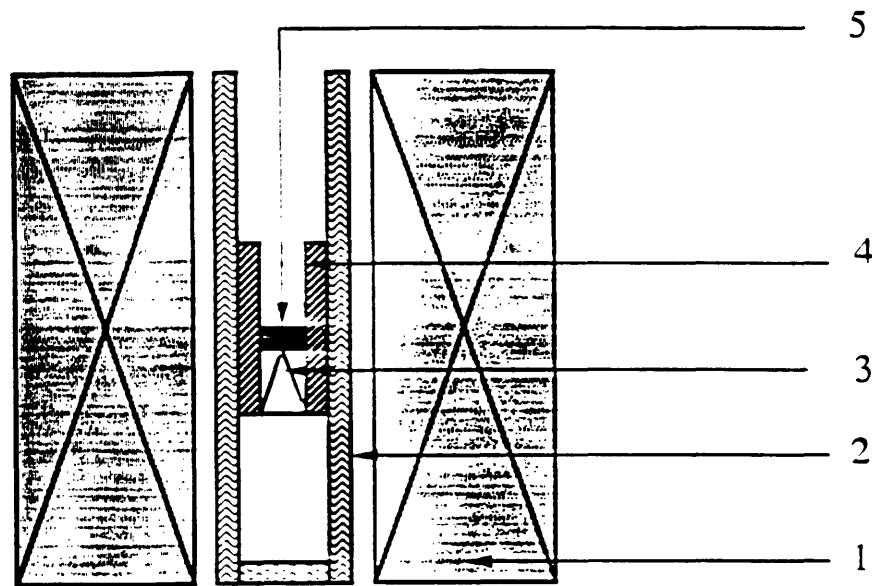
1. Superconducting Magnet
2. Water cooling jacket
3. Thermal couple
4. Furnace
5. Sample

Fig. 3-1.   High magnetic field and high temperature processing
              system.

Section 2.3. X- ray diffraction

The degree of the texture of the samples which were polished along transverse directions, were evaluated by pole figures and X - ray diffraction. X-ray diffraction was performed in a Rigaku 300 X - Ray diffractometer, using CuK_α X-ray at 50 KV and 200mA. The Lotgering factor, F [22], was calculated to quantify the degree of c - axis orientation as

$$F = (P - P_o)/(1 - P_o)$$

where $P = \Sigma I_{(00\ell)}/\Sigma I_{(hk\ell)}$, is the sum of integrated intensities for all (00ℓ) reflections divided by the sum of all intensities $(hk\ell)$ in the textured specimen. P_o is an equivalent parameter for a random specimen where the intensities were obtained from powder diffraction patterns. The factor F varies from 0 (unoriented) to 1 (completely oriented).

Section 3.4. Temperature dependence of resistance and J_c measurement

R - T curves were measured by a standard four - probe method during cooling down or warming up cycles. The critical current of the samples were measured at 4.2 K or 77 K in zero field or in an elevated magnetic field and determined from I - V curves using a criterion of 1 $\mu V/cm$. The measurement system is shown in Fig. 3-2.
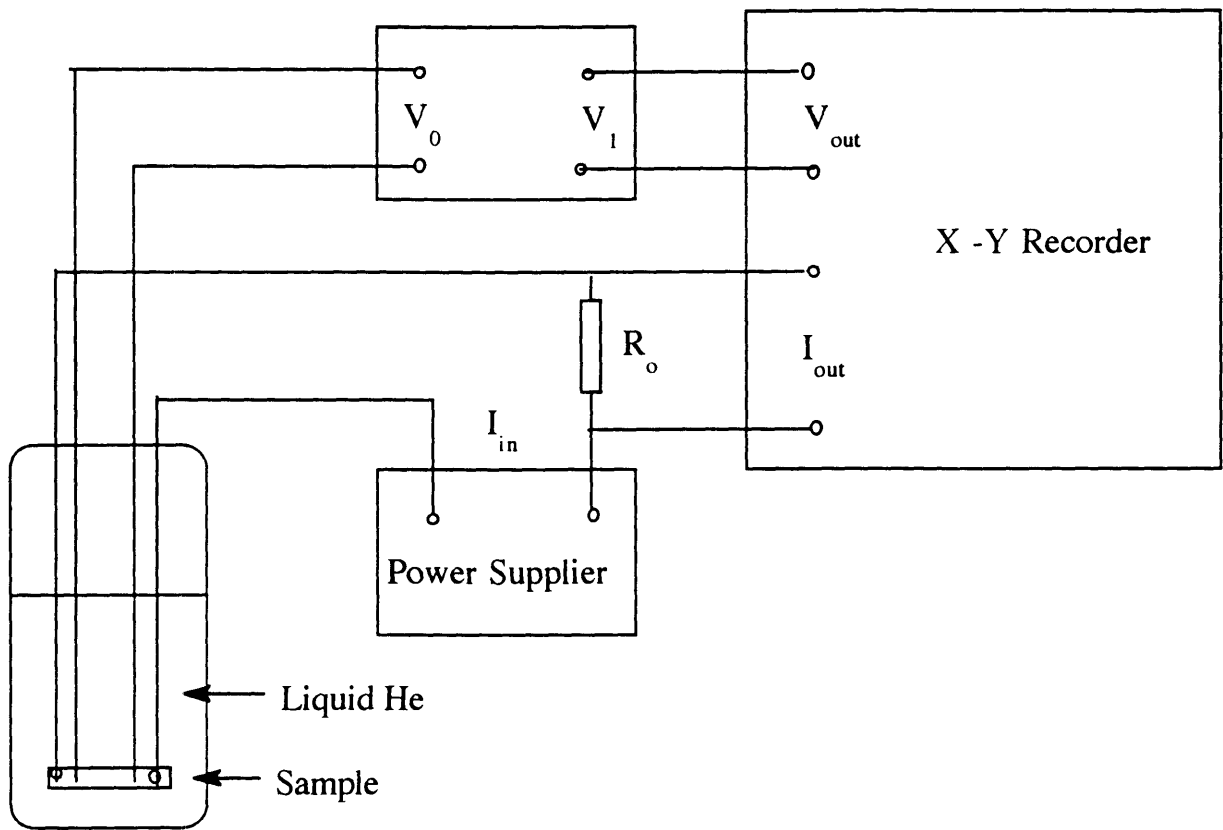
Fig. 3-2. J_c measurement system.

Section 3.5. Magnetization and magnetic anisotropy.

Superconducting transitions were determined from the measurement of Meissner diamagnetic susceptibility as a function of temperature using a Quantum Design SQUID magnetometer. The field was first set at 30 Oe and was held constant throughout the measurements. The sample was then introduced in the cryostat at ~ 100 K and was cooled to 4.2 K in the magnetic field. The amount of flux expulsion was recorded during the warm up. Magnetic hysteresis was measured at 4.2 K under zero field cooling the sample from room temperature to 4.2 K. The samples were placed in the SQUID magnetometer in two directions, i.e. H_α // H and $H_\alpha \perp$ H, H_α is the magnetic field during high temperature processing and H is the measurement magnetic field at low temperature. The magnetic anisotropy factor was defined as $\eta = \Delta M(H_\alpha$ // H) / $\Delta M(H_\alpha \perp$ H).

Chapter 4. Rotating Grains of High - T$_c$ Superconductor in A High Magnetic Field by Introducing A Liquid Phase.

Section 4.1. Influence of a 10 T magnetic field on the texture development of Bi - 2212 superconductors

Bi - 2212 superconductors were processed under a 10 T magnetic field at 870°C ~ 940°C. The grain orientation and superconducting properties were characterized by SEM, XRD, SQUID and J$_c$ measurement. It was found that: (a) A high magnetic field can not introduce anisotropic nucleation and anisotropic growth during the early stage of growth. (b) A liquid phase is important for texture development of Bi - 2212 via application of a 10 T magnetic field.   (c) Substitution of a small amount of Ca by Ho in Bi - 2212 increases the degree of texture in Bi - 2212 superconductors by application of a 10 T magnetic field during partial melt - growth.

4.1.1. Experimental Procedure

The starting materials were first prepared by solid state reaction. Highly pure Bi_2O_3, $SrCO_3$, $CaCO_3$, Ho_2O_3 and CuO were weighed in the ratios according to the desired compositions $Bi_2Sr_2CaCu_2O_8$ and $Bi_2Sr_2Ca_{0.9}Ho_{0.1}Cu_2O_8$. The mixed powders were first reacted at 800°C for $Bi_2Sr_2CaCu_2O_8$ and 820°C for $Bi_2Sr_2Ca_{0.9}Ho_{0.1}Cu_2O_8$ for 12 hours in air to form the precursors. The precursors were then ground in an agate mortar and pestle, pressed into pellets and sintered in a 10 T magnetic field at elevated temperature. For high magnetic field experiments, the furnace is placed in the room temperature bore of a superconducting magnet. Magnetic fields of up to 10 T can be applied parallel to the long axis of the furnace throughout the processing cycle. The field was increased to 10 T, then the

temperature was raised. After the processing, the temperature was decreased to room temperature and the magnetic field was reduced to zero.

4.1.2. The influence of a high magnetic field on anisotropic nucleation and growth during the early stage of growth

For the first set of experiments, the pellets of $Bi_2Sr_2CaCu_2O_8$ composition were annealed at 870°C and 880°C under a 10 T magnetic field for a short time (1 hour). Figs. 4-1-1(a) and 1(c) show the images of polished cross sections. It is clear that there is no apparent grain orientation for this short time annealing at 870°C even near the onset of the melting point, i.e. 880°C. In other words, a 10 T magnetic field does not introduce anisotropic nucleation and anisotropic growth during the early stages of growth.

By application of a high magnetic field, the driving force for grain alignment is the normal anisotropy energy which is given by $\Delta E = \Delta\chi H^2 V_c / 2$ [15], where V is the volume of a grain (cm^3), and H is the magnetic field (in Oe). It is clear that the anisotropy energy depends on the volume of the grain. Thus there is a critical volume of a grain, V_c, which corresponds to a magnetic anisotropy energy equal to the thermal disorder energy kT, i.e $\Delta\chi H^2 V_c / 2 = kT$. Thus,

$$V_c = 2kT / H^2 \Delta\chi .$$

When $V < V_c$ the magnetic field can not overcome thermal disorder and introduce grain alignment. This implies that the application of a high magnetic field can not introduce anisotropic nucleation, or anisotropic growth at an early stage of grain growth, as observed.

For $Bi_2Sr_2CaCu_2O_y$, the difference in the normal state susceptibility is $\Delta\chi \sim 1.4 - 11.3 \times 10^{-5}$ [13] [14]. Using a room temperature value of $\Delta\chi \sim 10^{-5}$ and assuming a cubic grain with edge length ℓ, at 870°C and a 10 T magnetic field, we estimate that the critical grain size is approximately 120 Å. When $V > V_c$, the grains should be rotated with the c - axis parallel to the magnetic field direction. After 1 hour processing at 870°C and 880°C, the average grain edge length ℓ is larger than 120 Å, but there is no apparent grain orientation observed. According to the Curie law, the paramagnetic susceptibility will decrease with increasing temperature, i.e. $\chi = c / T$. If we assume that $\Delta\chi = c / T$, we can obtain the critical grain edge $\ell_c \sim 10$ μm for Bi - 2212 at around 1000 K (the processing temperature). This implies that if $\ell < 10$ μm, a 10 T magnetic field can not introduce any anisotropic grain growth for the Bi - 2212 system at these processing temperatures.

From the SEM images, although the average grain size of Bi - 2212 is larger than 10 μm, i.e. $\ell > \ell_c$, there is still no apparent grain alignment (Figs. 4-1-1(a) and (c)). This observation will be explained in the next section.

4.1.3. Grain rotation by a high magnetic field

In order to enhance texture development in Bi - 2212, we increase the processing time to 10 hours under a 10 T magnetic field. First the pellet was sintered via solid state reaction under a 10 T magnetic field at 870°C, which is 10°C below the onset of melting in Bi - 2212 [32]. After 10 hours annealing, although $\ell > \ell_c$, the SEM image of the polished cross section does not show any apparent grain orientation (see Fig. 4-1-1(b)). X - ray diffraction patterns of the sample polished along the transverse direction also shows almost pure Bi
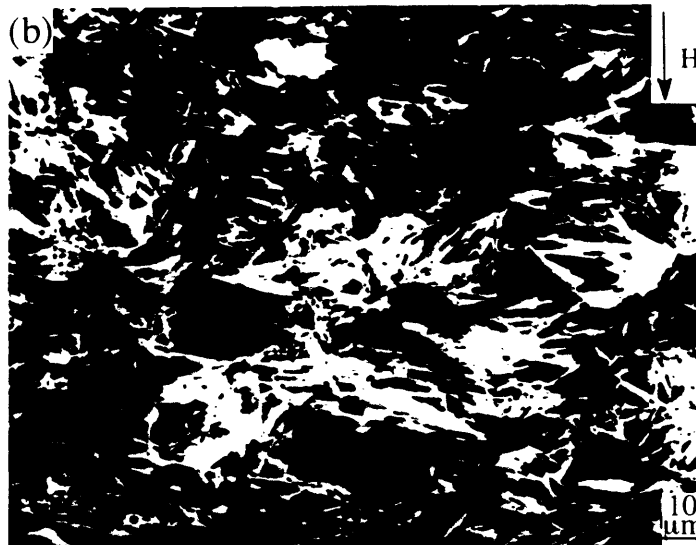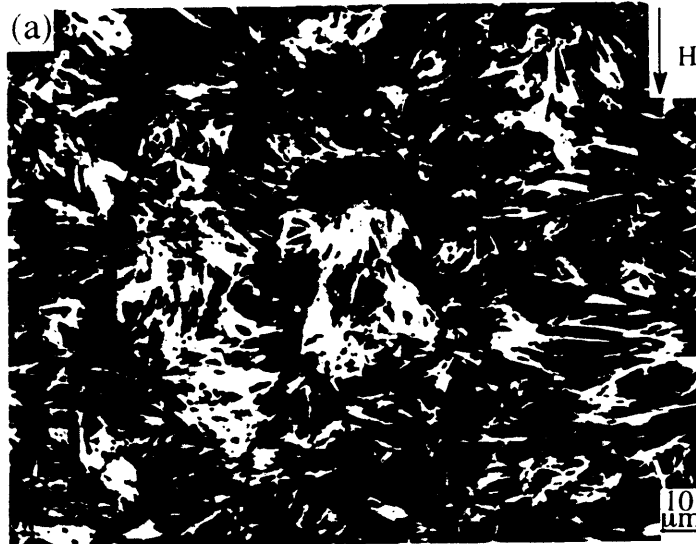
Fig. 4-1-1:   SEM images of polished cross section of $Bi_2Sr_2Ca_1Cu_2O_y$
annealed under a 10 T magnetic field in air. (a) 870°C for 1
hour, (b) 870°C for 10 hours.
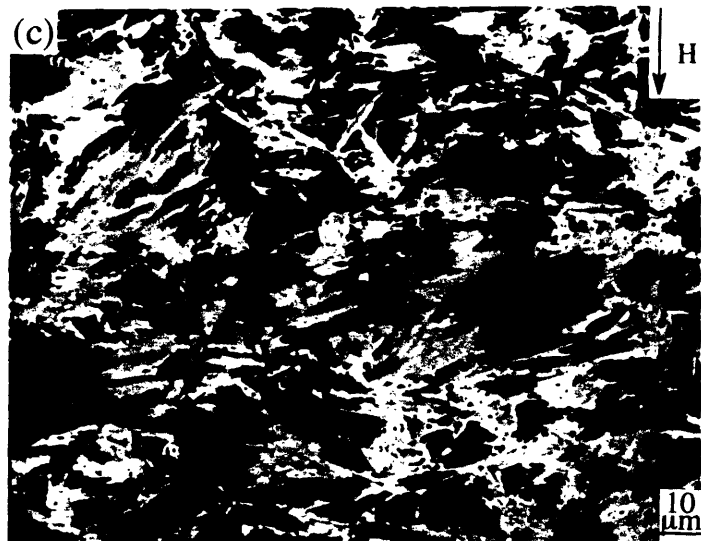
Fig. 4-1-1:   SEM images of polished cross section of $Bi_2Sr_2Ca_1Cu_2O_y$

annealed under a 10 T magnetic field in air. (c) 880°C

for 1 hour, (d) 880°C for 10 hours.

2212 phase with F = 0.09 (Fig. 4-1-4(a)), a very low degree of grain alignment. It is clear that a high magnetic field does not introduce a textured structure in $Bi_2Sr_2CaCu_2O_y$ when processed in the solid state.

When the annealing temperature was increased to 880°C (the onset of the melting point of Bi - 2212), a liquid phase begins to appear and some degree of grain orientation was observed after 10 hours of processing (see Fig. 4-1-1(d)). X - ray diffraction patterns of the sample polished along the transverse direction shows that the relative intensity of (00ℓ) peaks increases and the F factor increases to 0.24.

As discussed above, when $V > V_c$, the magnetic field will tend to rotate grains with c // H_α. If the sample is in the solid state, the magnetic field will rotate the grains involving mechanical interaction between the grains. It is difficult to rotate the grains in the solid state even 10°C below the melting point. At 880°C a liquid phase appears between the grains, thus the grains can be more easily rotated by a 10 T magnetic field and the degree of texture increases (Figs. 4-1-1(d) and Fig. 4-1-4). Unfortunately, an impurity phase (Sr, Ca)CuO_x begins to appear when the oxide melts.. The impurity phase (Sr, Ca)CuOx will block the texture development of the Bi - 2212 phase. Thus, it is necessary to create a liquid phase, but reduce the fraction of the impurity phase during texture development by application of a high magnetic field.

4.1.4. Partial melt growth of Bi - 2212 under a 10 T magnetic field

In order to increase the degree of texture, first we tried to create a liquid phase during texture development under a high magnetic field. We know that above 880°C, (Sr,Ca)$Cu)_x$ and (SrCa)$_2CuO_x$ will appear [30]. In order to

avoid the nucleation and growth of these impurity phases, the temperature is quickly raised to 900°C for a short time, then the sample is quickly cooled to 880°C and the temperature reduced to 870°C with a cooling rate of 1°C / hour. Bi - 2212 phase will be nucleated and grown when the temperature decreases to 880°C. In a 10 T magnetic field and after $V > V_c$, grains will be rotated in the undercooled liquid and the entire sample should be textured.

Figs. 4-1-2(a) and (b) show the SEM images of polished cross sections of the samples prepared as described above. It is clear that long plate- like grains were formed and grown parallel to each other. Unfortunately, under this processing condition, there is the impurity phase (Sr, Ca)CuO$_x$ in the sample with an average size around 50 μm. In order to increase the volume fraction of the superconducting 2212 phase, the melt-grown sample was annealed at 860°C and 0 T for 65 hours in air to convert the impurity phase to the 2212 phase and recover the superconductivity. This diffusion controlled growth processes will not effect the degree of texture in the sample.

The SEM images of polished cross sections of the annealed sample are shown in Figs. 4-1-2(c) and (d). Good local texture is shown in Fig. 4-1-2(d). After the 860°C long time annealing, the X - ray diffraction pattern of a polished transverse cross section shows stronger (00ℓ) peaks (Fig. 4-1-5(a)) with F = 0.44. The degree of texture is higher in this case (F = 0.44) than that in the 880°C case (F = 0.24) as discussed above.

3.1.5. Ho doping effect on melt - texture of Bi - 2212 in a 10 T magnetic field
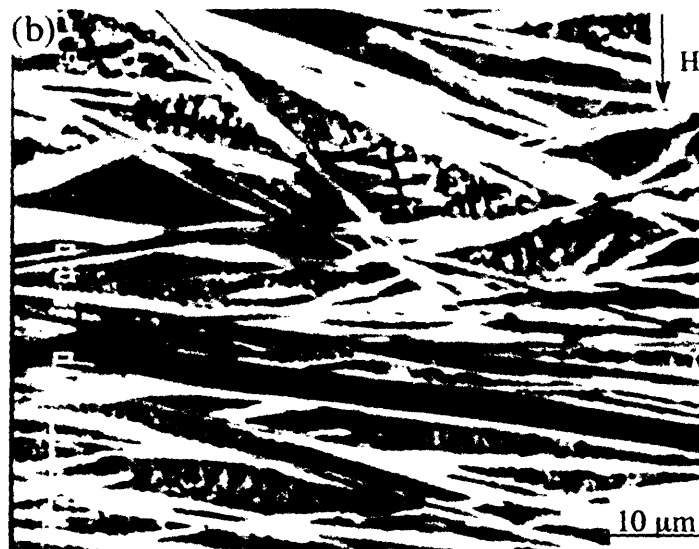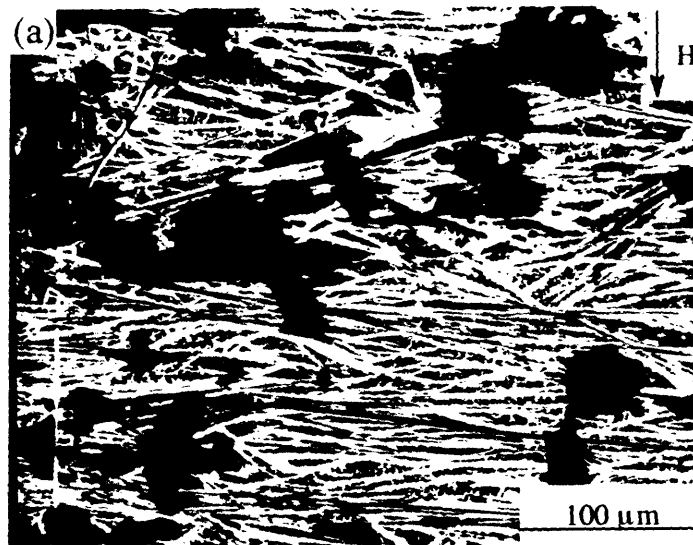
Fig. 4-1-2: SEM images of polished cross section of $Bi_2Sr_2Ca_1Cu_2O_y$ annealed under a 10 T magnetic field in air: 900°C for a short time, then fast cooled to 880°C and 1°C / min cooled to 870°C. (a) and (b) as grown sample.
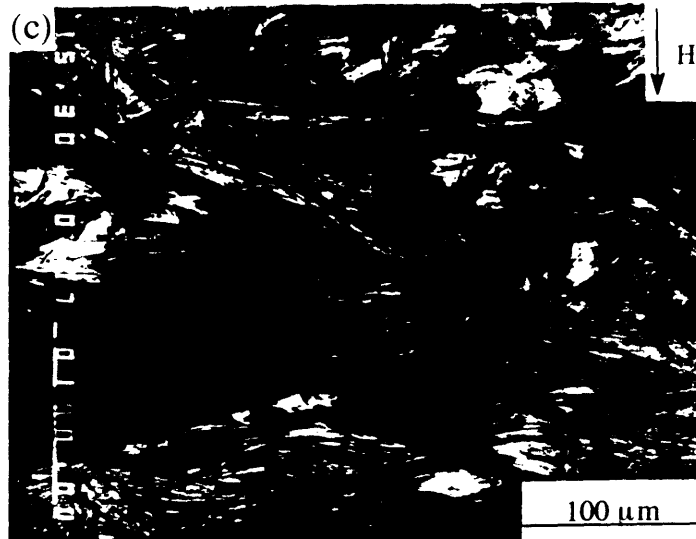
Fig. 4-1-2:   SEM images of polished cross section of $Bi_2Sr_2Ca_1Cu_2O_y$

annealed under a 10 T magnetic field in air: 900°C for a

short time, then fast cooled to 880°C and 1°C / min cooled

to 870°C. (c) and (d) the sample was annealed at 860°C for 65

hours under zero field in air after the partial melt - growth

under a 10 T magnetic field.

Pure Bi - 2212 has been melt - textured as discussed in section (c) above. It is clear that the degree of texture is still low and the impurity phase present is a major problem for texture development. Basically, there are two approaches that can be used to improve the degree of texture in melt- textured Bi - 2212 by application of a high magnetic field. First, to determine the best processing conditions and optimize the composition of Bi -2212. Second, to increase the melting point of Bi - 2212 above the melting point of $(Sr,Ca)CuO_x$ and $(Sr,Ca)_2CuO_x$ by doping, allowing the material to be processed above the melting point of the impurity phases to avoid $(Sr,Ca)CuO_x$ and $(Sr,Ca)_2CuO_x$ phase formation.

Because of the peritectic phase transformation in the Bi - 2212 system, it is impossible to eliminate the impurity phase during the melt - growth of Bi - 2212 for bulk material by altering the processing conditions. Thus in the present work, we choose the second approach to improve the texture of Bi - 2212 superconductor, i.e. doping the oxide with Ho. There are two advantages in choosing Ho as a doping element. First, because $Bi_2Sr_2Ca_1Cu_2O_y$ is an over-doped material when it is prepared in air, substitution of Ca^{2+} by Ho^{3+} will create excess electrons in the oxide while a small amount of doping will not influence T_c very much. At the same time, the melting point of a $Bi_2Sr_2Ca_{0.9}Ho_{0.1}Cu_2O_y$ precursor increases to 930°C. Even without a complete understanding of the phase diagram of $Bi_2Sr_2Ca_{0.9}Ho_{0.1}Cu_2O_y$, we can anneal the oxide above 920°C to avoid the formation of $(Sr,Ca)Cu)_x$ and $(Sr,Ca)_2CuO_x$. Second, the effective moment of Ho^{3+} is along the c - axis direction [18], and its presence will enhance the anisotropic paramagnetic susceptibility of Bi - 2212, i.e. it will increase the anisotropic
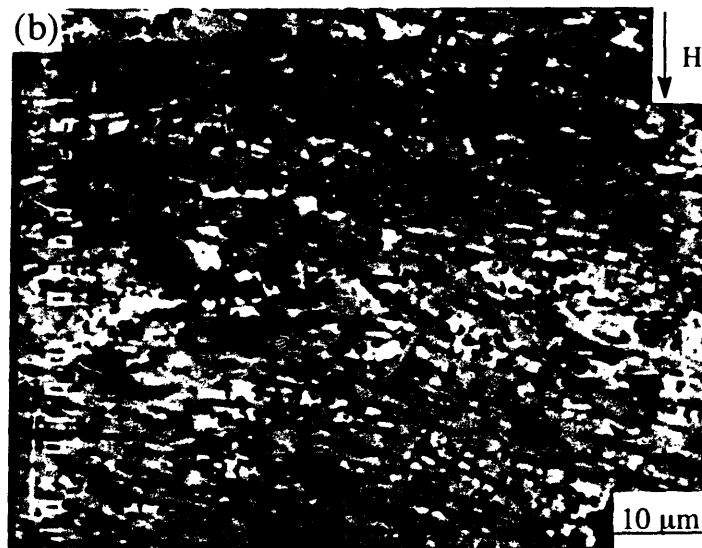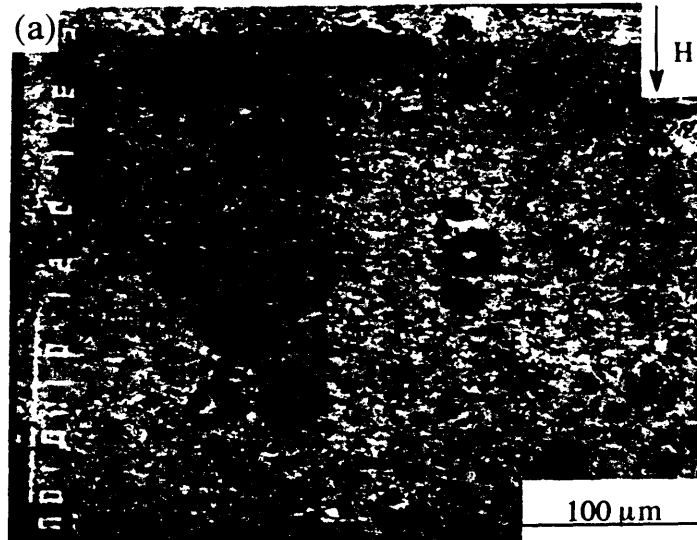
Fig. 4-1-3:   SEM images of polished cross section of

Bi$_2$Sr$_2$Ca$_{0.9}$Ho$_{0.1}$Cu$_2$O$_y$ annealed under a 10 T magnetic

field in air: 940°C for a short time, then fast cooled to

930°C and 1°C / min cooled to 920°C. (a) and (b) as grown

sample.
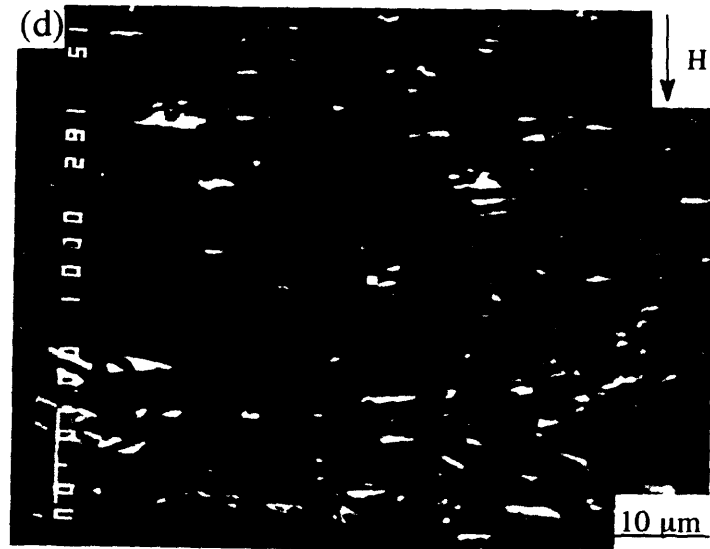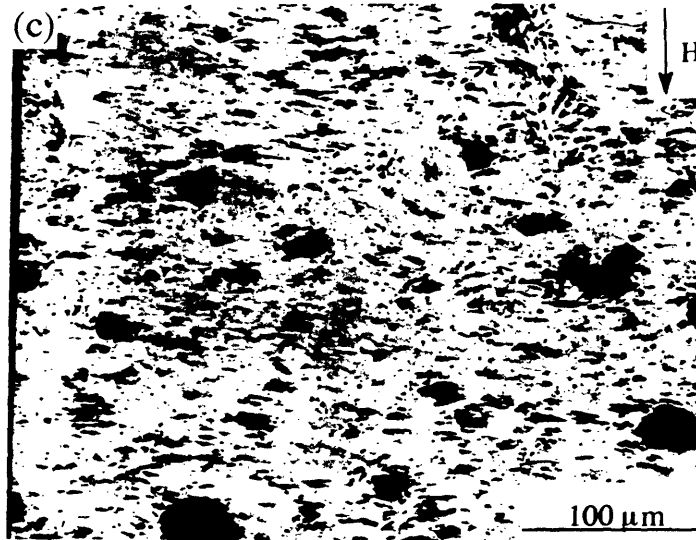
Fig. 4-1-3: SEM images of polished cross section of $Bi_2Sr_2Ca_{0.9}Ho_{0.1}Cu_2O_y$ annealed under a 10 T magnetic field in air: 940°C for a short time, then fast cooled to 930°C and 1°C / min cooled to 920°C.
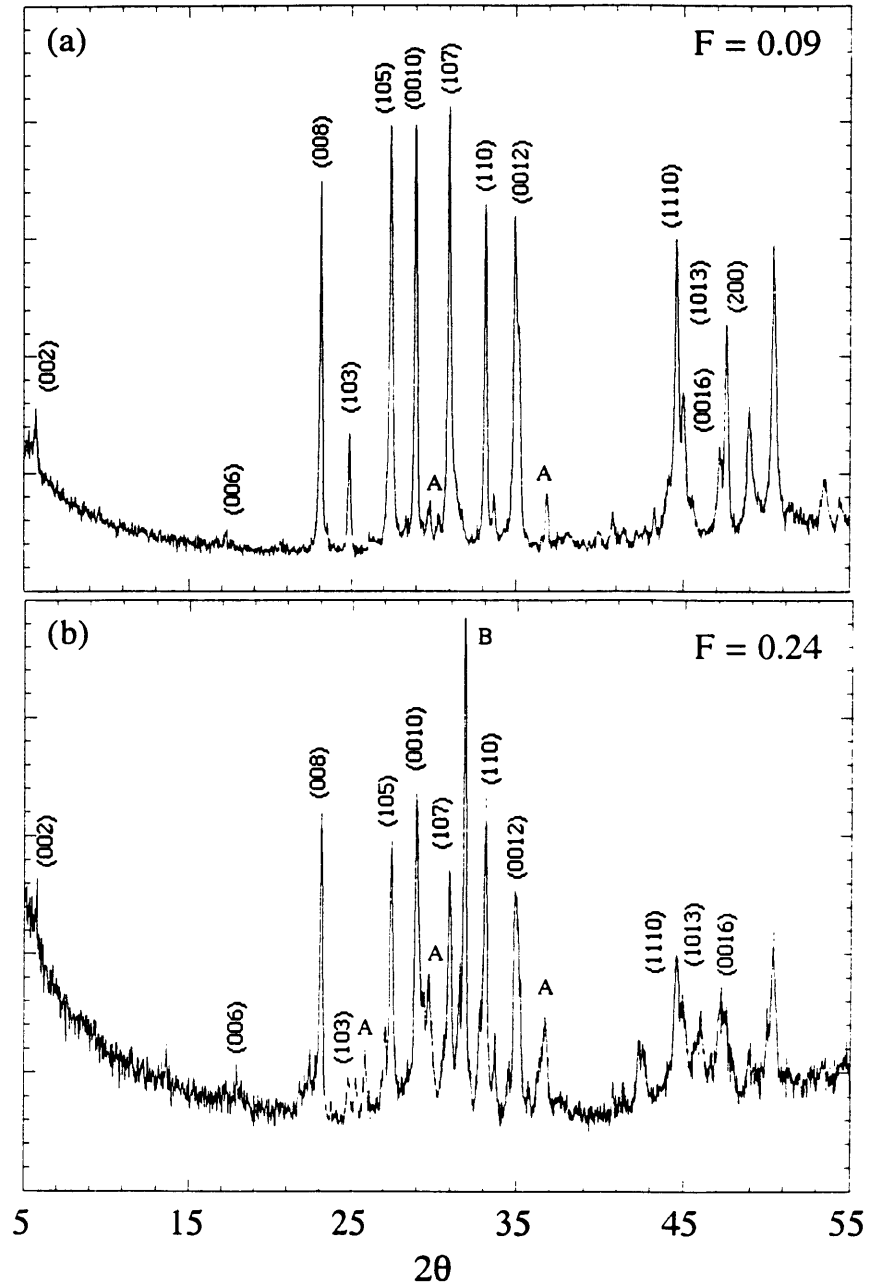
Fig. 4-1-4:   X - ray diffraction pattern of the sintered $Bi_2Sr_2Ca_1Cu_2O_y$

polished along transverse direction of applied field $H_\alpha =$

10 T. (a) sample was sintered at 870°C for 10 hours, (b)

sample was sintered at 880°C for 10 hours.
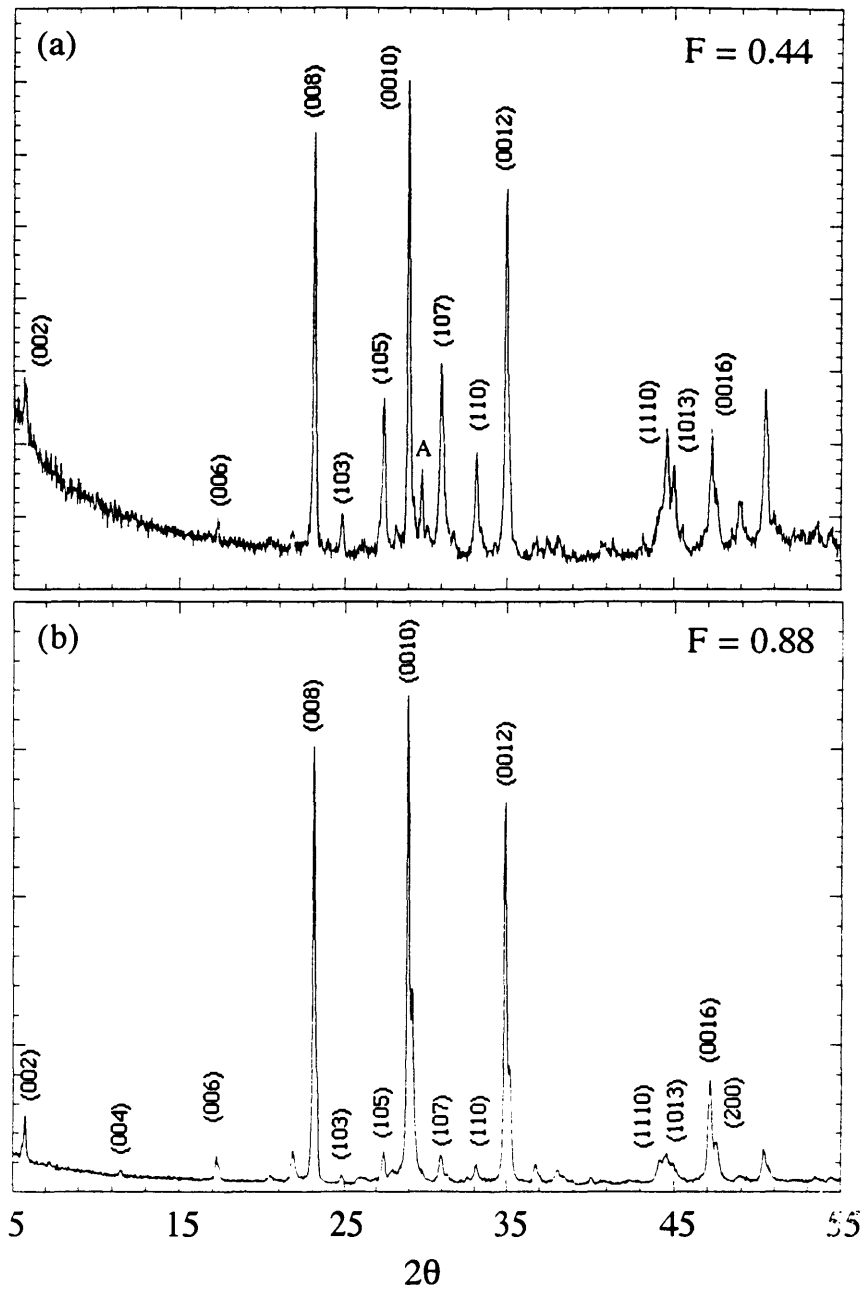
Fig. 4-1-5:   X - ray diffraction pattern of the melt - growth samples

polished along transverse direction of applied field H_α =

10 T.   (a) $Bi_2Sr_2Ca_1Cu_2O_y$, 900°C for a short time, then fast

cooled to 880°C and 1°C / min cooled to 870°C, (b)

$Bi_2Sr_2Ca_{0.9}Ho_{0.1}Cu_2O_y$, 940°C for a short time, then fast

cooled to 930°C and 1°C / min cooled to 920°C.

energy $\Delta E = \Delta\chi H^2 V_c/2$ and increase the driving force for texture development.

A pellet of $Bi_2Sr_2Ca_{0.9}Ho_{0.1}Cu_2O_y$ precursor material was heated at rate 20°C/min to 940°C for 30 minutes and fast cooled to 930°C. Then the sample was cooled at a rate of 1°C/ hour to 920°C and fast cooled to room temperature to avoid impurity phase formation. The SEM images of as - grown samples are shown in Figs. 4-1-3(a) and (b). It is clear that the fraction of impurity phase is dramatically decreased and the Bi - 2212 grains are well textured. At the same time the grain size is smaller than that of pure Bi - 2212 which was prepared by a similar process. A relatively low temperature and long time annealing is necessary to recover the superconductivity. The best annealing temperature is 860°C; if the annealing temperature increases to above 880°C, the impurity phase $(Sr,Ca)CuO_x$ will be formed. Figs. 4-1-3(c) and (d) show the SEM images of polished cross sections of the sample annealed at 860°C for 65 hours in air. X - ray diffraction patterns of polished transverse cross sections of $Bi_2Sr_2Ca_{0.9}Ho_{0.1}Cu_2O_y$ show very strong (00ℓ) peaks (Fig. 4-3-5(b)) with F = 0.88. Thus, substitution of a small amount of Ca by Ho in Bi - 2212 increases the degree of the texture of the superconductor and decreases the amount of the impurity phase by application of a 10 T magnetic field in the melt-growth of Bi - 2212 material.

4.1.6. Superconductivity and anisotropic magnetization

The temperature dependence of resistance and diamagnetic susceptibility of the samples which were processed under a 10 T magnetic field are shown in Figs. 4-1-6(a) and (b). After annealing in air, the temperature dependence of the resistance shows good metallic behavior for

both $Bi_2Sr_2Ca_1Cu_2O_y$ and $Bi_2Sr_2Ca_{0.9}Ho_{0.1}Cu_2O_y$. The $T_{c,zero}$ of $Bi_2Sr_2Ca_1Cu_2O_y$ is around 82 K and $T_{c,zero}$ of $Bi_2Sr_2Ca_{0.9}Ho_{0.1}Cu_2O_y$ is around 79 K. The onset of the temperature dependence of diamagnetic susceptibility is around 86 K for $Bi_2Sr_2Ca_1Cu_2O_y$ and 81 K for $Bi_2Sr_2Ca_{0.9}Ho_{0.1}Cu_2O_y$. Thus a small amount of Ho only reduces T_c by a few degrees, but dramatically increases the degree of texture (F = 0.88) and decreases the amount of the impurity phase.

Figs. 4-1-7(a) and (b) show the diamagnetic hysteresis at 4.2 K. The ratio of $\Delta M(H_\alpha//H)/ \Delta M(H_\alpha \perp H)$ for both $Bi_2Sr_2Ca_1Cu_2O_y$ and $Bi_2Sr_2Ca_{0.9}Ho_{0.1}Cu_2O_y$ are shown in Fig. 4-1-8(a). When $H_\alpha // H$, the curves always show a larger $\Delta M(H)$ for both samples. This implies that a 10 T magnetic field indeed introduces a textured structure with the c - axis // H_α for both $Bi_2Sr_2Ca_1Cu_2O_y$ and $Bi_2Sr_2Ca_{0.9}Ho_{0.1}Cu_2O_y$. $\Delta M(H_\alpha//H) / \Delta M(H_\alpha \perp H)$ has almost a constant value of 1.4 for $Bi_2Sr_2Ca_1Cu_2O_y$, but strongly depends on the field for $Bi_2Sr_2Ca_{0.9}Ho_{0.1}Cu_2O_y$. The overall $\Delta M(H_\alpha//H) / \Delta M(H_\alpha \perp H)$ of $Bi_2Sr_2Ca_{0.9}Ho_{0.1}Cu_2O_y$ is always larger than that of $Bi_2Sr_2Ca_1Cu_2O_y$ for all fields. For $Bi_2Sr_2Ca_{0.9}Ho_{0.1}Cu_2O_y$, the zero field $\Delta M(H_\alpha//H) / \Delta M(H_\alpha \perp H)$ is as high as 4.2 and the high field $\Delta M(H_\alpha//H) / \Delta M(H_\alpha \perp H)$ is almost 1.8 ~ 2.0. These results show that the degree of texture for the whole body $Bi_2Sr_2Ca_{0.9}Ho_{0.1}Cu_2O_y$ is higher than that of $Bi_2Sr_2Ca_1Cu_2O_y$.
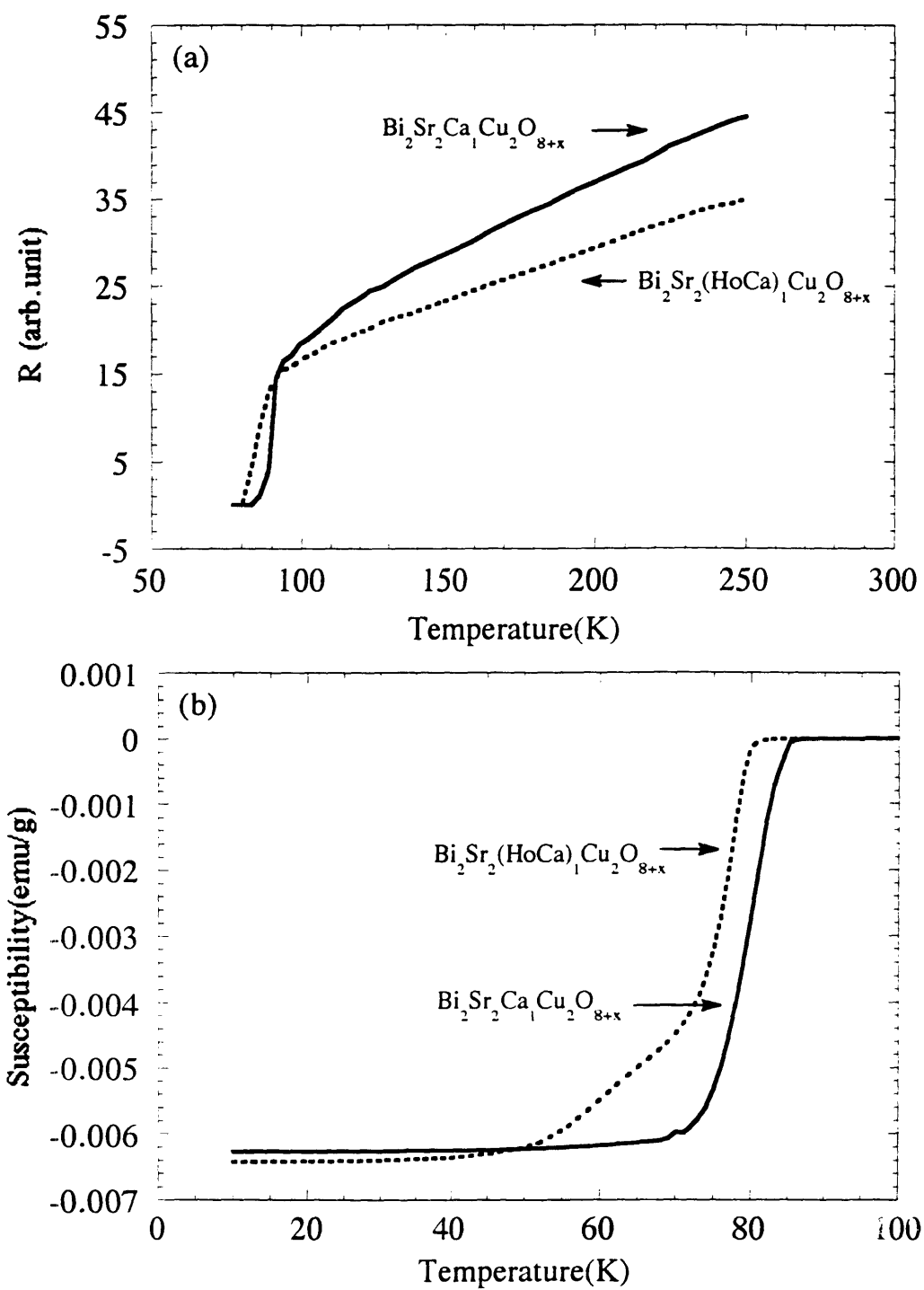
Fig. 4-1-6: (a) Temperature dependence of resistance of the samples,

(b) Temperature dependence of diamagnetic susceptibility

of the samples.
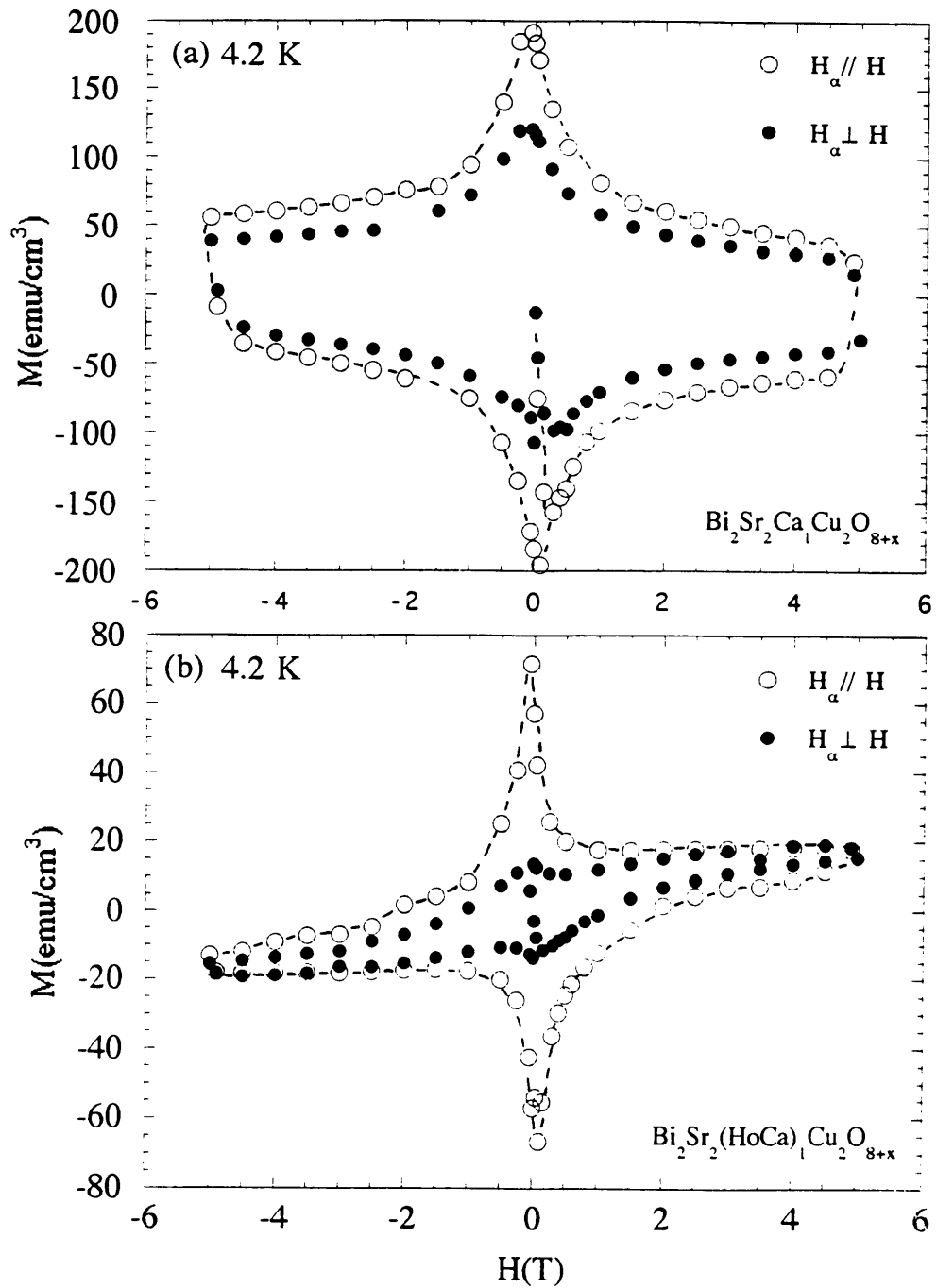
Fig. 4-1-7: Magnetic hysteresis at 4.2 K of samples with $H_\alpha//H$ and $H_\alpha \perp H$. H_α is the annealing field and H is the measuring field. (a) $Bi_2Sr_2Ca_1Cu_2O_y$. (b) $Bi_2Sr_2Ca_{0.9}Ho_{0.1}Cu_2O_y$.
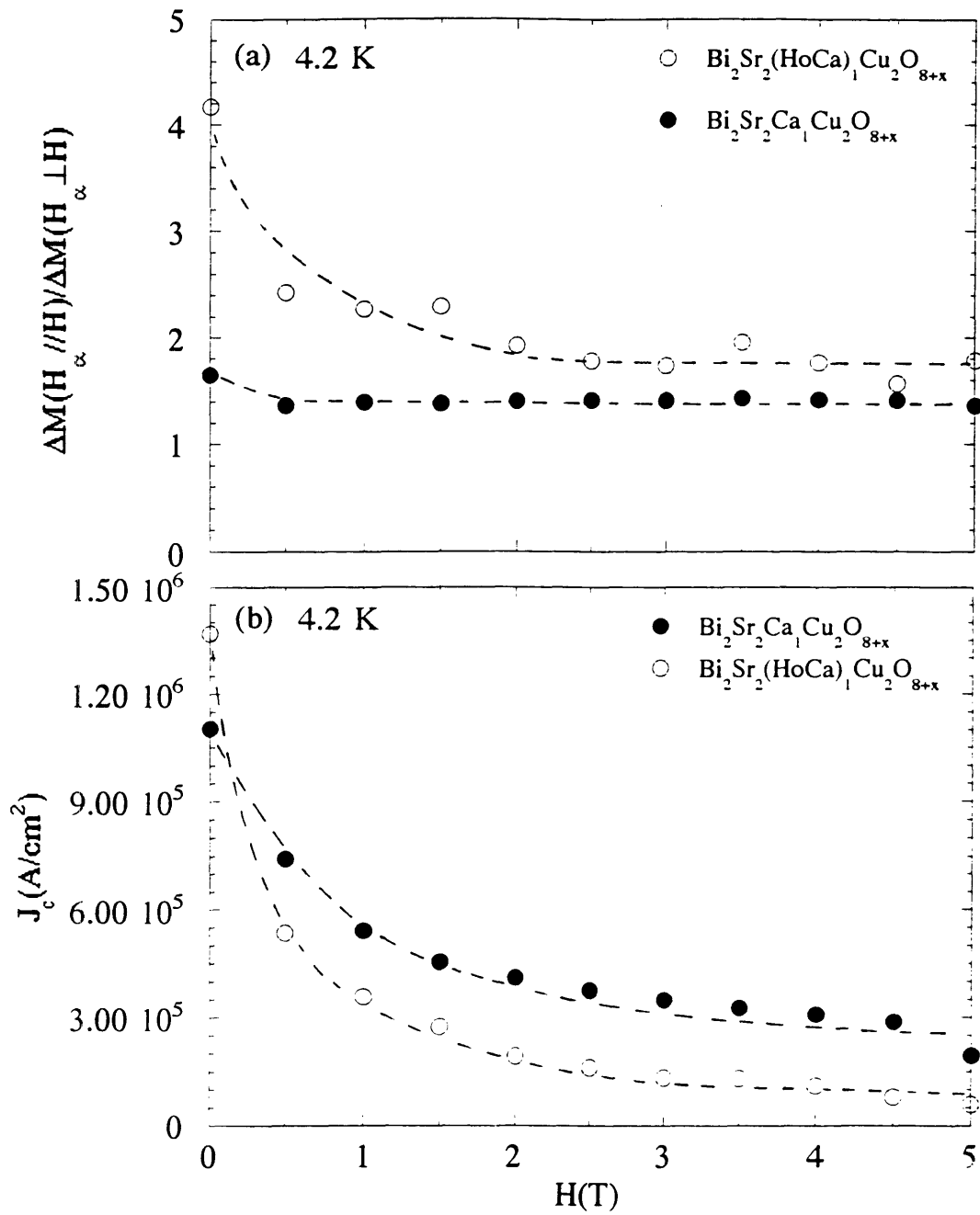
Fig. 4-1-8: (a) $\Delta M(H_\alpha//H)$ / $\Delta M(H_\alpha \perp H)$ dependence of field H for

$Bi_2Sr_2Ca_1Cu_2O_y$ and $Bi_2Sr_2Ca_{0.9}Ho_{0.1}Cu_2O_y$. (b) $J_{c,m}$

dependence of field H for $Bi_2Sr_2Ca_1Cu_2O_y$ and

$Bi_2Sr_2Ca_{0.9}Ho_{0.1}Cu_2O_y$.

4.1.7. Critical current density

The intragrain critical current density $J_{c,m}(H)$ with $H_\alpha//H$ was estimated by using the Bean model [23], $J_c = 30\Delta M/d$, where ΔM is the magnetization difference for increasing and decreasing magnetic field, and d is the average diameter of the current loop [24]. We chose d = 100μm for $Bi_2Sr_2Ca_1Cu_2O_y$ and d = 25μm for $Bi_2Sr_2Ca_{0.9}Ho_{0.1}Cu_2O_y$ based on the SEM images in Figs. 4-1-2 and 4-1-3. The $J_{c,m}$ vs H is plotted in Fig. 4-1-8(b). Although ΔM of $Bi_2Sr_2Ca_1Cu_2O_y$ is larger than that of $Bi_2Sr_2Ca_{0.9}Ho_{0.1}Cu_2O_y$ for all fields, the grain size of $Bi_2Sr_2Ca_1Cu_2O_y$ is also larger than that of $Bi_2Sr_2Ca_{0.9}Ho_{0.1}Cu_2O_y$ and $J_{c,m}(H)$ is the same order of magnitude for both samples. At high fields, intragrain critical current density for both samples is almost independent of the magnetic field and of order 10^5 A/cm^2. The smaller grains in $Bi_2Sr_2Ca_{0.9}Ho_{0.1}Cu_2O_y$ lead to better grain - to - grain contact and improve the weak links between the grains. The zero field transport critical current density at 4.2 K is $J_c(0)$ = 570 A/cm^2 for $Bi_2Sr_2Ca_1Cu_2O_y$ and $J_c(0)$ = 2400 A/cm^2 for $Bi_2Sr_2Ca_{0.9}Ho_{0.1}Cu_2O_y$.

4.1.8. Conclusion

Bi - 2212 superconductors were processed under a 10 T magnetic field at 870°C ~ 940°C. A high magnetic field can not introduce anisotropic nucleation and anisotropic growth during early stages of growth. The presence of a liquid phase is important for texture development by application of a high magnetic field. Substitution of a small amount of Ca by Ho in Bi - 2212 increases the degree of texture in Bi - 2212 by application of a 10 T magnetic field during partial melt - growth.

Section 4.2.   Rotating $Bi_2Sr_2(CaHo)Cu_2O_8$ by a high magnetic field with pure $Bi_2Sr_2CaCu_2O_8$ as a liquid phase

It is known that $Bi_2Sr_2CaCu_2O_8$ melts at 880^oC and $Bi_2Sr_2Ca_{0.9}Ho_{0.1}Cu_2O_8$ melts at about 930^oC. If the powder of the two materials is mixed and the mixture annealed between 880^oC and 930^oC, the mixture is an ideal liquid with co - existing solid phase. Under a high magnetic field, the grains of the solid phase should be rotated by the high magnetic field in due to the presence of the liquid phase. We can vary the content of the liquid, magnetic field, time and temperature, and determine which parameter is critical to texture development.

In this section, the mixtures $(Bi_2Sr_2Ca_{0.9}Ho_{0.1}Cu_2O_8)_{1-x}$ $(Bi_2Sr_2CaCu_2O_8)_x$ with x = 0, 0.1, 0.2, 0.3 and 0.4 were annealed under elevated magnetic fields.   The texture development dependence on processing temperature T_a, time t, magnetic field and liquid phase content was studied systematically. The $Bi_2Sr_2Ca_{0.9}Ho_{0.1}Cu_2O_8$ superconductor was textured by rotating the grains under an elevated magnetic field with $Bi_2Sr_2Ca_1Cu_2O_8$ as a liquid phase. The degree of texture increases with increasing temperature T_a under a high magnetic field for a fixed time.   For constant liquid phase content x, the degree of texture increases with increasing time and increasing magnetic field.   The degree of texture also depends on the liquid phase content for a fixed magnetic field, temperature and time. The transport critical current density J_c increases with increasing degree of the texture. This method can be used as a pre - texturing process to reduce the rolling process and optimize powder - in - tube technology for Bi - 2212 and Bi-2223 tapes.

4. 2. 1: Experimental Procedure

The starting materials were prepared by solid state reaction. Highly pure Bi_2O_3, $SrCO_3$, $CaCO_3$, Ho_2O_3, and CuO are weighed according to the normal composition $Bi_2Sr_2Ca_{0.9}Ho_{0.1}Cu_2O_8$ and $Bi_2Sr_2CaCu_2O_8$. The mixed powders were reacted at 820^oC for 12 hours in air. The precursors were then ground in an agate mortar and pestle, pressed into pellets and sintered at 880^oC for $Bi_2Sr_2Ca_{0.9}Ho_{0.1}Cu_2O_8$ and at 860^oC for $Bi_2Sr_2CaCu_2O_8$ for 48 hours in air. Then the pellets were ground into powder again. The powder of the two materials was mixed as $(Bi_2Sr_2Ca_{0.9}Ho_{0.1}Cu_2O_8)_{1-x}(Bi_2Sr_2CaCu_2O_8)_x$ with $x = 0, 0.1, 0.2, 0.3$ and 0.4 by grinding in acetone. The mixture was then pressed into pellets. Finally the pellets were annealed under elevated magnetic fields for different temperature, time and liquid phase contents x. After the annealing processes were finished, the samples were fast cooled to room temperature under the magnetic field. After fast cooling under the elevated magnetic field, the samples are semiconductors due to the 'liquid phase' between the grains, and the loss of oxygen. The 'liquid phase' can be converted to the superconducting phase and the oxygen can be restored by annealing the samples at 860^oC for a long period of time in zero field. At 860^oC, if there is small amount of 'liquid phase', the annealing process is a diffusion controlled growth and the atoms in the small amount of 'liquid phase' will be incorporated into the textured grains to form the superconducting 2212 phase. The annealing process does not influence the well textured structure, after the annealing process, the highly textured structure is retained.

4.2.2: Texture development dependence on the temperature under a 10 T magnetic field.

X - ray diffraction patterns of the samples with x = 0.1, which were annealed at 890°C and 930°C under a 10 T magnetic field for 1 hour, are shown in Fig. 4-2-1(a) and (b). The degree of the texture is low for the sample annealed at 890°C, i.e. F = 0.23. When the temperature was increased to 930°C, X - ray diffraction patterns show very strong (00ℓ) peaks and the F factor increases to 0.82. From Fig. 4-2-2, it can be clearly seen that increasing temperature T_a not only increases the degree of the texture, but also increases the density of the sample. A poorly textured structure with low density was obtained under a lower temperature i.e. $T_a = 890$°C (see Fig. 4-2-2(a)). When the temperature T_a was increased to 930°C, both the degree of texture and density were increased (see Fig. 4-2-2(b)). The relation between the degree of the texture and temperature for liquid phase content x = 0.1 and 0.3 is shown in Fig. 4-2-3. For different liquid phase content x, the F factor increases with increasing the temperature T_a under a 10 T magnetic field for 1 hour. At a fixed temperature, the difference in the F factor for different liquid phase content x, is much smaller than the difference for different temperatures. At the same temperature, the difference in the F factor for different x can not be seen clearly in the F vs T_a curve. The liquid phase content x correlation with of texture development will be plotted on an expanded scale and discussed in section (d).

Fig. 4-2-1: X - ray diffraction patterns of samples with x = 0.1 polished along transverse direction of annealing magnetic field, with H_α = 10 T and t = 1 hour. (a) T = 890°C and (b) T = 930°C.
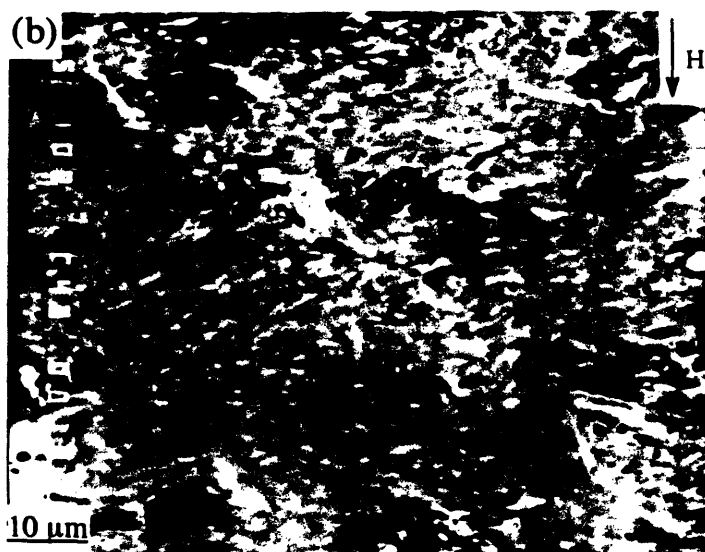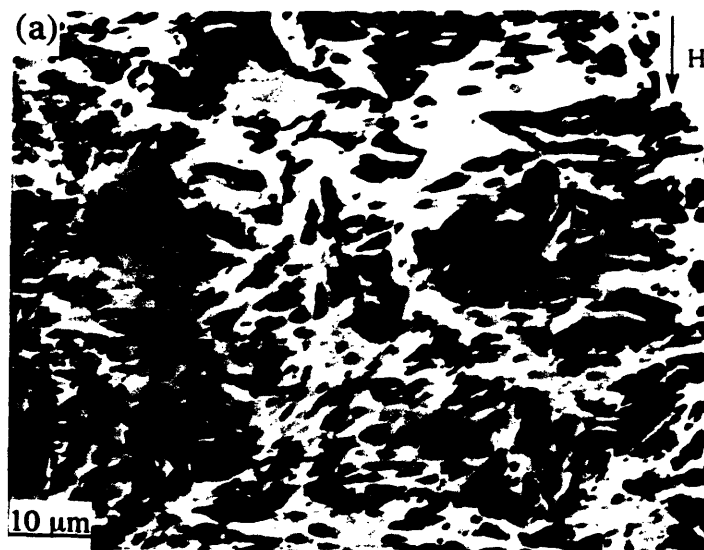
Fig. 4-2-2:   SEM images of polished cross section of samples with x =

0.1 for H_α = 10 T and t = 1 hour. (a) T = 890°C and (b) T_m =

930°C.
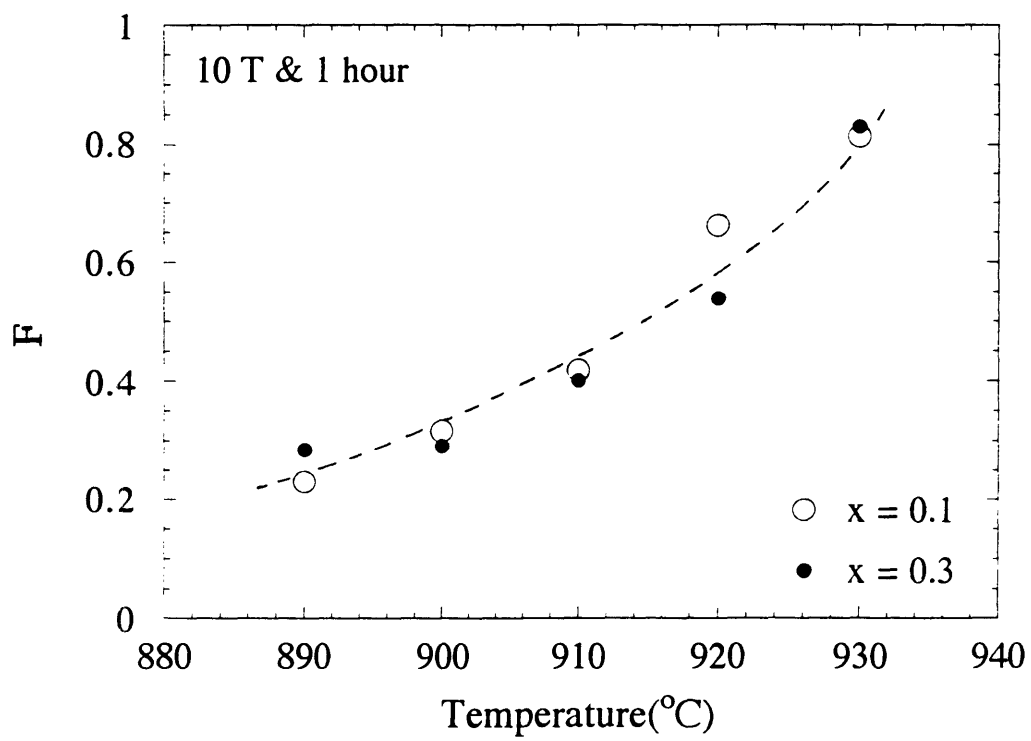
Fig. 4-2-3: Temperature dependence of the F factor with $H_\alpha = 10$ T

and t = 1 hour for different liquid phase content, i.e. x = 0.1

and 0.3.

It is known that pure $Bi_2Sr_2CaCu_2O_8$ melts at 880°C and the melting point of $Bi_2Sr_2Ca_{0.9}Ho_{0.1}Cu_2O_8$ is around 930°C. When the mixture of pure $Bi_2Sr_2CaCu_2O_8$ and $Bi_2Sr_2Ca_{0.9}Ho_{0.1}Cu_2O_8$ was annealed above 880°C, $Bi_2Sr_2CaCu_2O_8$ will melt but $Bi_2Sr_2Ca_{0.9}Ho_{0.1}Cu_2O_8$ will be in the solid state. Because the time at temperature is short, only from 15 minutes to 1 hour, it is reasonable to neglect the inter-diffusion or homogenized process in this system. Thus the grains of $Bi_2Sr_2Ca_{0.9}Ho_{0.1}Cu_2O_8$ will be rotated by the 10 T magnetic field so that the c - axis $//H_\alpha$ direction in the liquid phase. The viscosity of the liquid phase decreases with increasing temperature, thus the higher the temperature, the easier it is for the grains to be rotated by the 10 T magnetic field. As seen in Fig. 4-2-3, the F factor increases with increasing temperature T_a under a 10 T magnetic field for only 1 hour. For this case, the temperature dominates the texture development process under a 10 T magnetic field. For fixed temperature, the difference between different liquid phase content is small. This fact indicates that the grains can be rotated by a high magnetic field during a short period of time when a small amount of liquid phase exists at an elevated temperature.

4.2.3: Texture development dependence on the magnetic field H_α.

X- ray diffraction patterns of the samples with x = 0.1, which were annealed at 920°C for 1 hour under a 0 T and 10 T annealing magnetic field, are shown in Fig. 4-2-4(a) and (b), respectively. Under 0 T magnetic field, the X - ray diffraction pattern shows strong (103), (105), (107) and (110) peaks. The F factor is low, i.e. F = 0.23, but not equal to zero. This low degree of texture was introduced by the mechanical deformation when
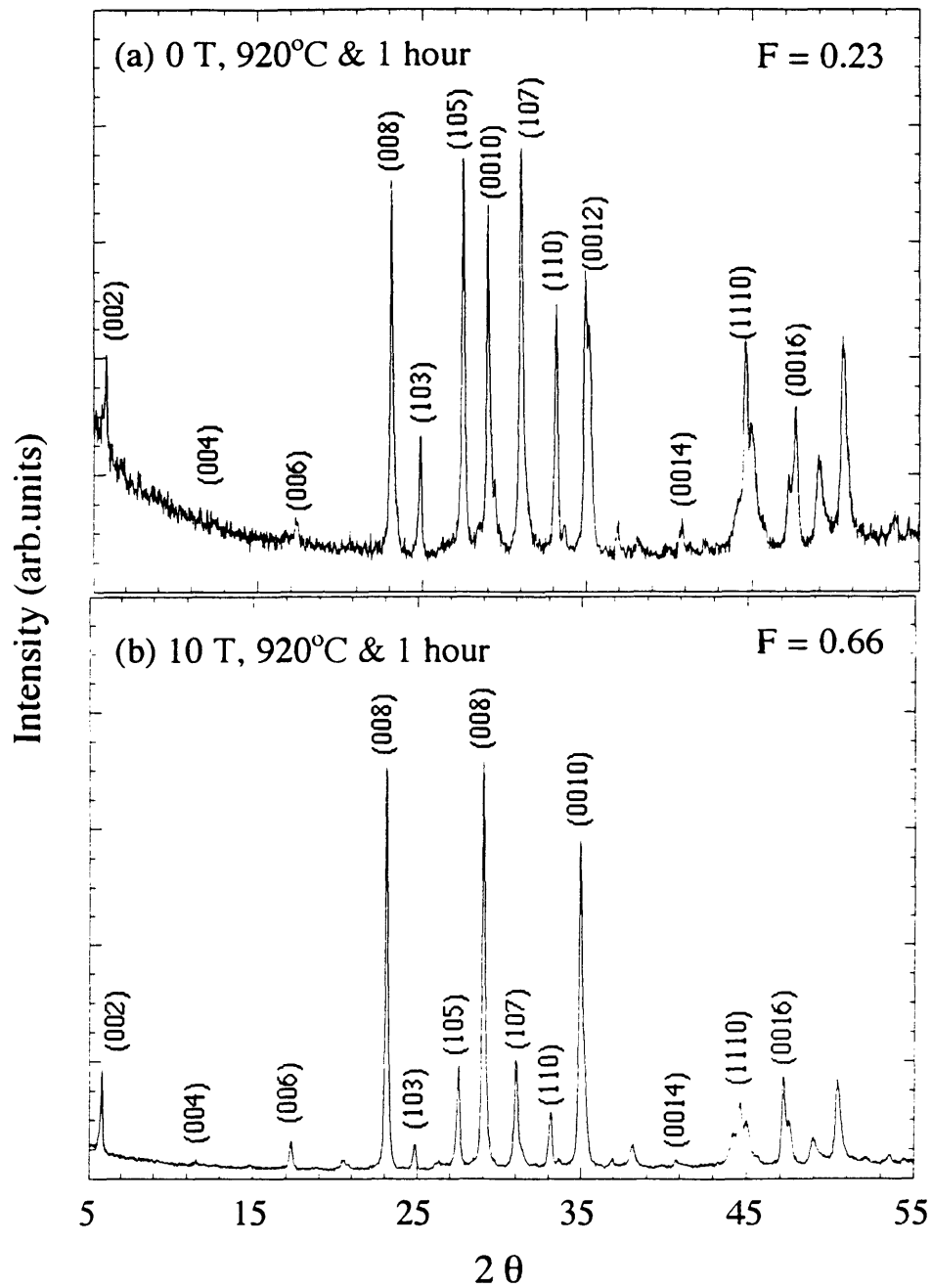
Fig. 4-2-4: X - ray diffraction patterns of samples with x = 0.1 polished along transverse direction of annealing magnetic field with T = 920°C and t = 1 hour. (a) H_α = 0 T and (b) H_α = 10 T.

Fig. 4-2-5:   SEM images of polished cross section of samples with x =

0.1 for T = 920°C and t = 1 hour. (a) $H_\alpha = 0$ T and (b) $H_\alpha = 10$

T.
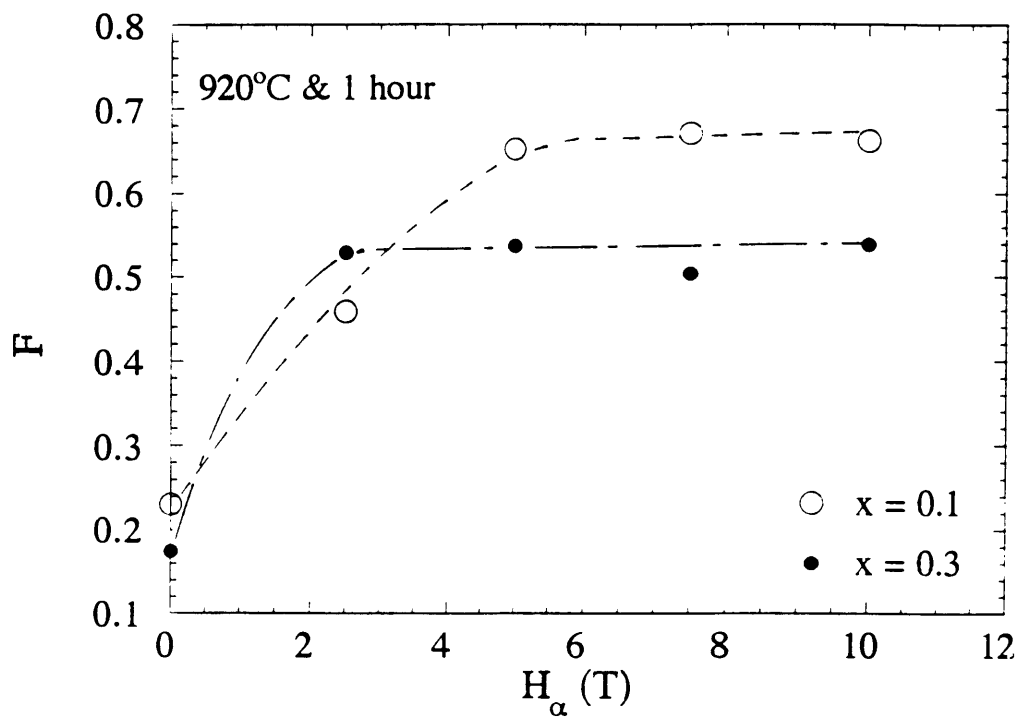
Fig. 4-2-6:   Magnetic field dependence of the F factor with T = 920°C and t = 1

hour for different liquid phase content, i.e. x = 0.1and 0.3.

the sample was pressed into a pellet. When the magnetic field is increased to 10 T, the X - ray diffraction pattern shows very strong (00ℓ) peaks and very weak (103), (105), (107) and (110) peaks. For this case, the F factor increases to 0.66. Thus for the same thermal sequence, i.e. $T_a = 920^oC$ and $t = 1$ hour, the textured structure can be introduced by application of a 10 T magnetic field during high temperature processing. The change in the grain orientation by application of a 10 T magnetic field can be clearly seen from the SEM images of the samples which were annealed at 920^oC for 1 hour under a 0 T and 10 T magnetic field (see Fig. 4-2-5(a) and (b)). When the magnetic field H_α increase from 0 T to 10 T, the grains of the samples were rotated so they became nearly parallel to each other.

The relation between the texture development and the magnetic field H_α for x = 0.1 and 0.3 is shown in Fig. 4-2-6. The F factor increases with increasing magnetic field H_α for fixed liquid phase content x. For fixed magnetic field, the F factor also depends on the liquid phase content x. For the sample with x = 0.1, the F vs H_α curve saturates around 5 T and for the sample with x = 0.3 the curve saturates around 2 T. Beyond the saturation point, the F factor of the sample with x = 0.1 is larger than that of the sample with x = 0.3. This means that if we want to texture the material under a lower magnetic field, more liquid phase should be present in the sample. If we want to improve texture with a resulting high F factor, less liquid should be present and a higher magnetic field should be applied. For x = 0.1 there is 10 percent liquid phase in the material and the interaction between the grains is strong, a higher magnetic field is required to rotate the grains. Thus the saturation field is higher. But due to the lower percentage of liquid phase for x = 0.1, the 860^oC zero field process was diffusion controlled growth and the

atoms in the small amount of 'liquid phase' join the textured grains to form the superconducting 2212 phase. For x = 0.1, the annealing process did not influence the well textured structure very much and a high degree of texture was maintained. For x = 0.3, there is more liquid phase in the material and the interaction between the grains is weaker. Thus only a weak magnetic field is required to rotate the grains and the saturation field shifts to a lower value. More liquid in the material also reduces the degree of the texture when the sample was annealed at 860°C in zero field. For x = 0.3, 30% 'liquid phase' will have more chance to nucleate and grow randomly in a zero field. This random growth will reduce the overall degree of the texture of the sample and the F factor decrease with increasing liquid phase content. More details on the F dependence of liquid phase content will be discussed in section (d).

4.2.4: Texture development dependence on the time t.

X - ray diffraction patterns of the samples with x = 0.1, which were annealed under a 10 T magnetic field at T = 920°C for t = 15 minute and 2 hours, are shown in the Fig. 4-2-7 (a) and (b). When the time increases from 15 minutes to 2 hour, the intensity of (00ℓ) peaks increases and F factor increases from 0.48 to 0.72. Increasing the time not only increases the degree of the texture, but also increases the density of the sample. This effect can be clearly seen in Fig. 4-2-8(a) and (b). We plot the F factor as a function of time for different liquid phase content x = 0.1 and 0.3 in Fig. 4-2-9. For constant x, the F factor increases with increasing time; for fixed time the F factor depends on the liquid phase content. At 920°C under 10 T magnetic field, the F factor saturates at 1.
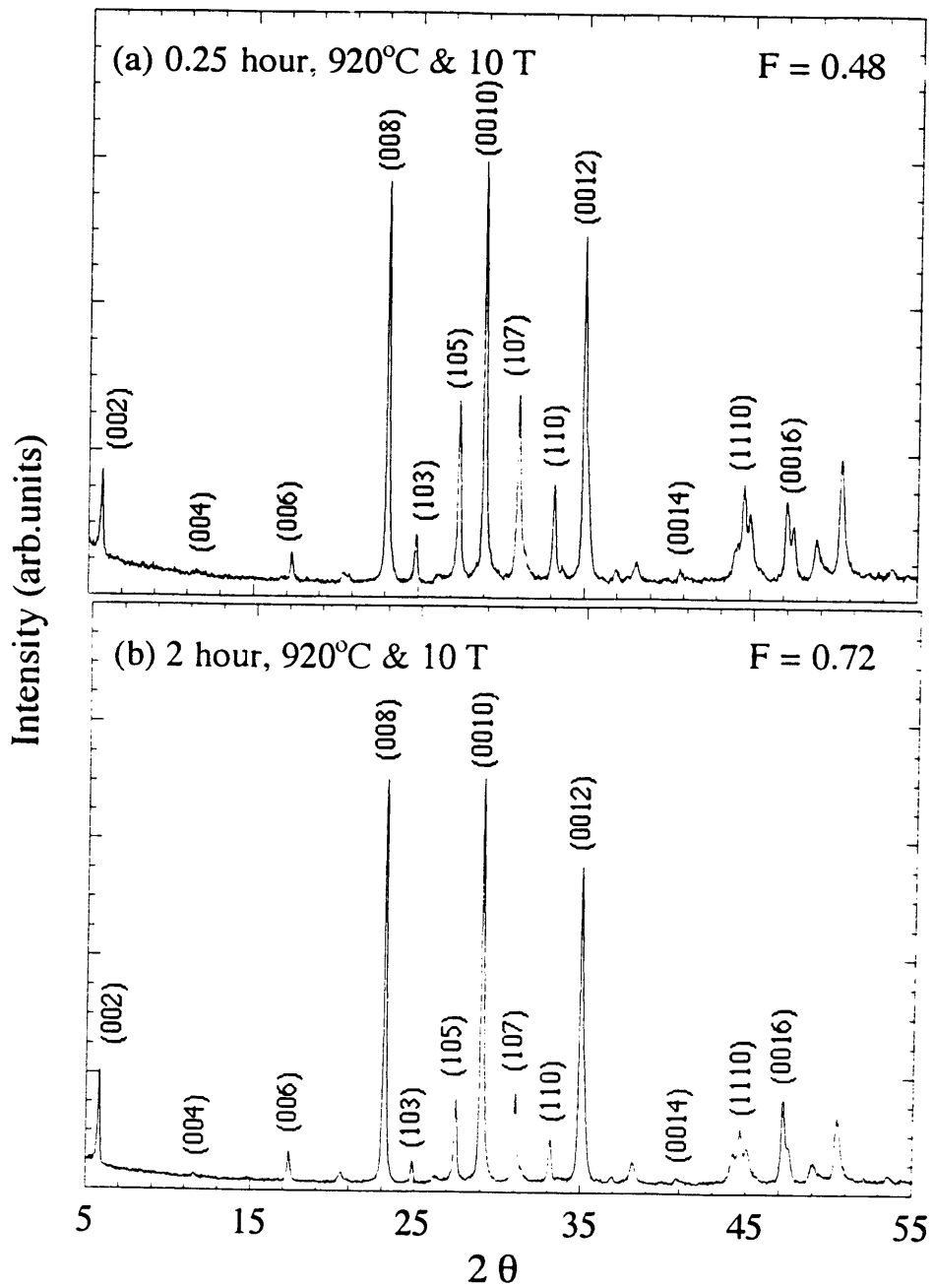
Fig. 4-2-7: X - ray diffraction patterns of samples with x = 0.1 polished along transverse direction of annealing magnetic field with T = 920°C and H_α = 10 T. (a) t = 0.25 hour and (b) t = 2 hour.
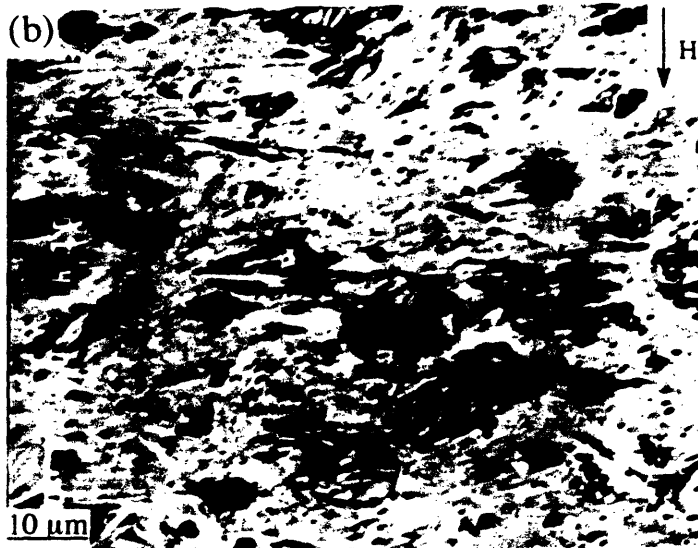
Fig. 4-2-8:   SEM images of polished cross section of samples with x =

0.1 for T = 920°C and H_α = 10 T. (a) t = 0.25 hour and (b) t =

2 hour.
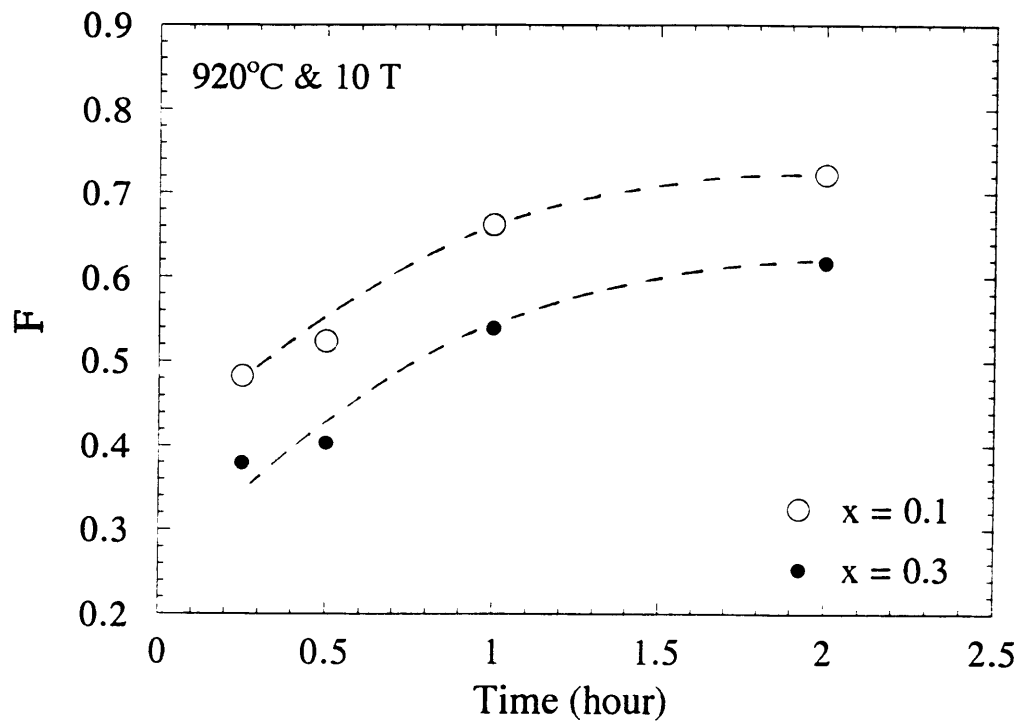
Fig. 4-2-9:   Time dependence of the F factor with T = 920°C and H_α = 10 T for different liquid phase content, i.e. x = 0.1 and 0.3.

hour. This means that the texture development process is a very fast process under a high magnetic field. Thus if a material were annealed properly under a high magnetic field, the pre - texturing process could be achieved in a very short period of time. This will dramatically reduce the fabrication time for superconducting tape. We will discuss the details of this x dependence in the next section.

4.2.5: Texture development dependence on the liquid phase content x.

X - ray diffraction patterns of the samples which were annealed under 10 T magnetic field at T_a = 920°C for liquid phase content x = 0.1 and 0.4 are shown in Fig. 4-2-10. It can be clearly seen that the degree of texture depends on the liquid phase content with T_a = 920°C, H_α = 10 T and t = 1 hour. For this case, the sample with x = 0.1 shows a higher degree of texture than that of the sample with x = 0.4. This fact tells us that only 10 percent liquid phase is required to induce texture via rotating grains under a high magnetic field. If there is too much liquid phase, the degree of texture will be reduced by the nucleation and growth of the glass phase under zero field at 860°C.

SEM images of three pairs of samples with different liquid phase content are shown in Fig. 4-2-11. In Fig. 4-2-11(a) and (b), the samples were annealed at 890°C under a 10 T magnetic field for 1 hour, (a) x = 0.0 and (b) x = 0.3. At this temperature, $Bi_2Sr_2CaCu_2O_8$ is a liquid phase and $Bi_2Sr_2Ca_{0.9}Ho_{0.1}Cu_2O_8$ is a solid phase. For x = 0.0, there is no liquid phase in the sample, the 10 T magnetic field can not overcome the interaction between the grains and introduce grain alignment. For x = 0.3, there is a liquid phase due to the melting of $Bi_2Sr_2CaCu_2O_8$, thus the $Bi_2Sr_2Ca_{0.9}Ho_{0.1}Cu_2O_8$ grains are rotated by the high magnetic field toward c - axis // H_α direction and the

grains are aligned. The liquid phase is not only responsible for the grain orientation in a high magnetic field, but also responsible for an increase in density. This fact can be clearly seen in Fig. 4-2-11 (a) and (b). In Fig. 4-2-11 (c) and (d), the samples with x = 0.0 and 0.3 were annealed at 920°C under a 10 T magnetic field for 15 minutes. More liquid phase increases the density of the samples faster than less liquid phase. In Fig. 4-2-11(e) and (f), the samples were processed at T_a = 920°C under a 2.5 T magnetic field for 1 hour, (e) x = 0 and (f) x = 0.3. This temperature is very close to the melting point of $Bi_2Sr_2Ca_{0.9}Ho_{0.1}Cu_2O_8$ and above the melting point of $Bi_2Sr_2CaCu_2O_8$. For x = 0.0, there is less liquid phase and the degree of texture is low. For x = 0.3, there is more liquid phase and the degree of texture and the density is high even under a lower magnetic field, i.e. H_α = 2.5 T.

We plot the F factor as a function of liquid phase content x for different conditions in Fig. 4-2-12(a), (b) and (c). In Fig. 4-2-12(a), the samples were processed at 890°C and 920°C under a 10 T magnetic field for 1 hour. For the higher temperature, i.e. T_a = 920°C, when x = 0.1 the F factor reaches the maximum then decreases with increasing liquid phase content. This means that if we want to introduce a textured structure under a high magnetic field at higher temperature, only 10 percent liquid phase is required. For the lower temperature, i.e. T_a = 890°C, the F factor increases with increasing liquid phase content. Thus if we want to introduce a textured structure under a high magnetic field at a lower temperature, more liquid phase is required. But the F factor of the samples with different x which were processed at higher temperatures is always larger than that of the samples with different x which were processed at a lower temperature. At lower processing temperatures the interaction between the grains is strong, thus more liquid

phase must be present to reduce the interaction and increase the degree of texture. If the magnetic field H_α or the time t at temperatures is reduced, the F factor for all samples will be reduced.

In Fig. 4-2-12(b), the samples were processed at 920°C under a 10 T magnetic field for 0.5 and 1 hour. The degree of the texture is higher for t = 1 hour than for t = 0.5 hour, the F factor reaches a maximum at x = 0.1 and then decreases with increasing liquid phase content x. Recalling the F vs time curve in the previous section, the F factor saturates at t = 1 hour, thus for different liquid phase content a maximum one hour is required to yield a well textured structure under a 10 T magnetic field. It is also clear that if the temperature T_a or magnetic field H_α was reduced, the saturation time will increase beyond 1 hour.

In Fig. 4-2-12(c), the samples were annealed at 920°C for 1 hour under different magnetic fields H_α = 2.5 T and 10 T. For H_α = 10 T, the F factor increases with increasing liquid phase content x and reaches a maximum at x = 0.1, then decreases with increasing liquid phase content. For H_α = 2.5 T, the F factor always increases with increasing liquid phase content. Thus if we want to texture the sample under a higher magnetic field, less liquid phase is required. If we want to texture the sample under a lower magnetic field, more liquid is required to reduce the interaction between the grains. If the temperature T_a or time t were reduced, the overall F factor would be decreased. From the relationships of F with the magnetic field, the temperature T_a and time, we can choose the processing parameters properly and texture the samples according to different experimental conditions or the final requirements for sample.
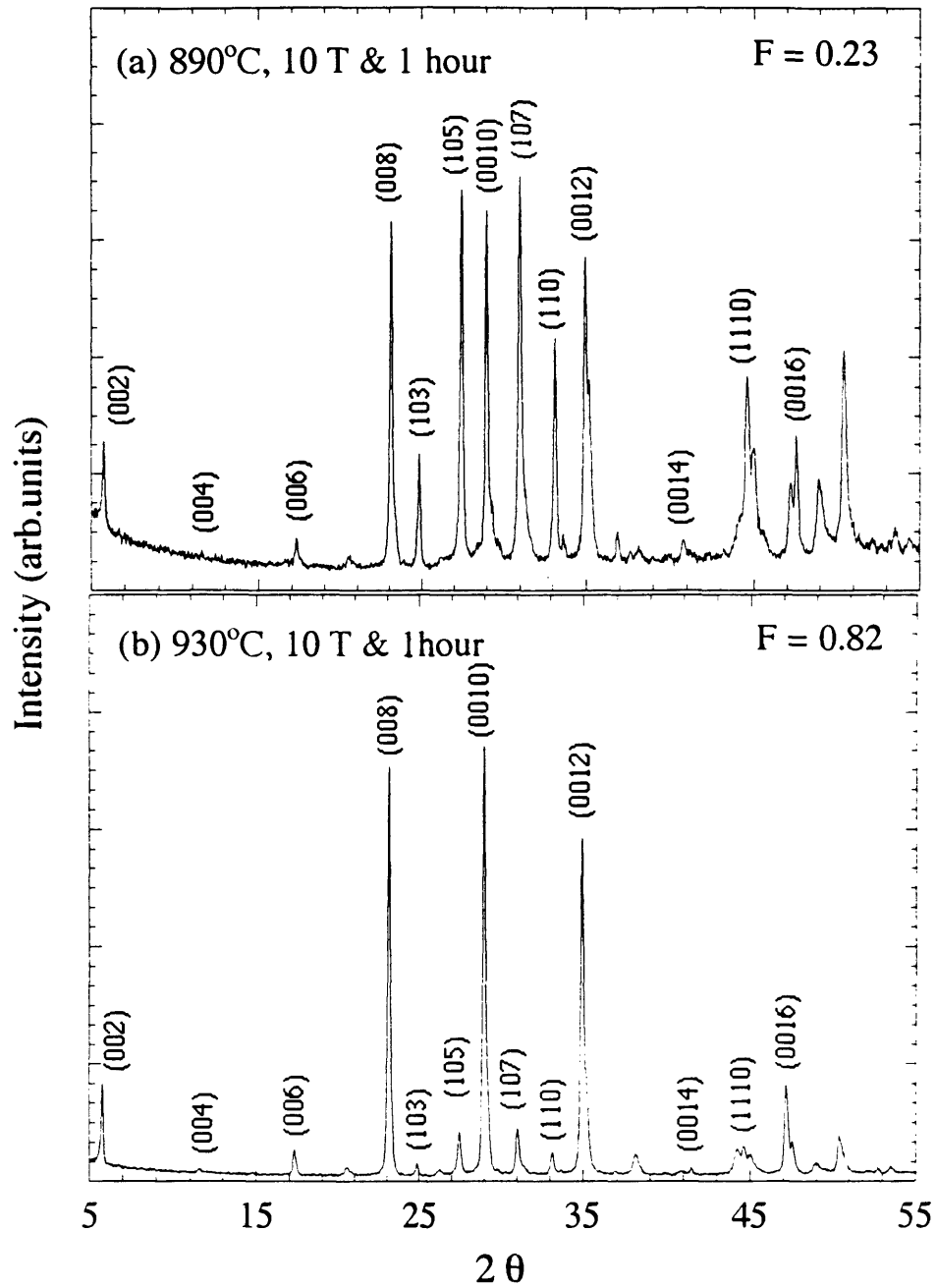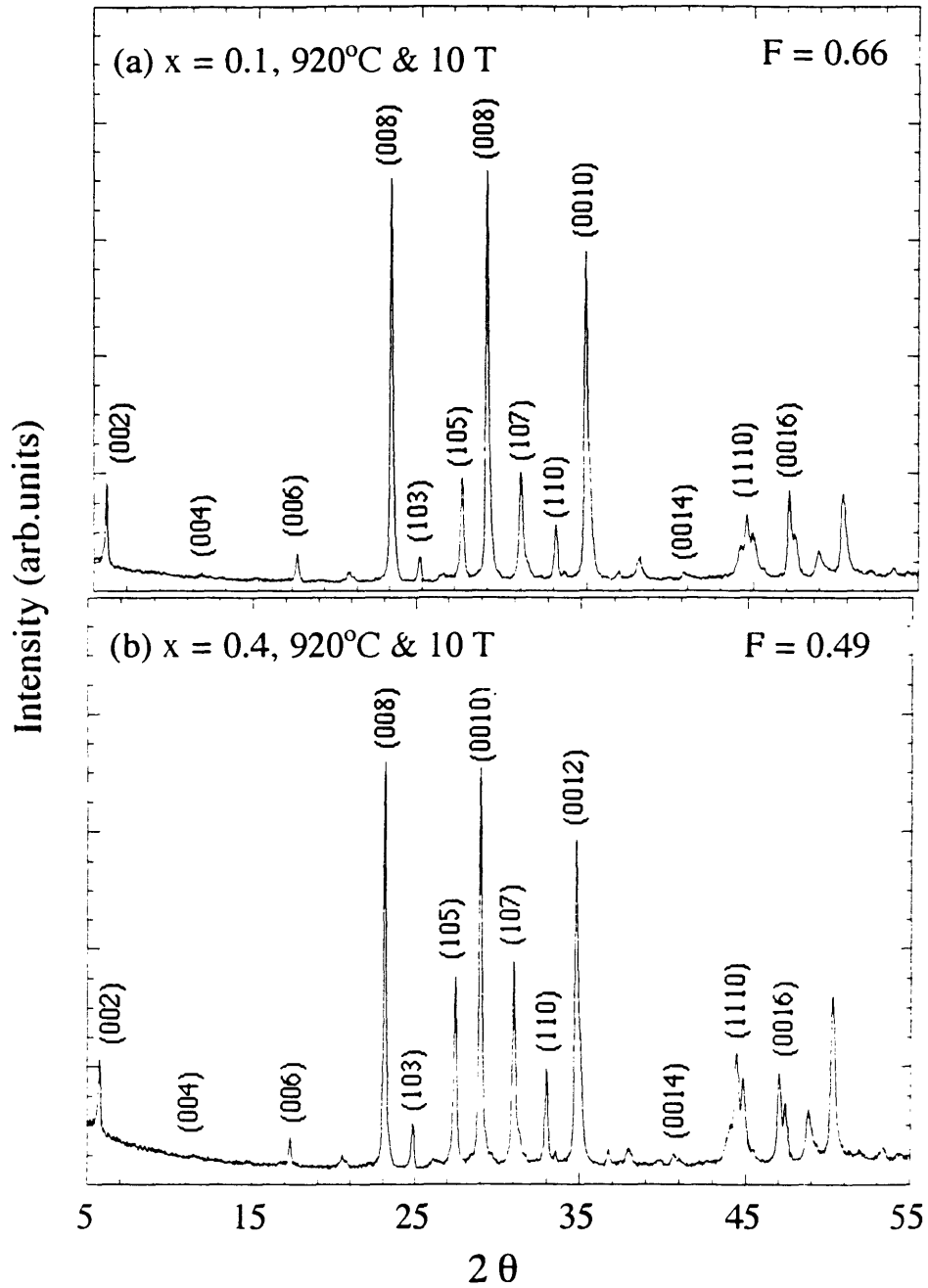
Fig. 4-2-10: X - ray diffraction patterns of samples polished along transverse direction of annealing magnetic field with T = 920°C, H_α = 10 T and t = 1 hour. (a) x = 0.1 and (b) x = 0.4.
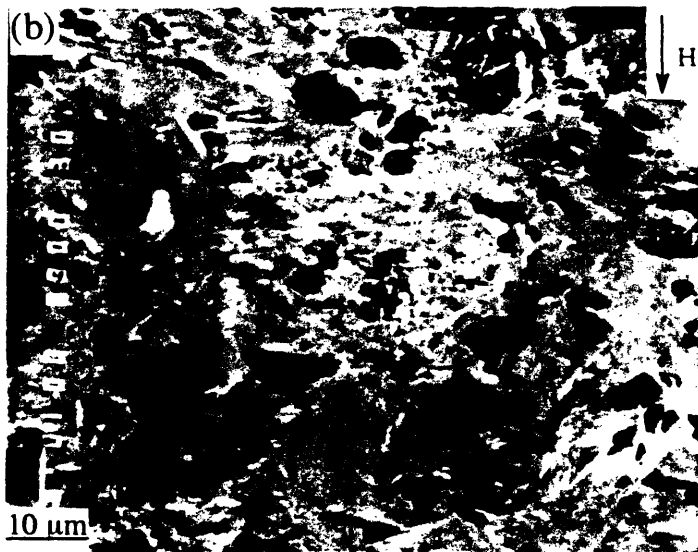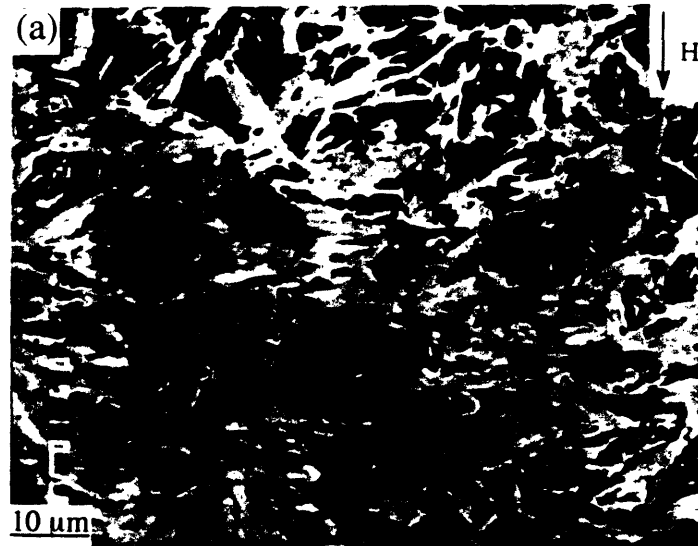
Fig. 4-2-11: SEM images of polished cross section of samples, with T = 920°C, H_α = 10 T and t = 1 hour (a) x = 0.0 and (b) x = 0.3.
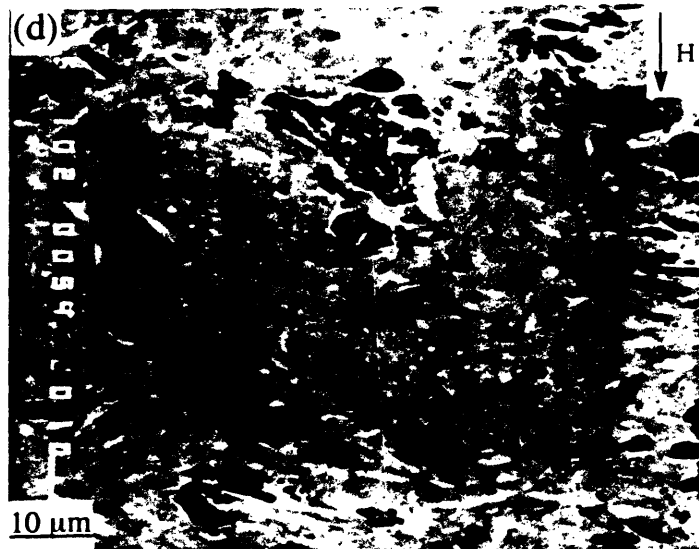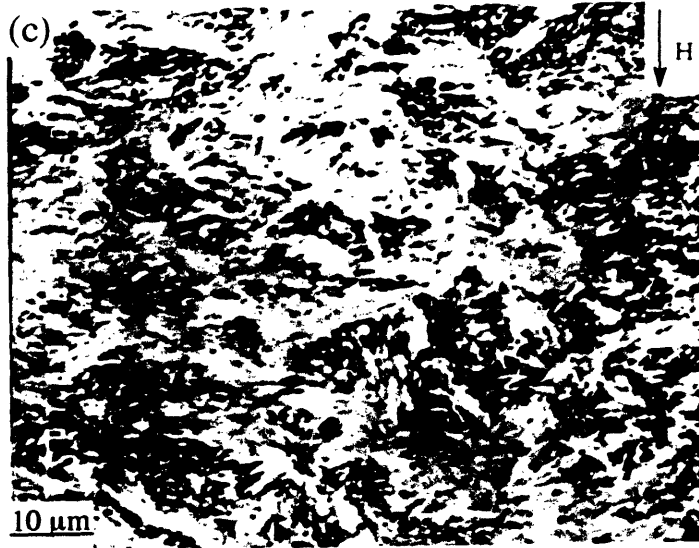
Fig. 4-2-11:   SEM images of polished cross section of samples,

with T = 920°C, H_α = 10 T and t = 0.25 hour (c) x = 0.0 and

(d) x = 0.3.
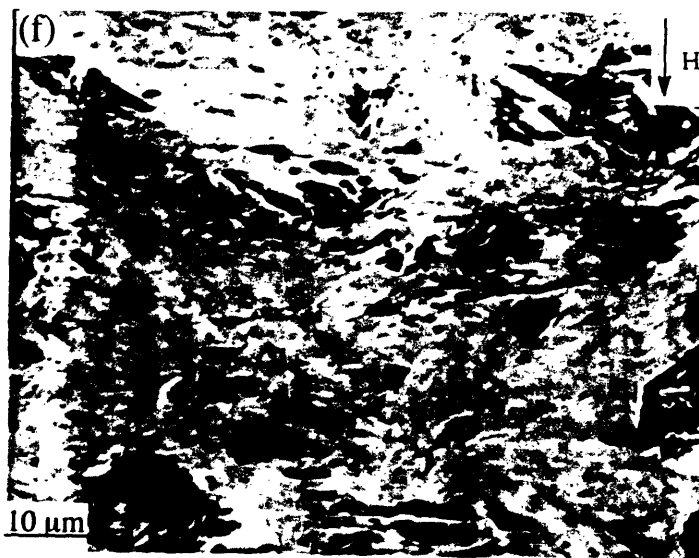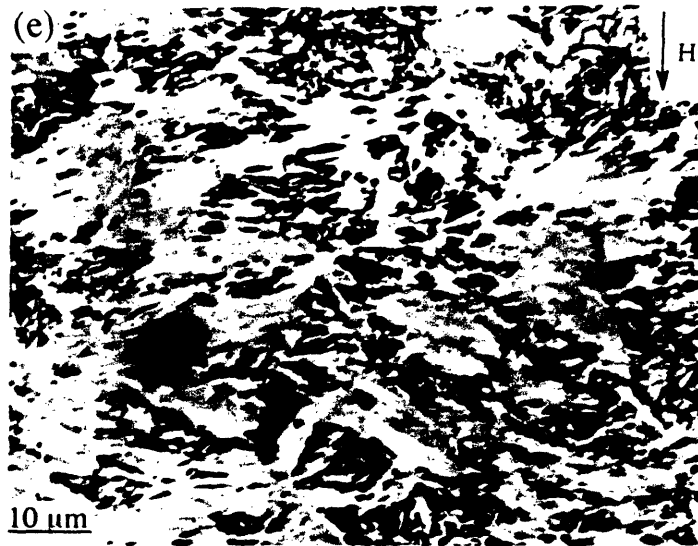
Fig. 4-2-11:   SEM images of polished cross section of samples, with T = 920°C,

H_α = 2.5 T and t = 1 hour (e) x = 0.0 and (f) x = 0.3.
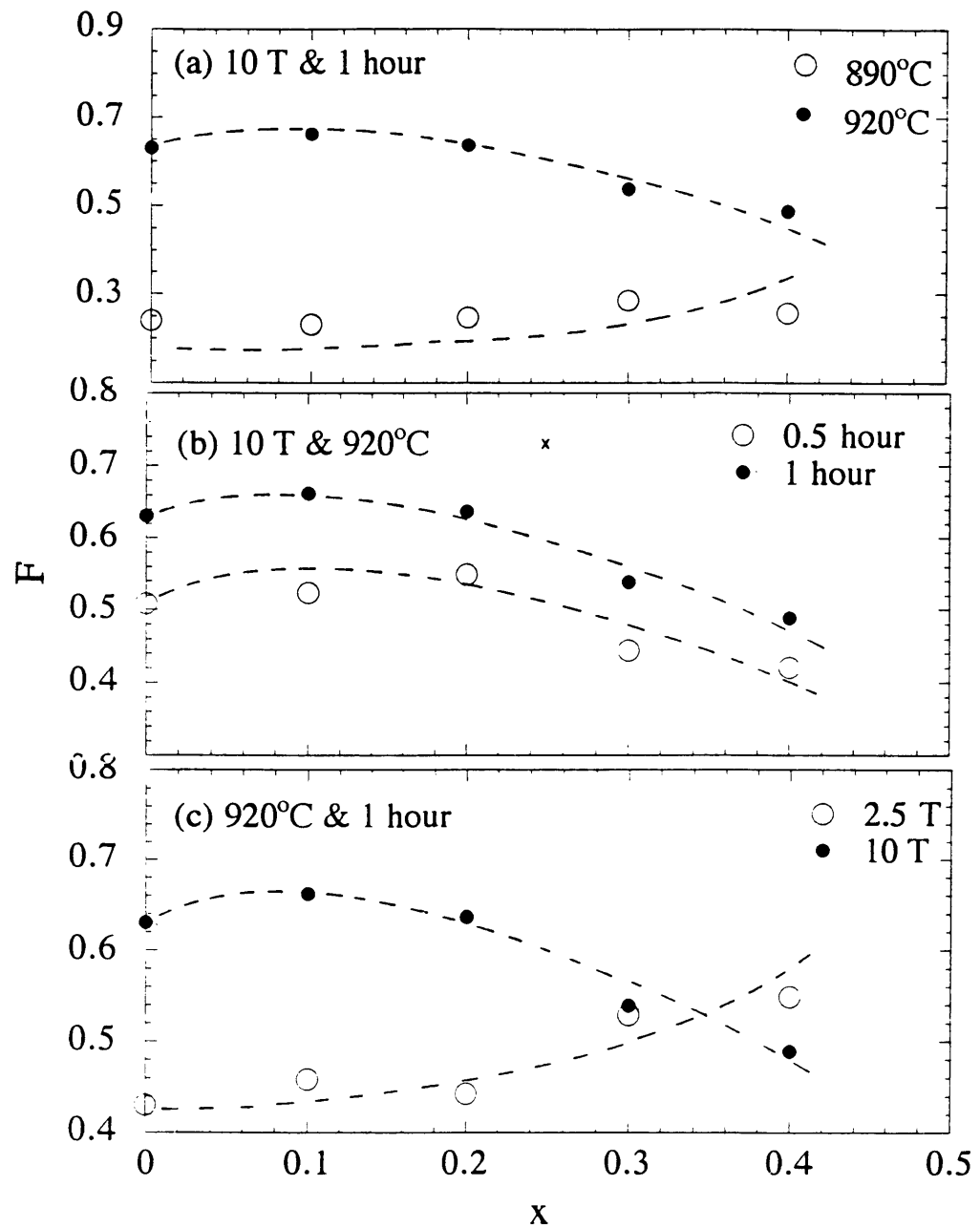
Fig. 4-2-12: Liquid phase content x dependence of the F factor. (a) $H_\alpha =$ 10 T and t = 1 hour for T = 890°C and 920°C, (b) H_α = 10 T and T = 920°C for t = 0.5 hour and 1 hour, (c) T = 920°C and t = 1 hour for H_α = 2.5 and 10 T.

4.2.6: Superconductivity, magnetic anisotropy and transport critical current density.

The temperature dependence of the diamagnetic susceptibility of the sample which was processed at 920°C for 1 hour under 10 T is shown in Fig. 4-2-13. The samples were placed with H_α // H. The transition temperature T_c is about 90 K. This fact indicates that the magnetic field only rotates the grains to the c // H_α direction and does not influence the intrinsic superconducting properties of the sample. $Bi_2Sr_2CaCu_2O_8$ and $Bi_2Sr_2Ca_{0.9}Ho_{0.1}Cu_2O_8$ have almost the same T_c, thus the mixture does not alter the superconducting properties and a T_c = 90K were obtained.

The magnetic anisotropy factor $\eta = \Delta M(H_\alpha // H) / \Delta M(H_\alpha \perp H)$ is plotted as a function of measurement magnetic field in Fig. 4-2-14. The magnetic anisotropy factor η is larger for the H_α = 10 T sample than for the H_α = 0 T sample over all measurement magnetic fields. This result is similar to the results for the melt growth of $Bi_2Sr_2Ca_{0.9}Ho_{0.1}Cu_2O_8$ superconductors under a high magnetic field presented in the next chapter.

The transport critical current density is plotted as a function of the F factor in Fig. 4-2-15. For the open - circle data, the textured structure was introduced by increasing the magnetic field H_α. For the filled - circle data, the textured structure was introduced by increasing T_m under a 10 T magnetic
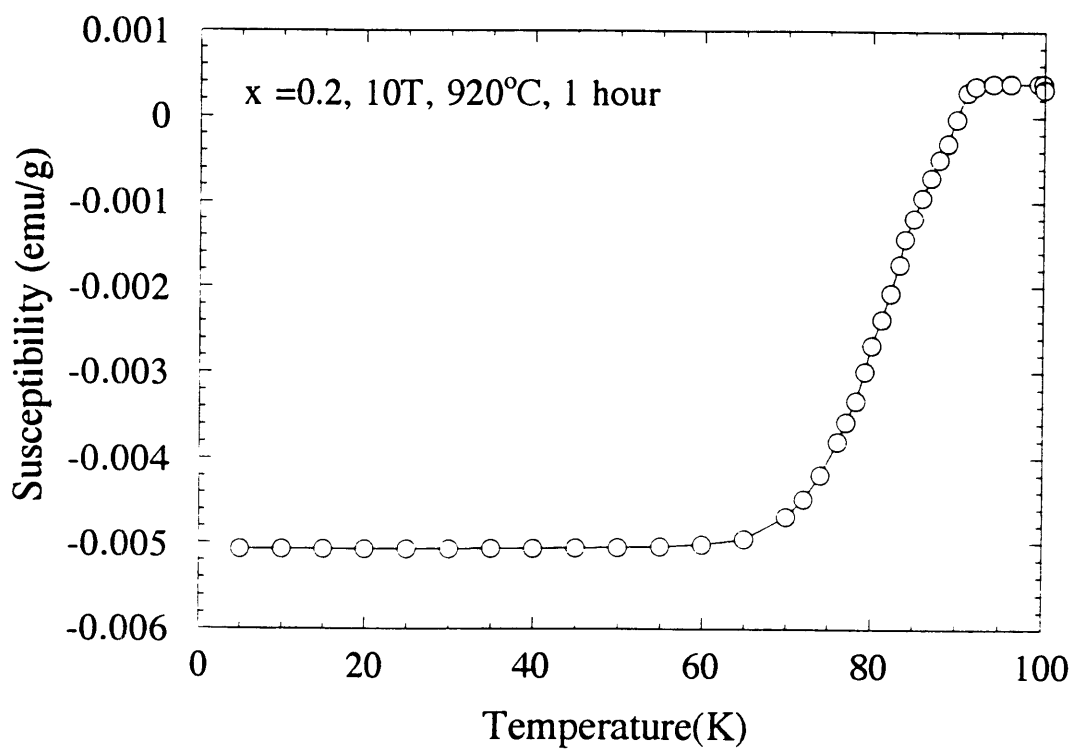
Fig. 4-2-13:   Temperature dependence of diamagnetic susceptibility of

sample with x = 0.2, H_α = 10 T, T = 920°C, and t = 1. The

sample was placed in H_α // H.
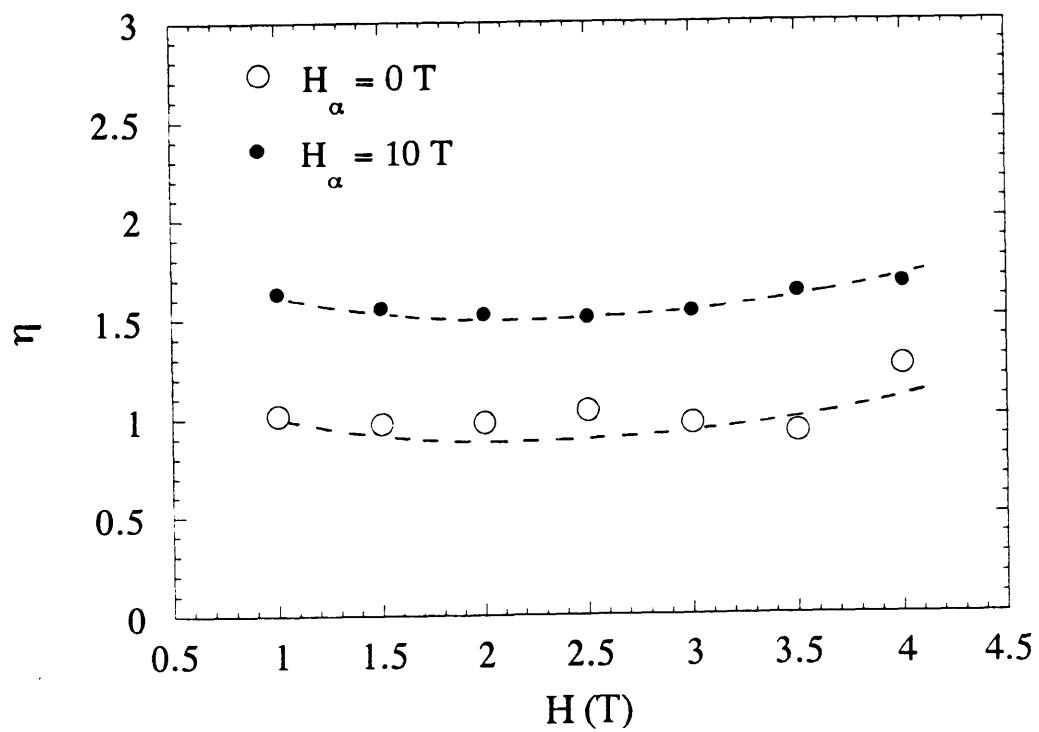
Fig. 4-2-14: Magnetic anisotropy factor $\eta = \Delta M(H_\alpha \mathbin{/\!/} H) / \Delta M(H_\alpha \perp H)$

dependence of measurement magnetic field H for $H_\alpha = 0$ T
and 10 T.
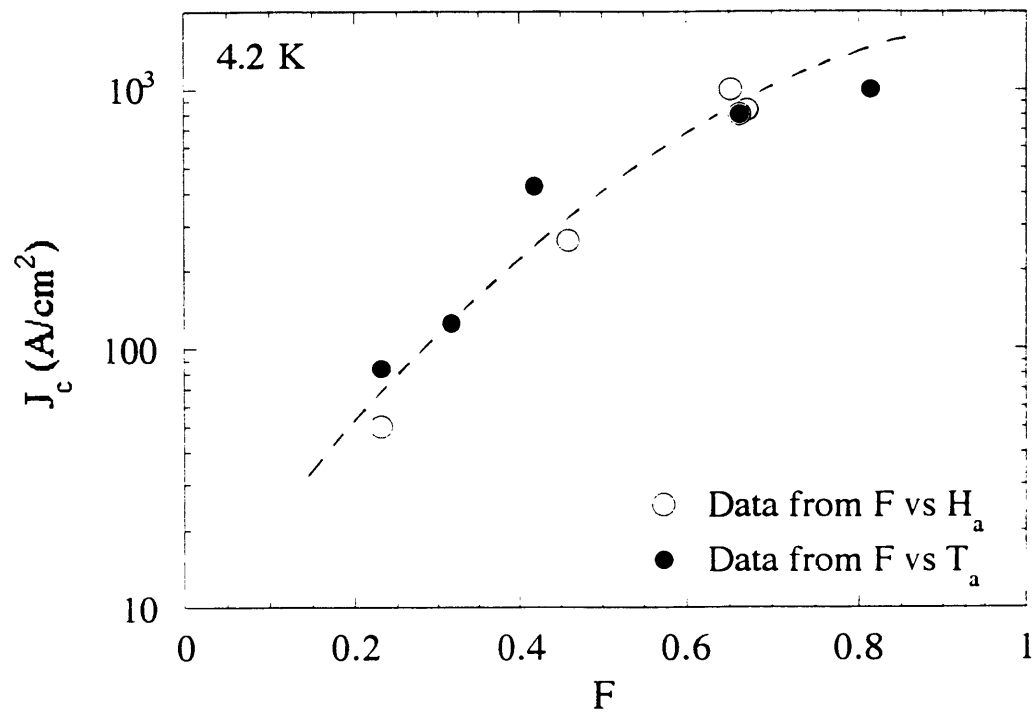
Fig. 4-2-15: Transport critical current density J_c at 4.2 K dependence of F factor.

field. For both cases, J_c increases with increasing F. But for the open - circle data, the thermal sequence is fixed ($T_a = 920^{\circ}C$, $H_\alpha = 10\ T$ and $t = 1$ hour) and the degree of the texture was improved by increasing the magnetic field H_α. For the filled - circle data, the magnetic field was fixed at 10 T, the degree of the texture was improved by increasing temperature T_a. For this case, log (J_c) also increases with increasing F factor. For both cases, the liquid phase content is x = 0.1. Even though the grains were textured by a high magnetic field, the contact between the grains is not improved. Increasing J_c requires an increase in the grain contact by, for instance, mechanical pressing along the H_α direction. Clearly this method can be used as a pre - texturing process before rolling in tape fabrication. The tape should first be annealed under a high magnetic field for a short period of time for texture development, then rolled to increase the connection between the grains. This pre - texturing processing under a high magnetic field provides a potential way to reduce the processing time for tape fabrication and increase the transport critical current density.

4.2.7: Conclusion

Bi$_2$Sr$_2$Ca$_{0.9}$Ho$_{0.1}$Cu$_2$O$_8$ superconductor was textured by rotating the grains in an elevated magnetic field in the present of a liquid phase. Texture development depends on temperature T_a, magnetic field H_α, processing time t and content of the liquid phase. The F factor increases with increasing magnetic field and the curve saturates at 2 - 5 T for different x content. By increasing T_a, the degree of texture increases under a high magnetic field for a fixed time. For a fixed liquid phase content x, the F factor also increases with increasing time, but for a fixed time the F factor depends on the liquid phase content x. The transport critical current density increase with increasing

degree of texture. Processing Bi - based materials under a high magnetic field provides a potential pre - texturing method for powder - in - tube technology for tape fabrication.

Chapter 5. Melt - Growth of High - T_c Superconductors Under an Elevated Magnetic Field

Section 5.1. Melt - growth of $Bi_2Sr_2(Ca,Ho)Cu_2O_8$ under an elevated magnetic field.

$Bi_2Sr_2Ca_{0.9}R_{0.1}Cu_2O_8$ (R = Y, Ho and Gd) superconductors were melt - grown under elevated magnetic fields. Texture development in these materials depends upon cooling rate, maximum processing temperature T_m, and magnetic field. A higher T_m is always desirable in obtaining a highly textured structure, and there is a trade off between the cooling rate and the magnetic field strength. Highly textured structures can be introduced either by a faster cooling rate under a stronger magnetic field, or by a lower cooling rate under a weaker magnetic field. The transport critical current density can be increased by improving both texture and connectivity between the grains. Processing Bi - based materials under a high magnetic field provides a potential way to increase transport critical current density.

5.1.1. Experimental Procedure

The starting materials were prepared by solid state reaction. Highly pure Bi_2O_3, $SrCO_3$, $CaCO_3$, Y_2O_3, Ho_2O_3, Gd_2O_3 and CuO are weighted according to the normal composition $Bi_2Sr_2Ca_{0.9}R_{0.1}Cu_2O_8$ with R = Y, Ho and Gd. The mixed powders were reacted at 820°C for 12 hours in air. Then the precursors were ground in an agate mortar and pestle, pressed into pellets and sintered at 880°C for 48 hours in air.   The pellets were re-ground and pressed into pellets again. Finally the pellets were melt - grown under elevated magnetic fields following the thermal sequence in Fig. 5-1-1.

5.1.2: Texture development dependence on cooling rate under a high magnetic field.

X - ray diffraction patterns of the samples with two different cooling rates at T_m = 950°C and H_α = 10 T are shown in Figs. 5-1-2(a) and (b). When the sample was cooled under a 10 T magnetic field with a slow cooling rate, i.e. $\mathcal{R}$ = 3°C/hr, X- ray diffraction patterns show very strong (00ℓ) peaks and very weak (103), (105), (107) and (110) peaks. For this case, the F factor reaches 0.80. When the sample was cooled under a 10 T magnetic field with a fast cooling rate, i.e. $\mathcal{R}$ =12°C/hr, the intensity of (103), (105), (107) and (110) peaks increases and the F factor decreases to 0.48. From a microstructural point of view, the sample with the low cooling rate not only has a higher degree of texture, but also has larger grains and better apparent connectivity between the grains (see Figs. 5-1-3(a) and (b)). The cooling rate dependence of the structural anisotropy factor F is plotted in Fig. 5-1- 4. The F factor decreases with increasing cooling rate under a 10 T magnetic field. Even when the cooling rate reaches 60°C / hr, the F factor is still larger than 0.4 . For T_m = 950°C, even under a 10 T magnetic field, a well textured structure can only be introduced with a slow cooling rate, thereby requiring a lengthy processing time.

From a processing point of view, a textured structure should be fabricated as fast as possible, i.e. reducing the processing time under a high magnetic field. There are two factors which can be adjusted to increase the degree of the texture [8] when the samples are processed under a high magnetic field. First, to increase the driving force ($\Delta E = \Delta\chi H^2 V_c/2$) for texture development by increasing the volume of the grains. In order to increase the grain size, a small under cooling ΔT and low nucleation rate is required. In
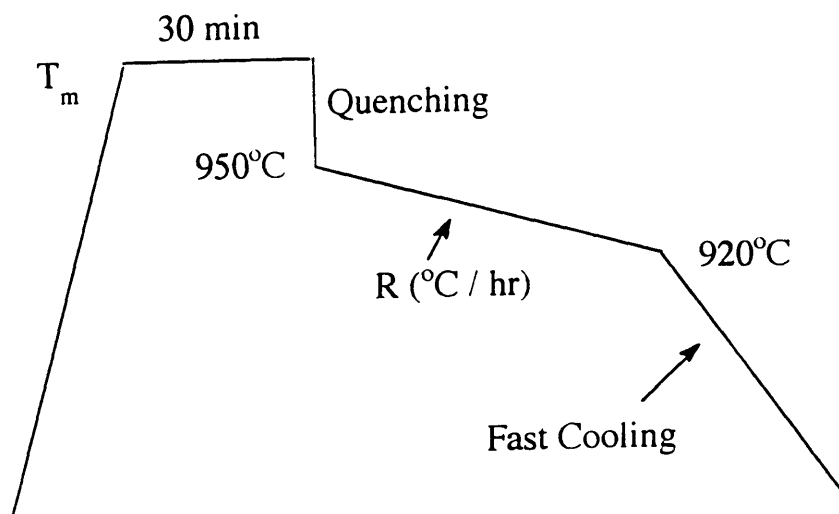
Fig. 5-1-1: Thermal sequence of melt - growth of $Bi_2Sr_2Ca_{0.9}Ho_{0.1}Cu_2O_y$ under elevated magnetic field.
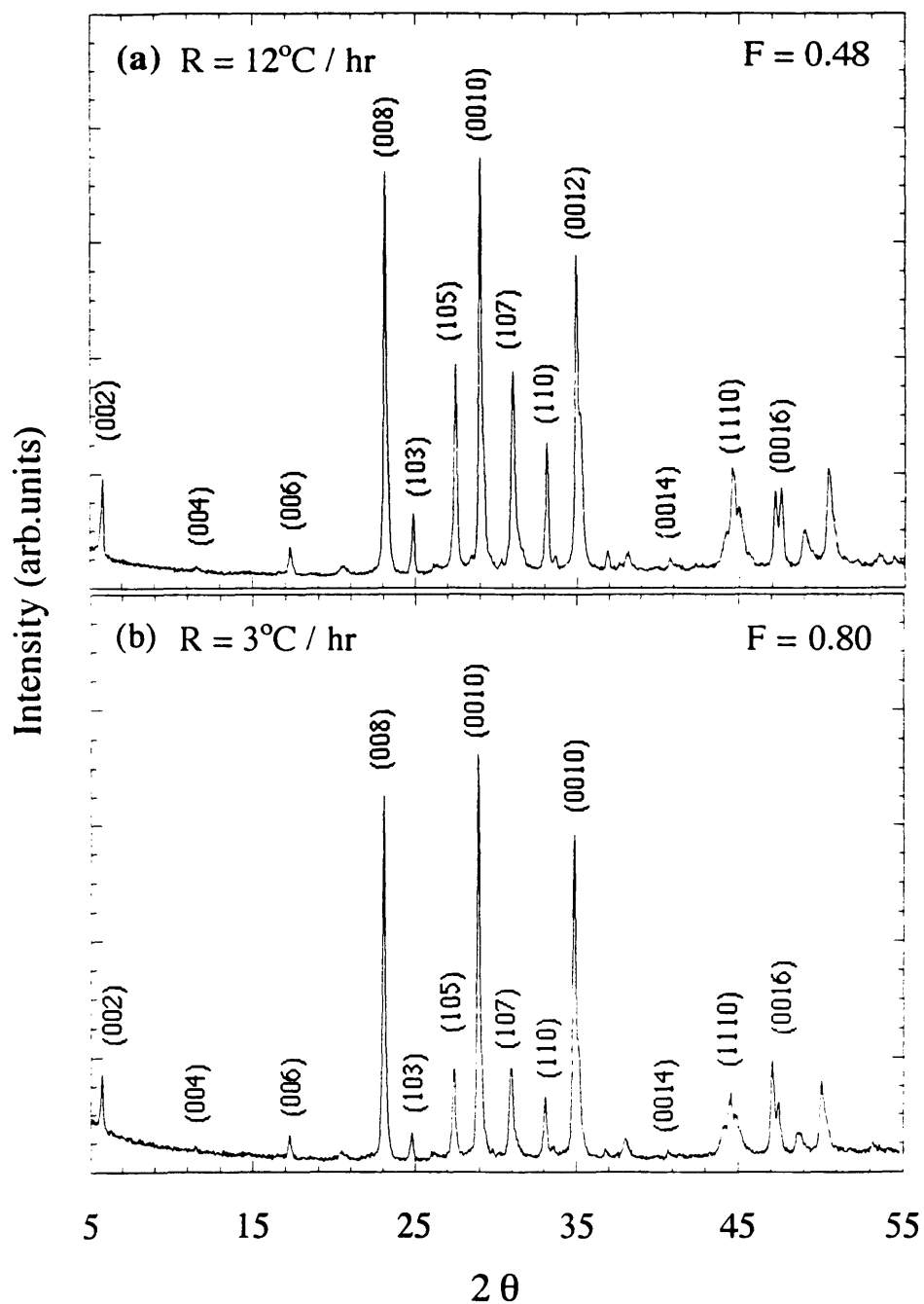
Fig. 5-1-2:   X - ray diffraction patterns of $Bi_2Sr_2Ca_{0.9}Ho_{0.1}Cu_2O_y$

polished along transverse direction of a magnetic field, with T_m

$= 950°C$ and $H_\alpha = 10$ T. (a) $\mathcal{R} = 12°C$ / hr and (b) $\mathcal{R} = 3°C$ / hr.
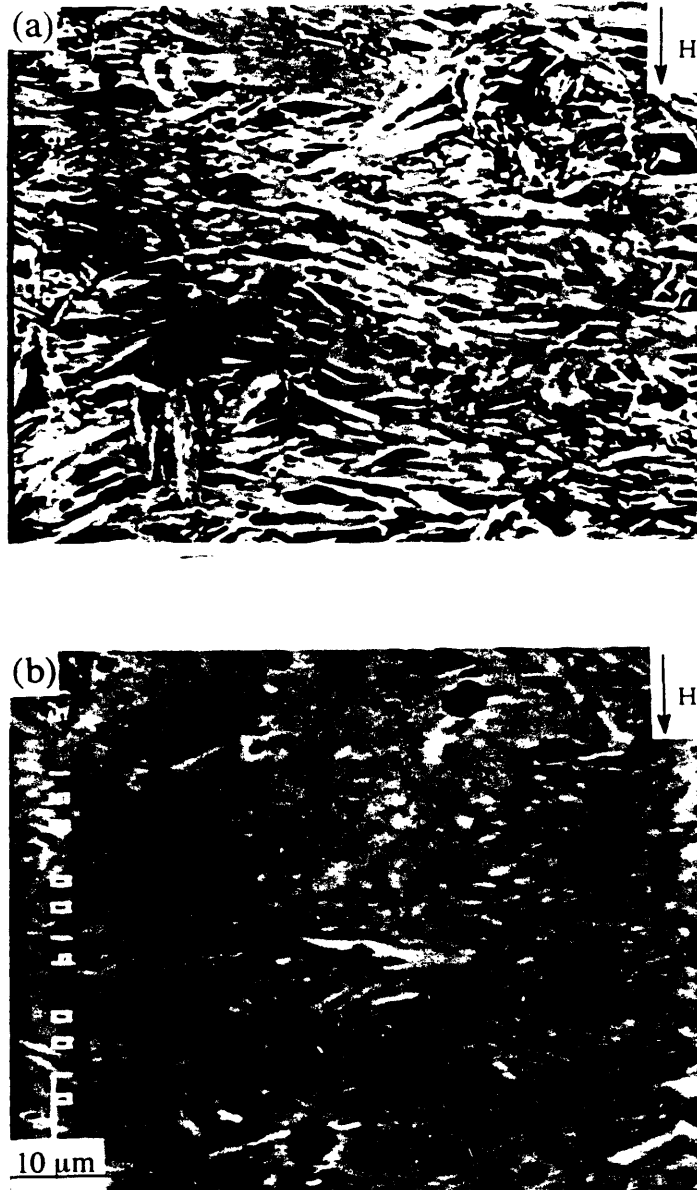
Fig. 5-1-3:   SEM images of polished cross section of $Bi_2Sr_2Ca_{0.9}Ho_{0.1}Cu_2O_y$

with $T_m = 950^oC$ and $H_\alpha = 10$ T, (a) $\mathcal{R} = 12^oC$ / hr and (b) $\mathcal{R} = 3^oC$ / hr.
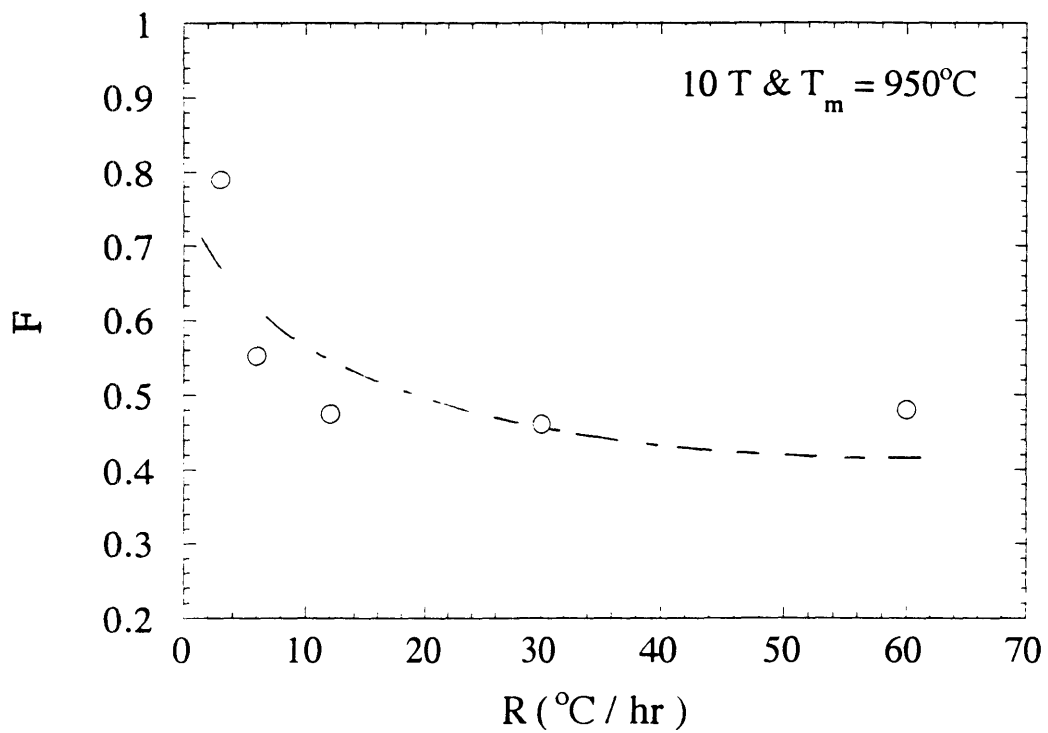
Fig. 5-1-4: F factor dependence of cooling rate for $T_m = 950^oC$ and $H_\alpha = 10$ T.

this case, it is impossible to increase the cooling rate and produce a highly textured structure quickly. Second, to reduce the interaction between the grains by creating more liquid phase. In this way, it is possible to reduce the processing time under a high magnetic field and obtain a highly textured structure. Thus our approach was to increase the processing temperature T_m to create more liquid phase and decrease the interaction between the grains, as discussed in the next section.

5.1.3: Texture development dependence on the maximum processing temperature T_m

X - ray diffraction patterns of samples with T_m = 950°C and 970°C are shown in the Figs. 5-1-5(a) and (b), respectively. Both samples were processed under a 10 T magnetic field and with a cooling rate of $\mathcal{R}$ = 30°C/hr. When T_m = 950°C, even though the (00ℓ) peaks are stronger than the (103), (105), (107) and (110) peaks, the degree of texture is still not very high, F = 0.46. When T_m increases to 970°C, the (00ℓ) peaks increase dramatically and the F factor increases to 0.84. The degree of texture increases with increasing maximum processing temperature T_m under the same magnetic field.

Increasing T_m not only produces a highly textured structure, but also increases the connection between the grains by creating more liquid phase. This fact can be seen from the SEM images of the cross section of the samples in Figs. 5-1-6(a) and (b). For the same degree of texture, the processing time has been reduced by a factor of 10 by increasing T_m from 950°C to 970°C under a 10 T magnetic field. The degree of texture increasing with increasing T_m also can be seen from the ΔM vs H curves in Fig. 5-1-7. When the sample was measured with H_α // H, the higher the degree of texture, the higher the ΔM
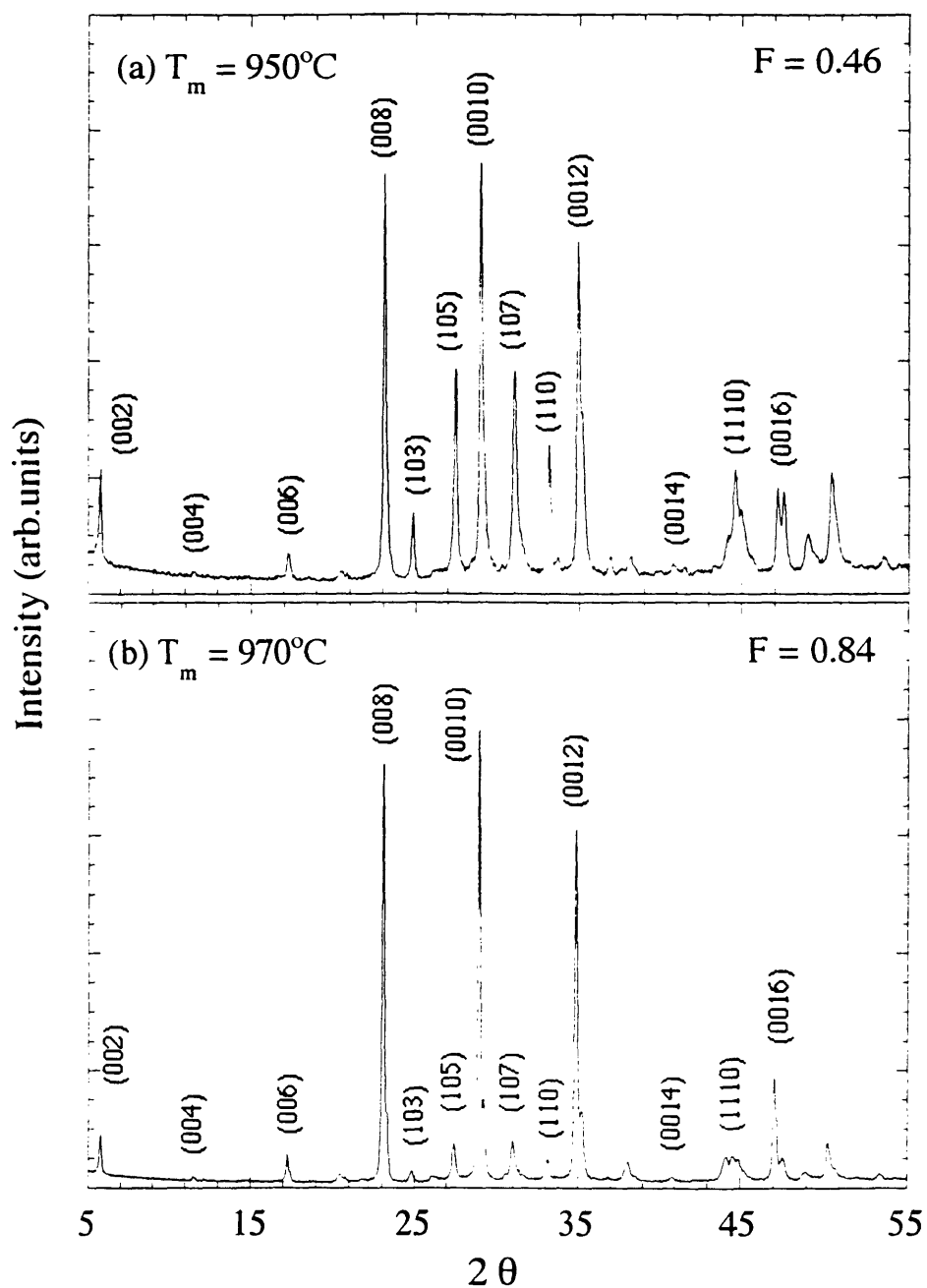
Fig. 5-1-5: X - ray diffraction patterns of $Bi_2Sr_2Ca_{0.9}Ho_{0.1}Cu_2O_y$

polished along transverse direction of magnetic field, with

cooling rate $\mathcal{R} = 30^oC$ / hr and $H_\alpha = 10\,T$, (a) $T_m = 950^oC$ and (b)

$T_m = 970^o$

Fig. 5-1-6:   SEM images of polished cross section of $Bi_2Sr_2Ca_{0.9}Ho_{0.1}Cu_2O_y$

with cooling rate $\mathcal{R} = 30^{\circ}C$ / hr and $H_\alpha = 10$ T, (a) $T_m = 950^{\circ}C$,

(b) $T_m = 970^{\circ}C$.
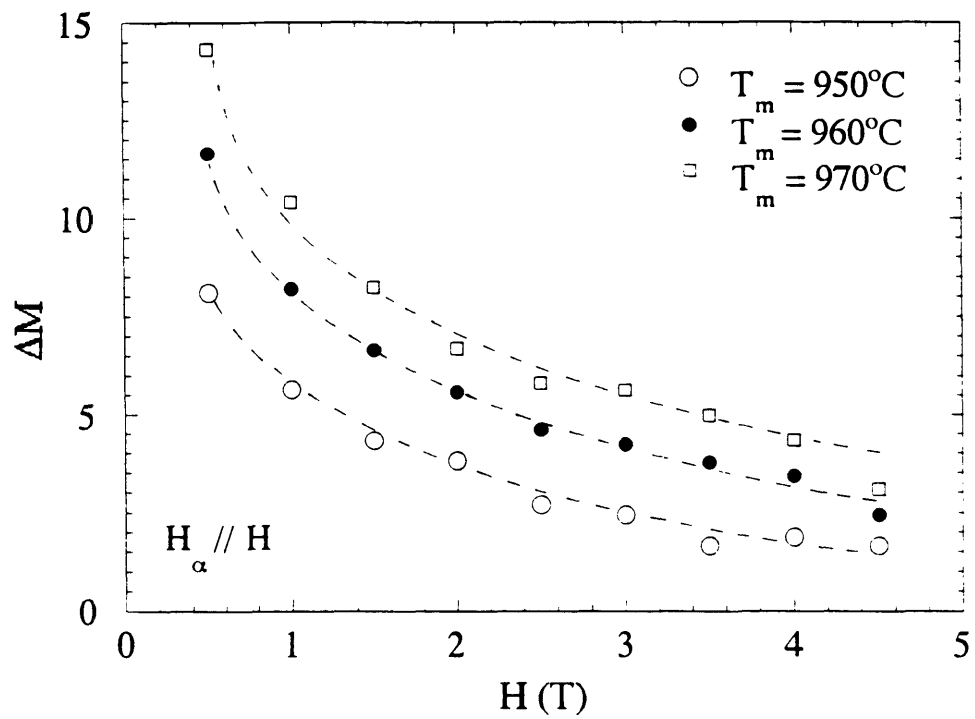
Fig. 5-1-7: Measurement magnetic field dependence of $\Delta M(H_\alpha // H)$ of $Bi_2Sr_2Ca_{0.9}Ho_{0.1}Cu_2O_y$ with cooling rate $R = 30^\circ C$ / hr, H_α = 10 T and $T_m = 950^\circ C$, $960^\circ C$ and $970^\circ C$.
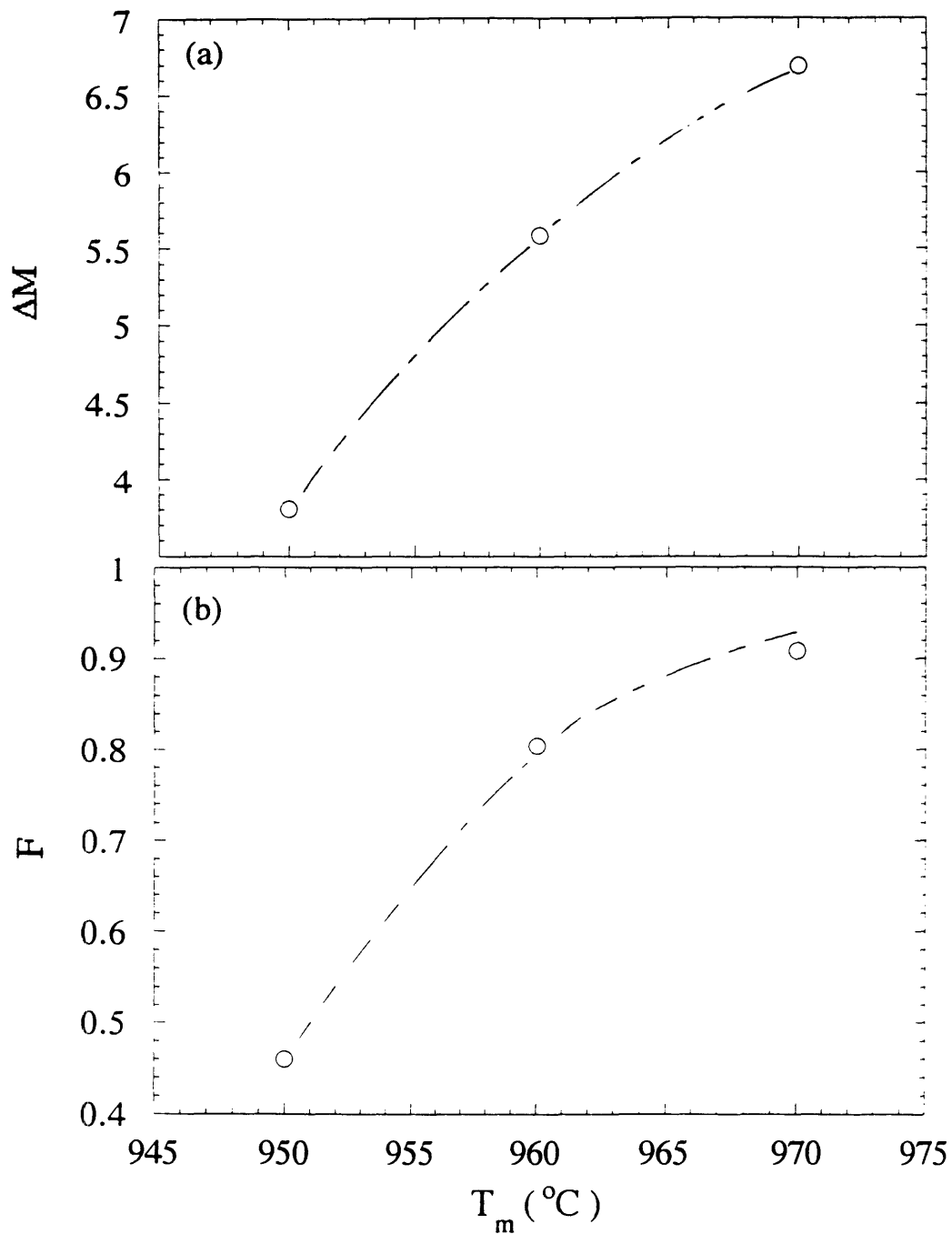
Fig. 5-1-8: (a) $\Delta M(H_\alpha // H)$ and (b) F factor dependence of T_m with cooling rate $\mathcal{R} = 30^\circ C$ / hr and $H_\alpha = 10$ T.

will be, if we assume the grain sizes are the same for the three samples. This assumption is reasonable, because the thermal sequences for the three samples are the same. Clearly, ΔM increases with increasing T_m for all H. We plot $\Delta M(2T)$ and F factor as a function of T_m in Fig. 5-1-8(a) and (b). Both ΔM and F increase with increasing T_m. The structural anisotropy and magnetic anisotropy are consistent with each other. Additional discussion will be given later.

By increasing T_m , a highly textured structure can be introduced by a 10 T magnetic field in a very short period of time, i.e. the processing time has been reduced 10 times by increasing T_m from 950°C to 970°C.

5.1.4: Texture development dependence on the magnetic field H_α.

X - ray diffraction patterns of the samples which were processed at T_m = 950°C under a field of 0 T, 2.5 T and 10 T are shown in Figs. 5-1-9(a), (b) and (c). When H_α = 0 T, the diffraction pattern is similar to the powder diffraction pattern, i.e. consistent with random grains in the sample (F = 0.03). When H_α increases to 2.5 T, the intensity of the (00ℓ) peaks increases and the F factor reaches 0.35. When H_α increases to 10 T, the X- ray diffraction pattern shows very strong (00ℓ) peaks and weak (103), (105), (107) and (110) peaks, and the F factor increases to 0.80.

When samples were processed at T_m = 970°C under magnetic fields of 0 T, 2.5 T and 10 T , the X - ray diffraction patterns of the samples exhibit differences (see Figs. 5-1-10(a), (b) and (c)). When H_α = 0 T, the X - ray diffraction pattern is similar to that of the powder sample. When H_α = 2.5 T, the intensity of the (00ℓ) peaks increases and the F factor increases to 0.59.

Comparing Fig. 5-1-9(b) with 10(b), the higher the T_m, the lower the magnetic field required to reach the same degree of texture. When $H_\alpha = 10$ T, a more fully textured structure is obtained. We plot the F factor as a function of magnetic field for $T_m = 950^\circ C$ with $\mathcal{R} = 3^\circ C/hr$ and $T_m = 970^\circ C$ with $\mathcal{R} = 30^\circ C$ in Fig. 5-1-11. For both cases, the F factor increases with increasing magnetic field. Under the same magnetic field, the F factor increases with increasing T_m. We should remember that the texture development depends on the cooling rate. The degree of texture decreases with increasing cooling rate for fixed T_m and H_α. In Fig. 5-1-11, although the cooling rate for $T_m = 970^\circ C$ is 10 times that for $T_m = 950^\circ C$, the degree of the texture still increases with increasing T_m under the same magnetic field. This means that the liquid phase plays a very important rule in texture development. Notice also that at a higher T_m, the same degree of texture can be obtained at a lower magnetic field. Thus if the sample was processed at a higher temperature with a slower cooling rate than $30^\circ C/hr$, the saturation magnetic field H_α will be shifted to a lower value. Thus a higher T_m is always desirable in attempting to obtain a highly textured structure, and there is a trade off between the cooling rate and the magnetic field. We can introduce a highly textured structure either with a faster cooling rate under a stronger annealing magnetic field, or with a lower cooling rate under a weaker magnetic field.

In order to observe the texture development of the grains under an elevated magnetic field, SEM images of the samples with $T_m = 950^\circ C$ and $H_\alpha = 0$ T, 5 T, and 10 T are shown in Figs. 5-1-12 (a), (b), (c), (d), (e) and (f). After melt - growth under an elevated magnetic field, the samples are semiconductors due to the Bi - rich liquid phase between the grains and the loss of oxygen. The "white" phase can converted to superconducting phase

and the oxygen can be restored by annealing the samples at 860°C for a long period of time in a zero field. At 860°C, the annealing process was diffusion controlled growth, the atoms in the small amount of the Bi - rich phase transform the textured grains to the superconducting 2212 phase. The annealing process did not influence the well textured structure; after the annealing process, the highly textured structure is retained. This fact is confirmed in Figs. 5-1-12(b), (d) and (e). Clearly, the grains were rotated by the magnetic field from a random structure ($H_\alpha = 0$ T) to a highly textured structure ($H_\alpha = 10$ T) (see Fig. 5-1-12).

The temperature dependence of the diamagnetic susceptibility of the samples which were processed under 0 T and 10 T are shown in Fig. 5-1-13. The samples were placed with $H_\alpha // H$. It is clear that the textured sample shows a larger diamagnetic susceptibility. The transition temperatures, T_c, are the same for both samples. This fact indicates that the magnetic field only rotates the grains to the $c // H_\alpha$ direction and does not influence the intrinsic superconducting properties of the samples.

The magnetic anisotropy factor $\eta = \Delta M(H_\alpha // H) / \Delta M(H_\alpha \perp H)$ is plotted as a function of measurement magnetic field in Fig. 5-1-14. The magnetic anisotropy factor η is larger for the $H_\alpha = 10$ T sample than for the $H_\alpha = 0$ T sample over the entire measurement magnetic field. We plot the magnetic anisotropy factor η at 2 T, i.e. $\eta = \eta(2\ \text{T})$, as a function of the magnetic field H_α in Fig. 5-1-15. The magnetic anisotropy factor increases with increasing magnetic field. The curve is similar to the F vs H_α curve in Fig 5-1-11. In Fig. 5-1-16, the magnetic anisotropy factor is plotted as a function of F factor, demonstrating the relationship of the magnetic anisotropy factor and the

structural anisotropy factor introduced by the magnetic field. This result is
similar to the results for $Y_1Ba_2Cu_3O_7$.
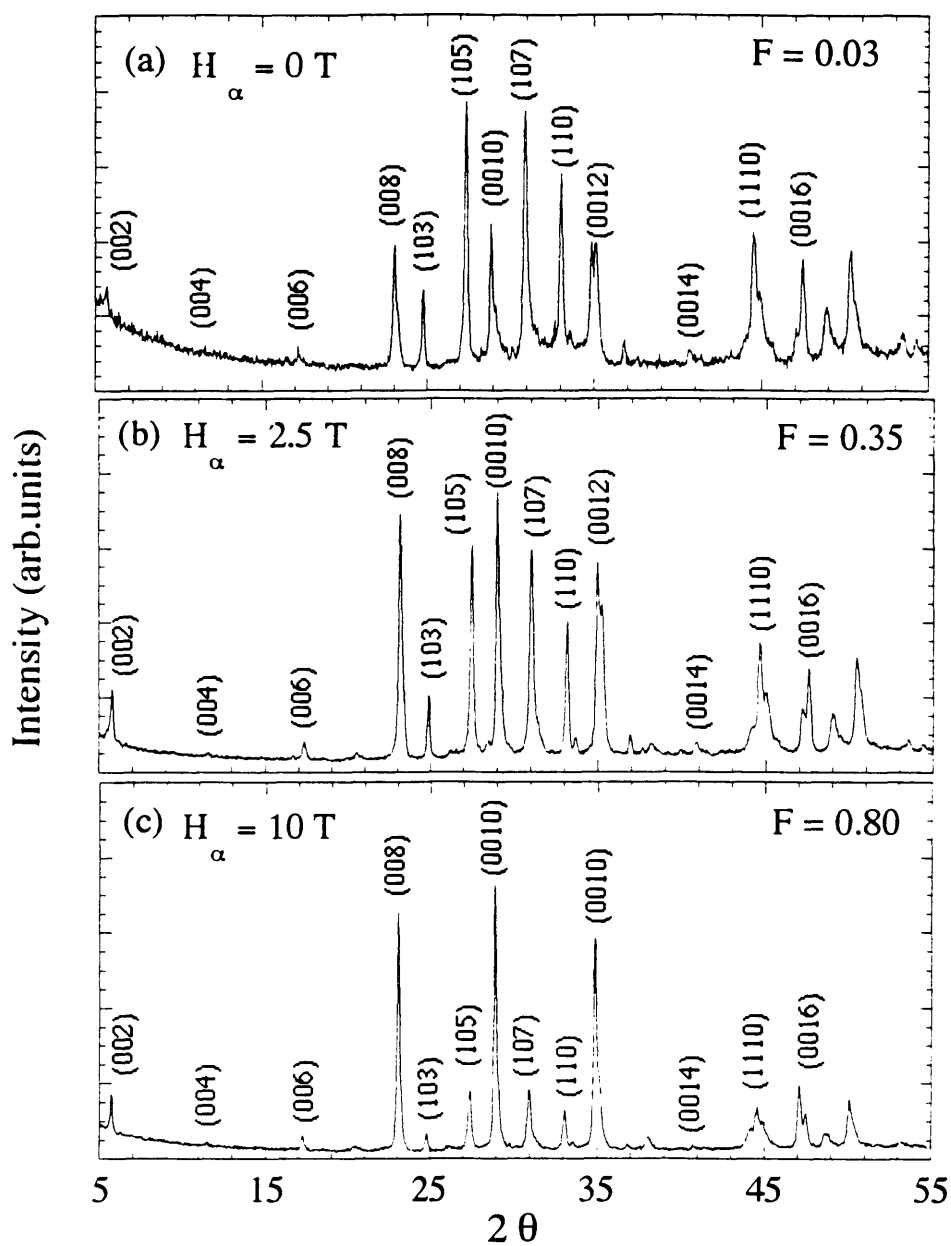
Fig. 5-1-9: X - ray diffraction patterns of $Bi_2Sr_2Ca_{0.9}Ho_{0.1}Cu_2O_y$ polished along transverse direction of magnetic field, with $T_m = 950°C$ and $\mathcal{R} = 3°C$ / hr. (a) $H_\alpha = 0$ T, (b) $H_\alpha = 5$ T and (c) $H_\alpha = 10$ T.
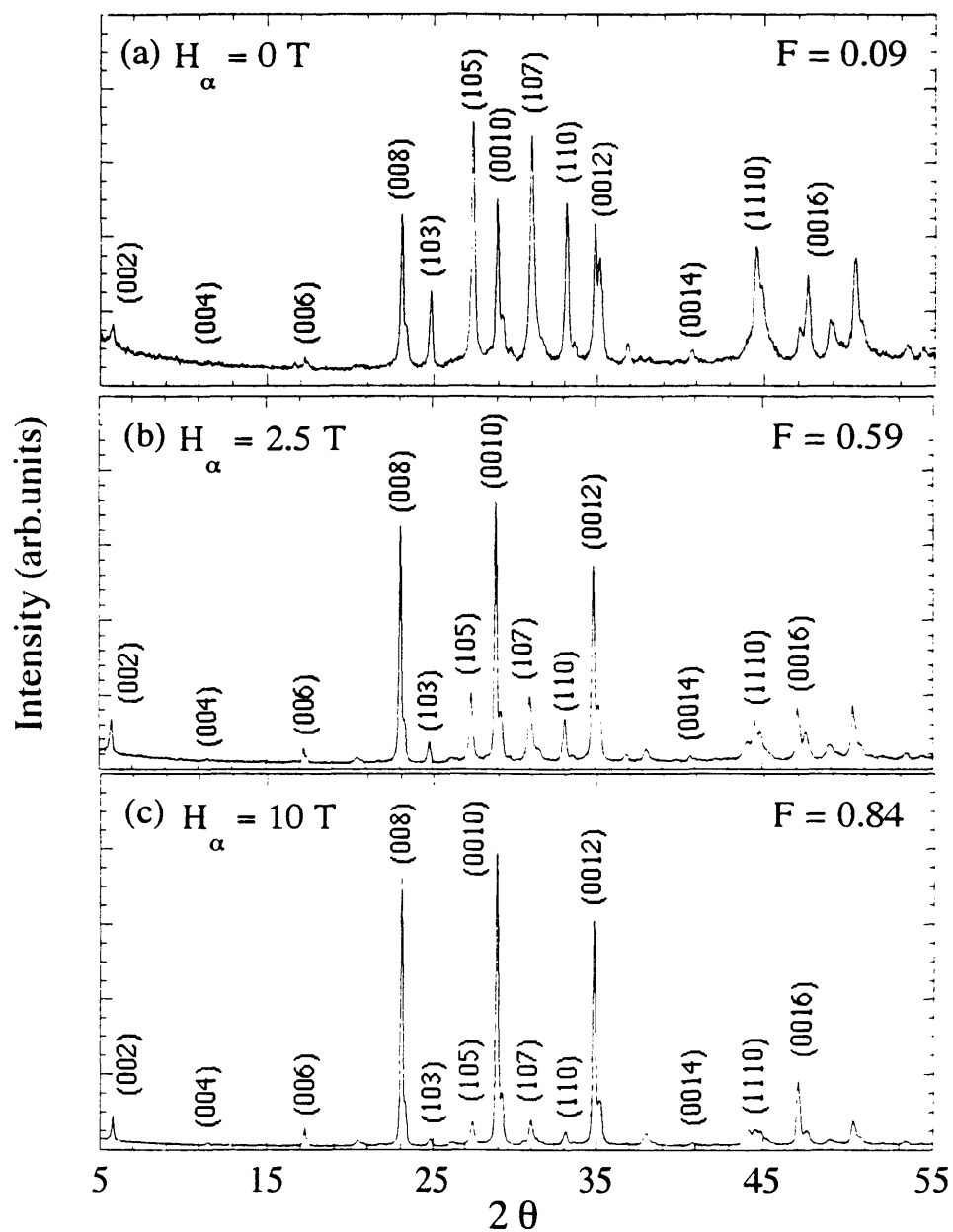
Fig. 5-1-10: X - ray diffraction patterns of $Bi_2Sr_2Ca_{0.9}Ho_{0.1}Cu_2O_y$

polished along transverse direction of magnetic field, with $T_m =$

970°C and $\mathcal{R} = 3$°C / hr. (a) $H_\alpha = 0$ T, (b) $H_\alpha = 5$ T and (c) $H_\alpha = 10$
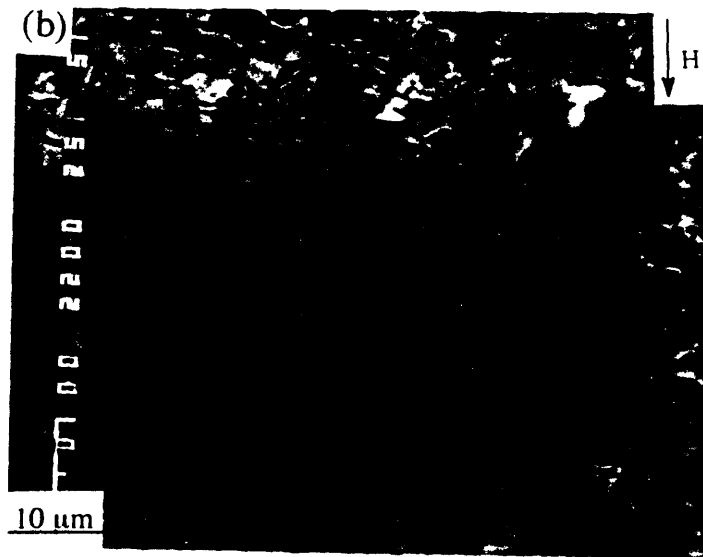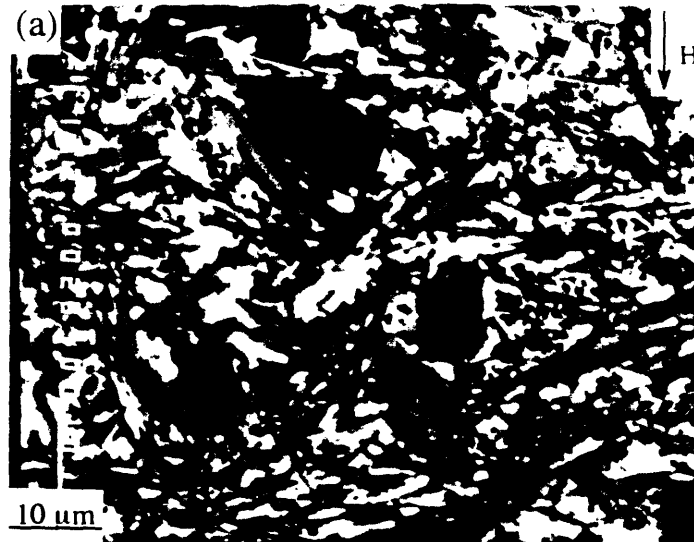
T.

Fig. 5-1-11: SEM images of polished cross section of $Bi_2Sr_2Ca_{0.9}Ho_{0.1}Cu_2O_y$ with cooling rate $\mathcal{R} = 3^oC$ / hr and $T_m = 950^oC$, (a) and (b) $H_\alpha = 0$ T, (b) is the sample after annealing at 860^oC.
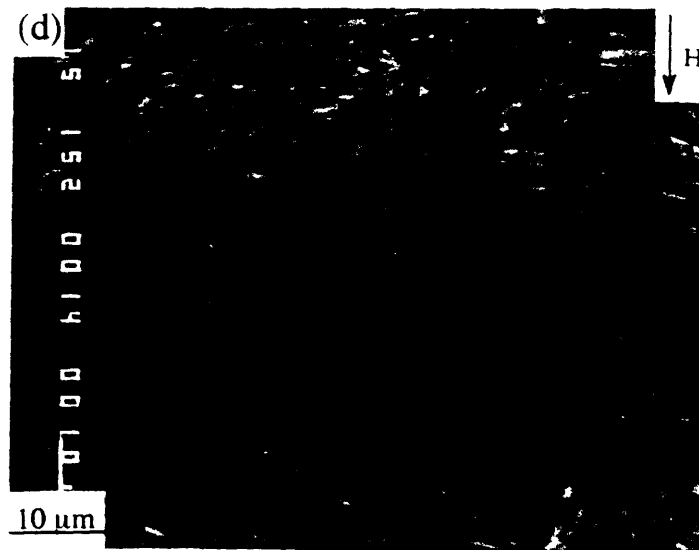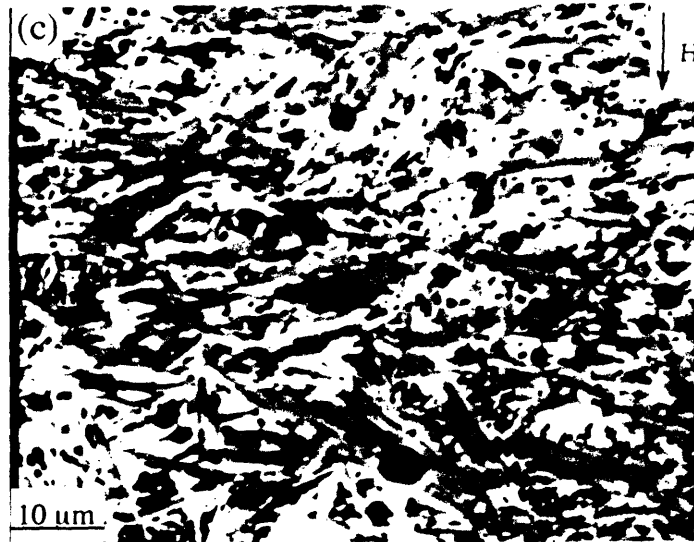
Fig. 5-1-11:   SEM images of polished cross section of $Bi_2Sr_2Ca_{0.9}Ho_{0.1}Cu_2O_y$ with cooling rate $\mathcal{R} = 3°C$ / hr and $T_m = 950°C$, (c) and (d) $H_\alpha = 5$ T, (d) is the sample after annealing at 860°C.

Fig. 5-1-11: SEM images of polished cross section of $Bi_2Sr_2Ca_{0.9}Ho_{0.1}Cu_2O_y$ with cooling rate $\mathcal{R} = 3^oC$ / hr and $T_m = 950^oC$, (e) and (f) $H_\alpha = 10$ T. (f) is the sample after annealing at 860°C.
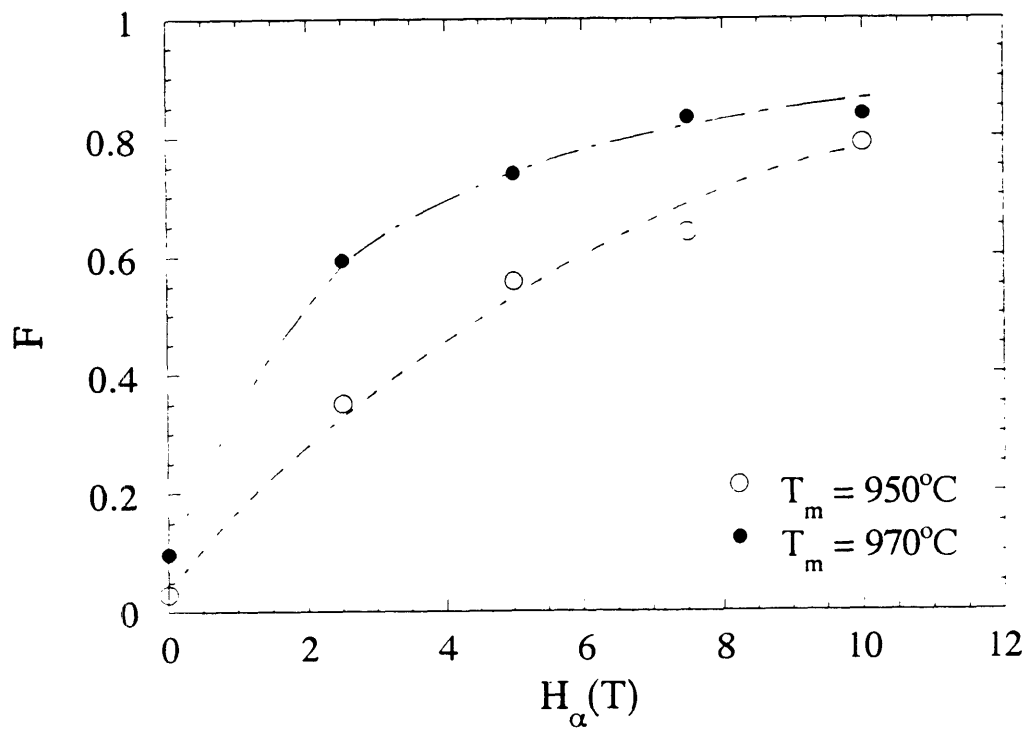
Fig. 5-1-12:   F factors as a function of magnetic field for (a)

$T_m = 950^{\circ}C$, $\mathcal{R} = 3^{\circ}C$ / hr and $H_\alpha = 10$ T, (b) $T_m = 970^{\circ}C$, $\mathcal{R} =$

$30^{\circ}C$ / hr and $H_\alpha = 10$ T.
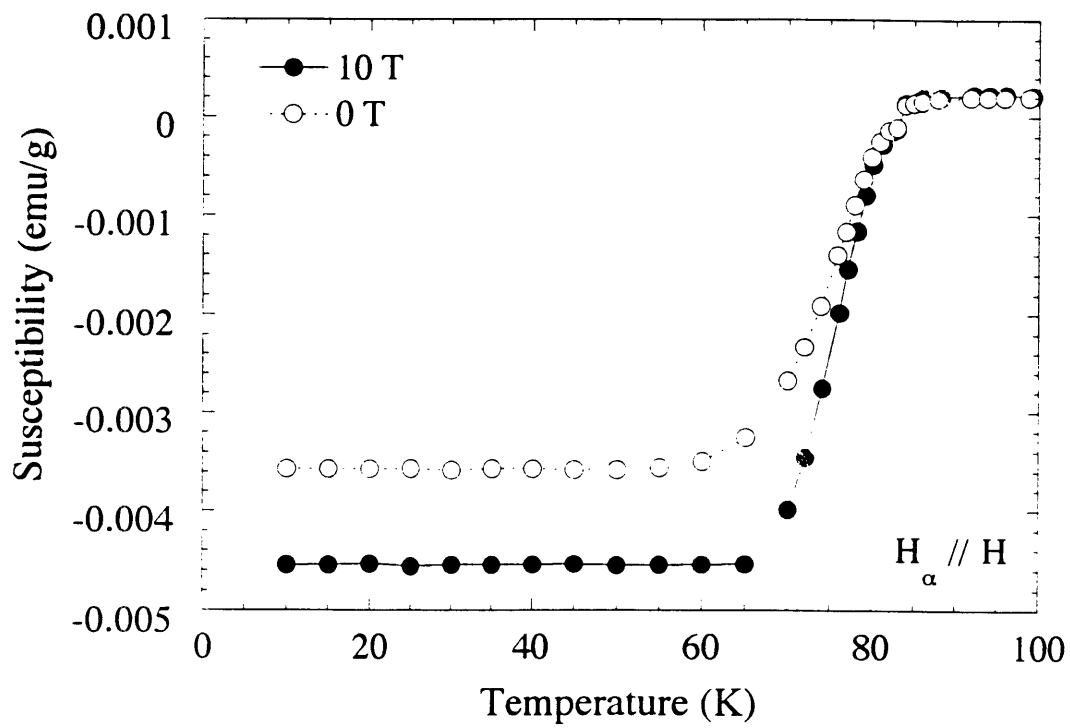
Fig. 5-1-13:   Temperature dependence of diamagnetic susceptibility of

$Bi_2Sr_2Ca_{0.9}Ho_{0.1}Cu_2O_y$ with $T_m = 950°C$, $\mathcal{R} = 3°C$ / hr and

$H_\alpha = 10$ T. The sample was placed in H_α // H.
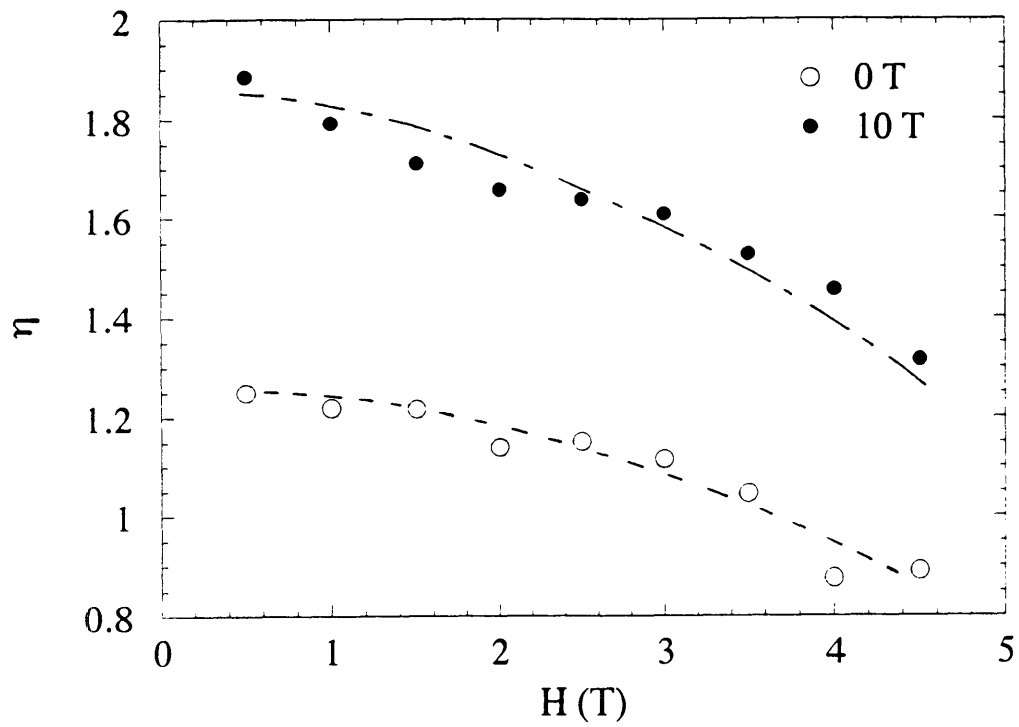
Fig. 5-1-14:   Magnetic anisotropy factor $\eta = \Delta M(H_\alpha /\!/ H) / \Delta M(H_\alpha \perp H)$

dependence of measurement magnetic field H for $H_\alpha = 0$ T

and 10 T.
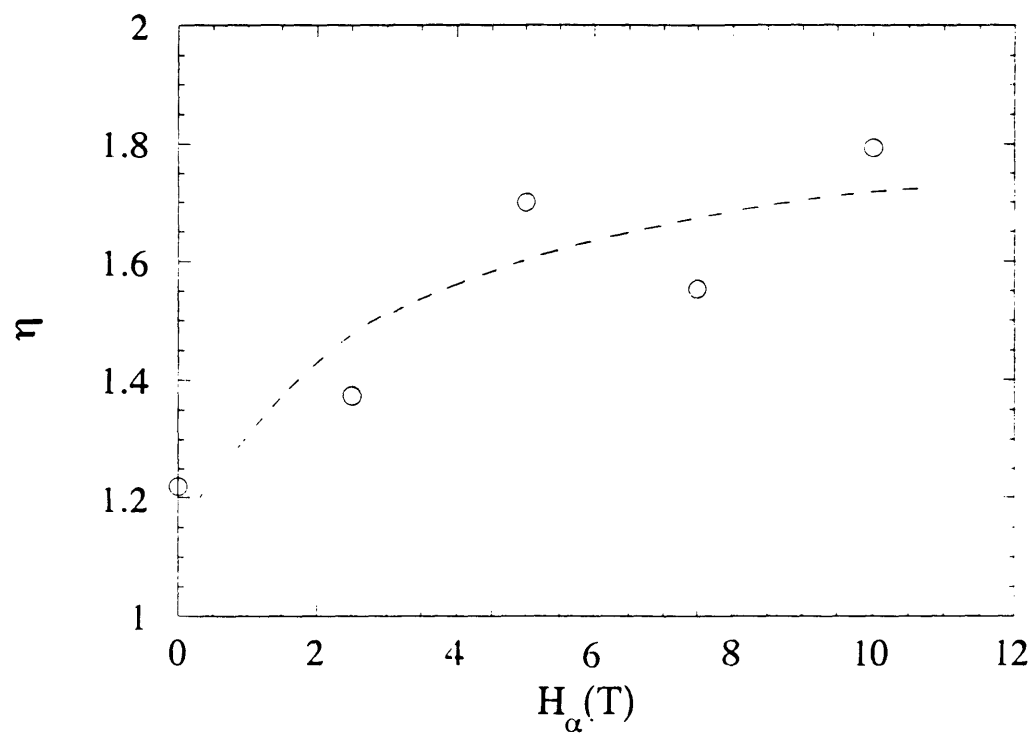
Fig. 5-1-15: Magnetic anisotropy factor $\eta = \Delta M(H_\alpha \mathbin{/\!/} H) / \Delta M(H_\alpha \perp H)$

at 1 T dependence of magnetic field H_α for $T_m = 950°C$ and
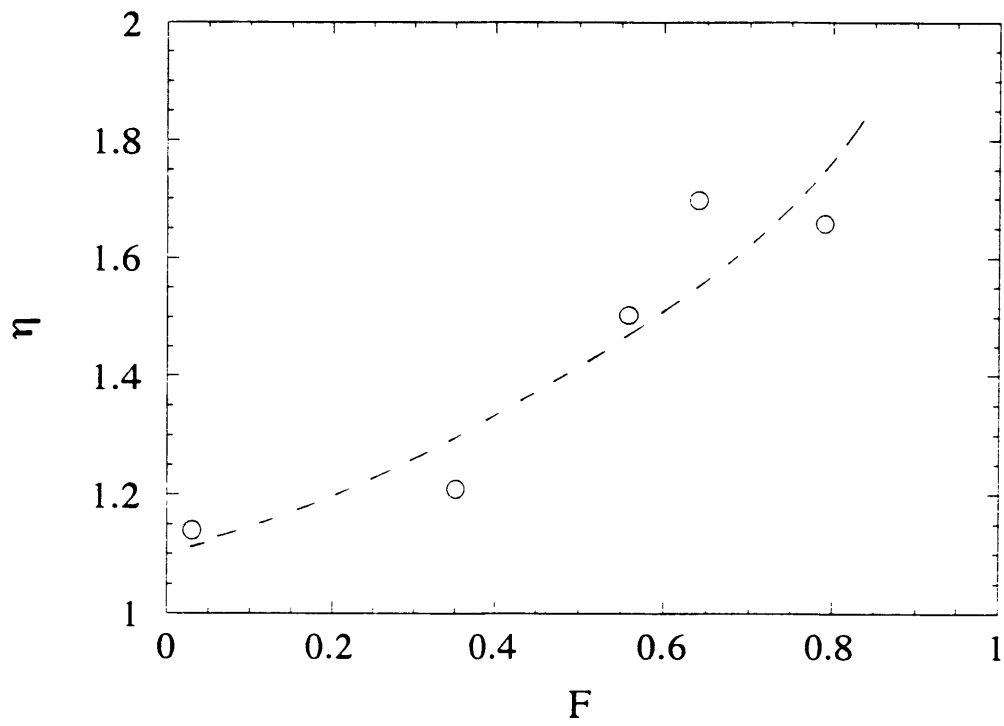
$\mathcal{R} = 3°C / hr.$

Fig. 5-1-16:   Relation between Magnetic anisotropy factor $\eta = \Delta M(H_\alpha$

// H) / $\Delta M(H_\alpha \perp$ H) at 1 T and F factor for $T_m = 950^{\circ}C$ and $\mathcal{R} =$

$3^{\circ}C$ / hr.

5.1.5: Transport critical current density increase with increasing F factor.

Transport critical current density was plotted as a function of the F factor in Fig. 5-1-17. For the open - circle data, the textured structure was introduced by increasing the magnetic field. For the filled - circle data, the textured structure was introduced by increasing T_m under a 10 T magnetic field. For both cases, J_c increases with increasing F. For the open - circle data, the thermal sequence is fixed ($T_m = 950^\circ C$ and $\mathcal{R} = 3^\circ C/hr$) and the degree of texture was improved by increasing the magnetic field. Although J_c increases with increasing F factor, the J_c saturates for a certain degree of texture. Thus the transport J_c can not be increased solely by increasing the degree of texture. For the filled - circle data, the annealing magnetic field was fixed at 10 T and the degree of the texture was improved by increasing T_m (creating more liquid phase.). For this case, log (J_c) increases linearly with the F factor. Thus the transport can be increased dramatically by improving both texture and connectivity between the grains. It is clear that processing Bi - based materials under a high magnetic field provides a potential way to increase the transport critical current density in these materials.
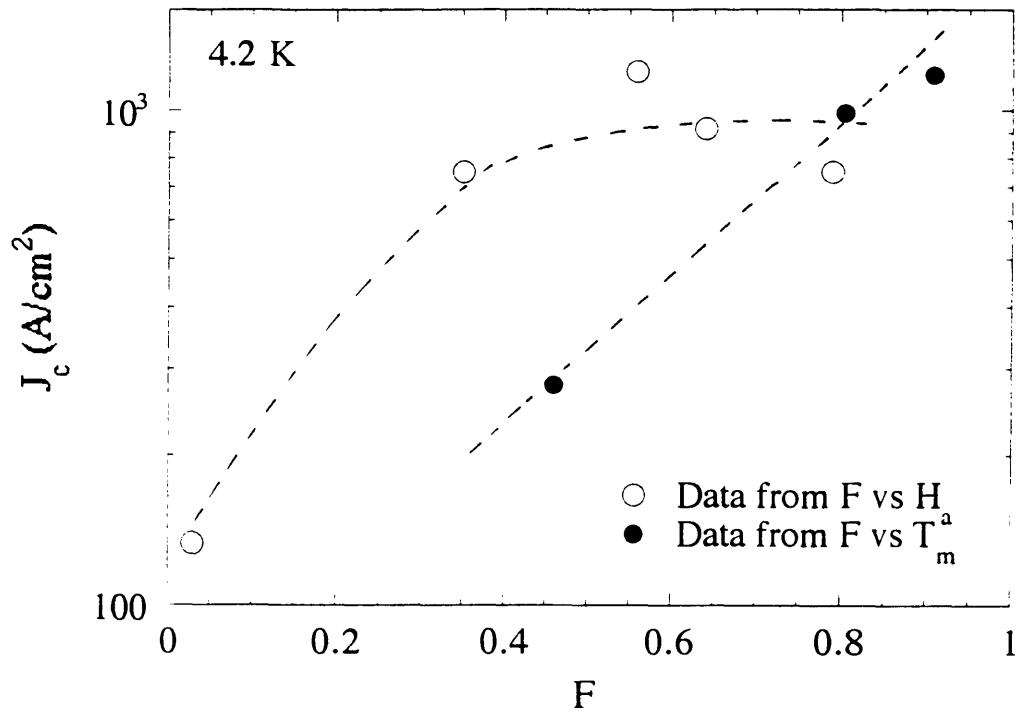
Fig. 5-1-17:   Transport critical current density J_c at 4.2 K dependence of
F factor.

5.1.6: Texture development of $Bi_2Sr_2Ca_{0.9}R_{0.1}Cu_2O_8$ with R = Y, and Gd under a high magnetic field.

Figs. 5-1-18(a) and (b) show SEM images of $Bi_2Sr_2Ca_{0.9}Y_{0.1}Cu_2O_8$ and $Bi_2Sr_2Ca_{0.9}Gd_{0.1}Cu_2O_8$ which were processed under a 10 T magnetic field with $T_m = 960°C$ and $\mathcal{R} = 30°C/hr$. It is clear that the c - axis for both materials are parallel to the magnetic field direction, i.e. c // H_α. The grain orientation is consistent with the result of Ref [18], in which the grains were textured by a high magnetic field in an organic solvent. Thus we can choose different rare earth elements and the amount of doping to change the melting point and other properties of the material. This family of materials can be textured under a high magnetic field for R = Ho. In addition, the relatively inexpensive $Bi_2Sr_2Ca_{1-x}Y_xCu_2O_8$ material can be textured under a high magnetic field.
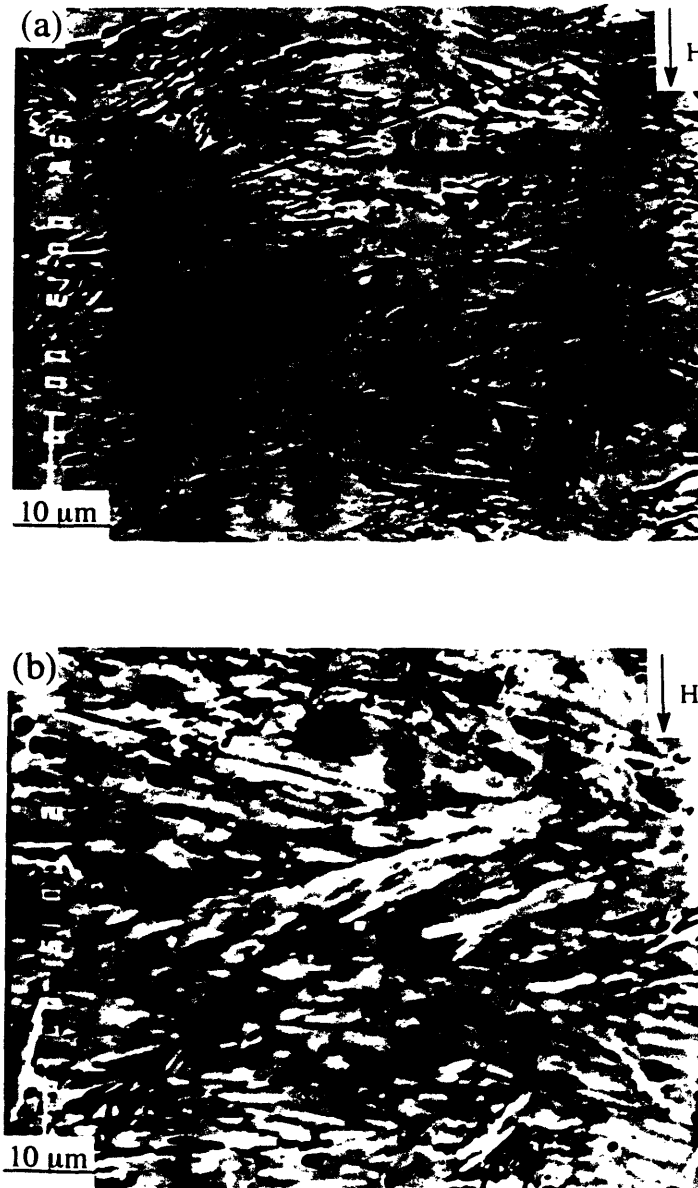
Fig. 5-1-18:   SEM images of polished cross section of $Bi_2Sr_2Ca_{0.9}R_{0.1}Cu_2O_y$

with cooling rate $\mathcal{R}$ = 30°C / hr and H_α = 10 T, (a) R = Y and (b) R

= Gd.

5.1.7: Conclusion

$Bi_2Sr_2Ca_{0.9}R_{0.1}Cu_2O_8$ with R = Y, Ho and Gd materials were melt - grown under elevated magnetic fields. Texture development depends upon the cooling rate, the maximum processing temperature T_m, and the magnetic field applied during processing. By increasing T_m, a textured structure can be introduced in a very short period of time, i.e. the processing time is reduced by a factor of 10 by increasing T_m from 950°C to 970°C under a 10 T magnetic field. There is a trade-off between the cooling rate and the magnetic field. We can introduce a highly textured structure with a faster cooling rate under a stronger magnetic field, or with a lower cooling rate under a weaker magnetic field. The transport critical current density can be increased dramatically by improving both texture and connection between the grains under a high processing magnetic field. Processing Bi - based materials under a high magnetic field provides a potential way to increase the transport critical current density.

Section 5.2 Melt - growth of $RBa_2Cu_3O_7$ under an elevated magnetic field.

Bulk $R_1Ba_2Cu_3O_7$ superconductors were melt - grown under elevated magnetic fields between 0 ~ 10 T. Highly textured, multi - domained structures were obtained by application of these high magnetic fields. Under a 10 T magnetic field, the degree of texture of $Y_1Ba_2Cu_3O_7$ increases with increasing maximum processing temperature, T_m. The domain alignment depends upon the cooling rate and applied magnetic field. There is a trade off between cooling rate and magnetic field, i.e. to obtain the same degree of texture, either a higher magnetic field and higher cooling rate, or lower magnetic field and lower cooling rate must be combined. During melt - growth under a high magnetic field, the domain orientation of $RBa_2Cu_3O_7$ (R = Ho, Gd and Er) is determined by the ionic moment orientation of the rare earth element in the superconductor.

5.2.1: Experimental Procedure

The starting materials were first prepared by solid state reaction. Highly pure Y_2O_3, Ho_2O_3, Gd_2O_3, Er_2O_3, $BaCO_3$ and CuO are weighed according to the normal composition $RBa_2Cu_3O_7$. The mixed powders were first reacted at 850°C for 24 hours in air to form a precursor. The precursor was then ground in an agate mortar and pestle, pressed into pellets and sintered at 950°C in flowing oxygen for 48 hours. The well formed R - 123 superconductors were re - ground and pressed into pellets, then the pellets were melt - grown under elevated magnetic field. The thermal processing sequence is shown in Fig. 5-2-1. T_m is the maximum processing temperature, $\mathcal{R}$ is the cooling rate with 4 ~ 60°C / hr and H_α is the annealing magnetic field between 0 and 10 T. For high magnetic field experiments, the furnace is

placed in the room temperature bore of a superconducting magnet. Magnetic fields of up to 10 T can be applied parallel to the long axis of the furnace throughout the annealing cycle. The field was increased to 0 ~ 10 T, then the temperature was raised. After processing, the temperature was decreased to room temperature, after which the magnetic field was reduced to zero.

The samples were placed in the SQUID magnetometer in two directions, i.e. H_α // H and $H_\alpha \perp$ H, H_α is the magnetic field at high temperature and H is the measurement magnetic field at low temperature. The magnetic anisotropy factor was defined as $\eta = \Delta M(H_\alpha$ // H) / $\Delta M(H_\alpha \perp$ H). For the magnetic measurement, the samples were cut in the shape of cubic 2 x 2 x 2 mm^3. There are many domains in the cubic samples for the magnetic measurement.

5.2.2: Texture development dependence on the maximum processing temperature T_m

Two samples with different maximum processing temperature T_m, i.e. $T_m = 1050^oC$ and 1075^oC, were grown under a 10 T magnetic field with the same cooling rate of $\mathcal{R} = 4^oC$ / hr. X - ray diffraction patterns of the cross section of these samples are shown in Fig. 5-2-2. The powder diffraction pattern of $YBa_2Cu_3O_7$ with F = 0.00 is also shown in Fig. 5-2-2(a). For $T_m = 1050^oC$, the X - ray diffraction pattern shows strong (00ℓ) peaks, but there are still (013) and (110) peaks, and F increases to 0.42. When T_m increases to 1075^oC, there are very strong (00ℓ) peaks and very weak (103) and (110) peaks, and in this case the F factor reaches 0.9. Clearly, the degree of texture increases with increasing maximum processing temperature T_m with fixed magnetic field and cooling rate. SEM images of the two samples are shown in Figs. 5-2-

3(a) and (b). When T_m = 1050°C, the grains formed are small in size and there is a small angular range between the c - axis of the grains and the magnetic field direction, H_α. When T_m increases to 1075°C, very large domains are formed and the c - axis of the domains are parallel to the magnetic field direction.

There are two factors which influence texture development in the samples under a 10 T magnetic field. The first one is liquid phase formation, which influences the grain rotation process. In the solid state, a 10 T magnetic field can not rotate grains due to the strong mechanical interaction between the grains. If there is a liquid phase present in the sample, the grains can be more easily rotated by the magnetic field. Y - 123 material melts peritectically at 1015°C and decomposes to 211 phase plus liquid phase. When T_m is increased to 1075°C, there will be more liquid phase present during grain growth. Thus the grains will be more easily rotated by the magnetic field in the under cooled liquid when the grain size is larger than the critical size, and the degree of the texture of the sample increases with increasing T_m, i.e., F = 0.48 with T_m = 1050°C and F = 0.90 with T_m = 1075°C. Second, the magnetic anisotropy energy ($\Delta E = \Delta\chi H^2 V/2$) depends on the volume of the grains. Even for samples where $\Delta\chi$ is constant and under similar magnetic fields (H_α = 10 T), the driving force for grain rotation increases with increasing volume of the grains. For melt - grown Y - 123, the higher the T_m, the larger the grains (as seen above). With higher T_m, the driving force for grain rotation increases due to the larger grain size. Thus, the degree of texture increases with increasing T_m. Actually, both of these factors influence the texture development of Y - 123 during melt - growth under a 10 T magnetic field.
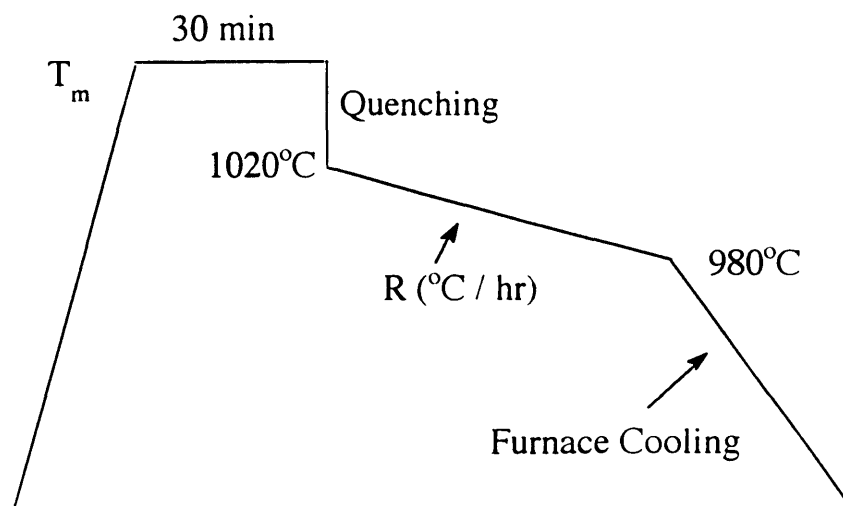
Fig. 5-2-1:   Thermal processing sequence of melt - growth of

RBa$_2$Cu$_3$O$_7$ under elevated magnetic field.
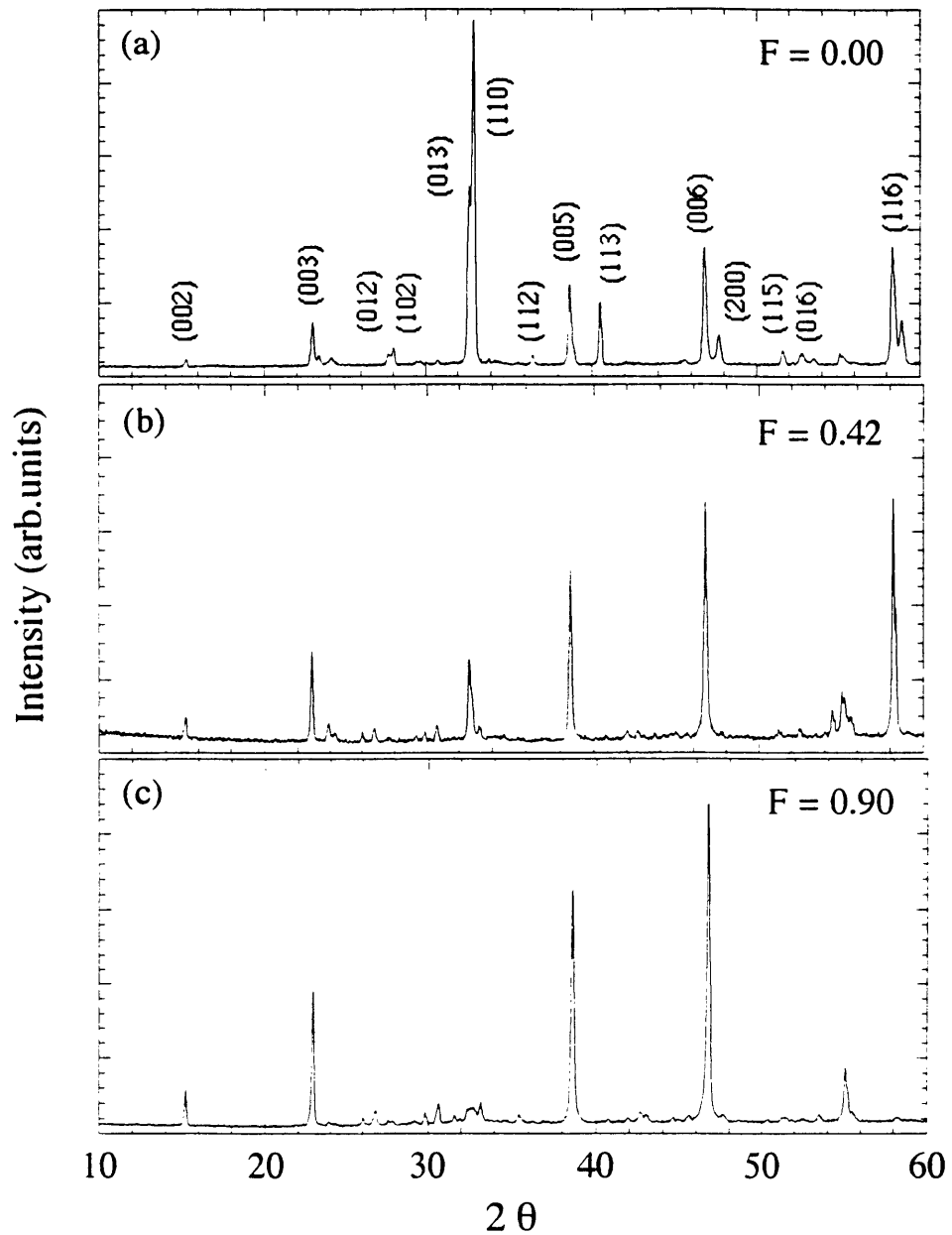
Fig. 5-2-2: X - ray diffraction patterns of $YBa_2Cu_3O_7$ polished along

transverse direction of magnetic field, with $\mathcal{R} = 4^{o}C$ / hr and

$H_{\alpha} = 10$ T. (a) powder diffraction pattern, (b) $T_m = 1050^{o}C$ and (c)
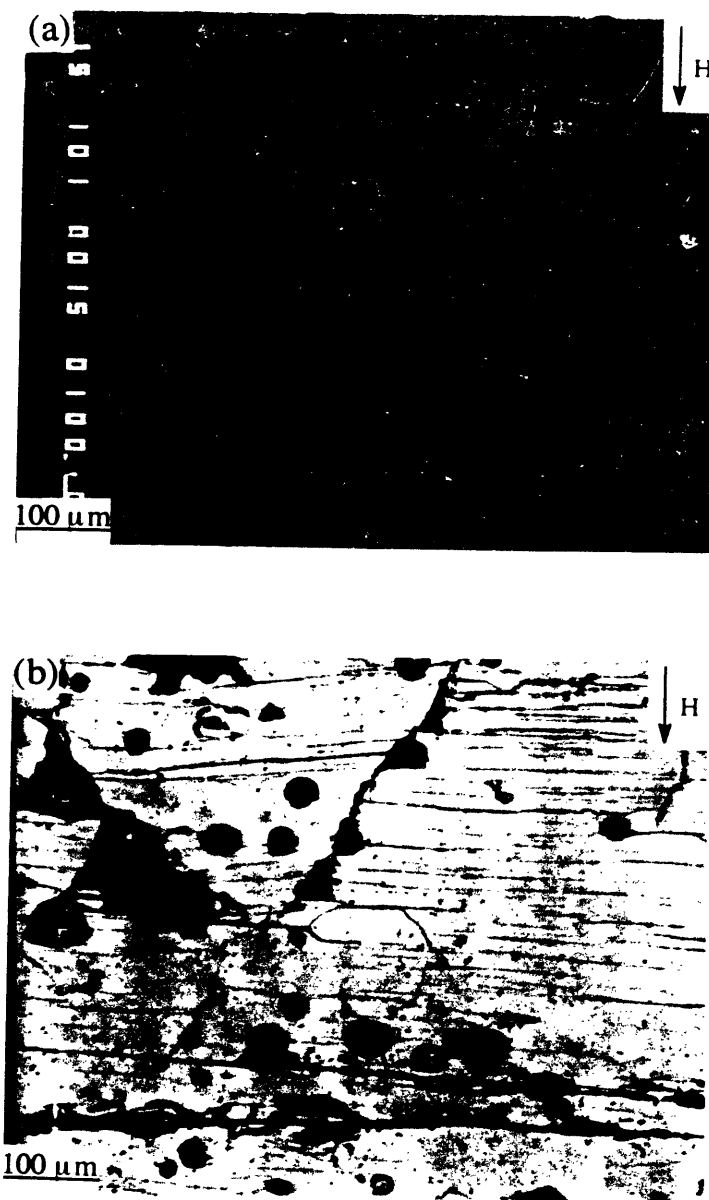
$T_m = 1075^{o}C$.

Fig. 5-2-3: SEM images of polished cross section of $YBa_2Cu_3O_7$ with $\mathcal{R} = 4^oC/hr$ and $H_\alpha = 10$ T. (a) $T_m = 1050^oC$ and (b) $T_m = 1075^oC$.

5.2.3: Texture development dependence on the cooling rate under a 10 T magnetic field.

X - ray diffraction patterns of samples with cooling rate $\mathcal{R} = 30^oC$ / hr, 12^oC / hr and 4^oC / hr are shown in Figs. 5-2-4(a), (b) and (c), respectively. The (00ℓ) peaks and F factor decrease with increasing cooling rate. At a fixed magnetic field $H_\alpha = 10$ T and maximum processing temperature $T_m = 1075^oC$, the slower the cooling rate, the higher the degree of texture. The degree of texture can also be seen in the anisotropic superconducting properties. When the sample is placed with H_α // H and $H_\alpha \perp$ H in the SQUID magnetometer, the temperature dependence of the weak field (H = 30 Oe) anisotropic susceptibility can be clearly seen in Fig. 5-2-5. The magnetic hysteresis of the samples with cooling rate $\mathcal{R} = 4^oC$ / hr and 30^oC / hr, which were placed with H_α // H and $H_\alpha \perp$ H, are shown in Figs. 5-2-6(a) and (b). For both cases, $\Delta M(H_\alpha$ // H) is always larger than $\Delta M(H_\alpha \perp$ H). This means that a textured structure with the c - axis // H_α was introduced by a 10 T annealing magnetic field. We plot the magnetic anisotropy factor $\eta = \Delta M(H_\alpha$ // H) / $\Delta M(H_\alpha \perp$ H) as a function of measurement field H for samples with cooling rate $\mathcal{R} = 4^oC$ / hr and 30^oC / hr in Fig. 5-2-7. The magnetic anisotropy factor η depends on the measurement field H, the two curves are almost parallel to each other, and $\eta(4^oC$ / hr) is always larger than $\eta(30^oC$ / hr). Thus we choose $\eta(H = 2T)$ to characterize the magnetic anisotropy and plot $\eta(H = 2T)$ as a function of cooling rate in Fig. 5-2-8.

The cooling rate dependence of the structural anisotropy factor F and magnetic anisotropy factor $\eta(H = 2T)$ are plotted in Figs. 5-2-8(a) and (b). Both the F and η factor decrease with increasing cooling rate under a 10 T magnetic

148

field. Even when the cooling rate reaches 60°C / hr, the F factor is still larger than 0.5 and η larger than 2.0. With a cooling rate in excess of 20°C / hr, a higher degree of texture can be obtained (see Fig. 5-2-8(a)). This means that a well textured bulk Y-123 can be fabricated in less than 3 hours total time under a 10 T magnetic field. Unlike directional solidification or the zone melt - growth method, the size of the sample depends on the pulling rate or the intrinsic growth rate of the grains, usually very slow. Under a 10 T magnetic field, in comparison, a long length of textured multi-domained bulk Y - 123 superconductor can be fabricated in a short period of time.
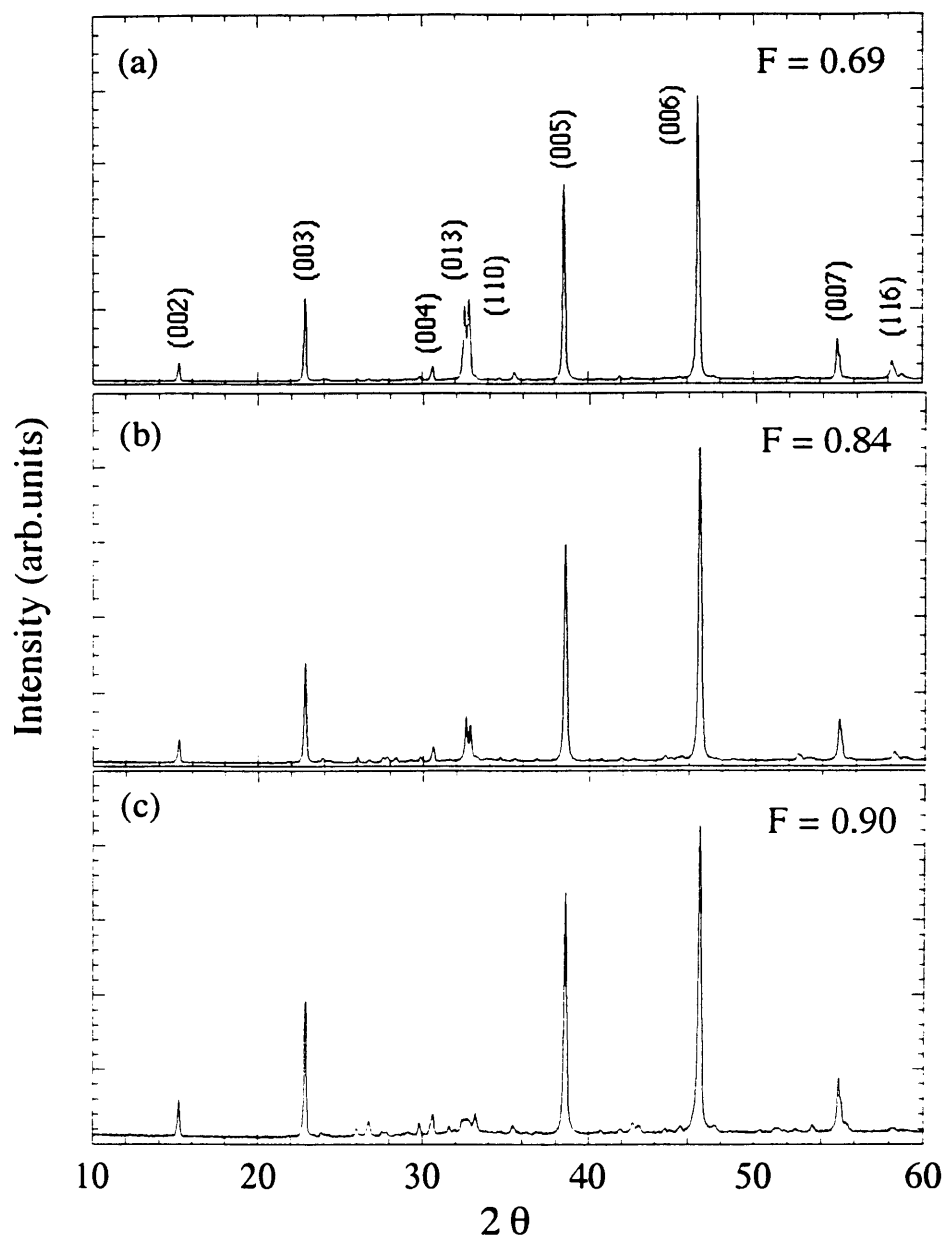
Fig. 5-2-4:   X - ray diffraction patterns of $YBa_2Cu_3O_7$ polished along

transverse direction of magnetic field,   with $T_m = 1075^oC$ and

$H_\alpha = 10$ T.   (a) cooling rate $\mathcal{R} = 30^oC$ / hr,   (b) cooling rate $\mathcal{R} = 12^oC$

/ hr and (c) cooling rate $\mathcal{R} = 4^oC$ / hr.
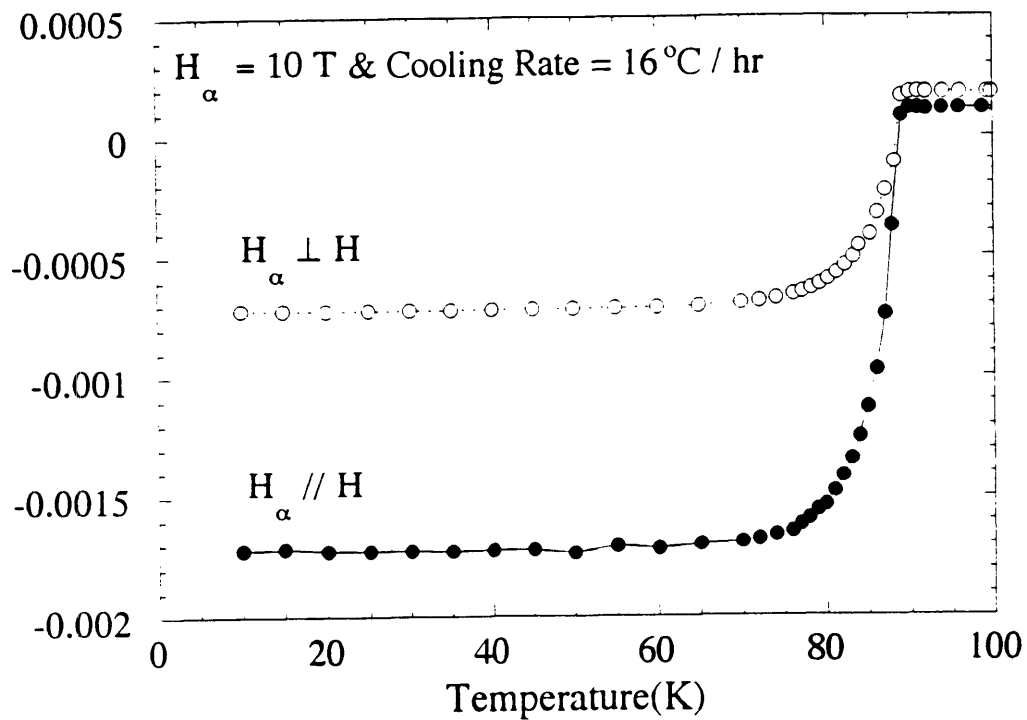
Fig. 5-2-5:   Temperature dependence of diamagnetic susceptibility of

YBa$_2$Cu$_3$O$_7$ with T$_m$ = 1075°C, $\mathcal{R}$ = 16°C / hr and H$_\alpha$ = 10 T.

The sample was placed in two orientations, i.e. H$_\alpha$ // H and

H$_\alpha$ ⊥ H.
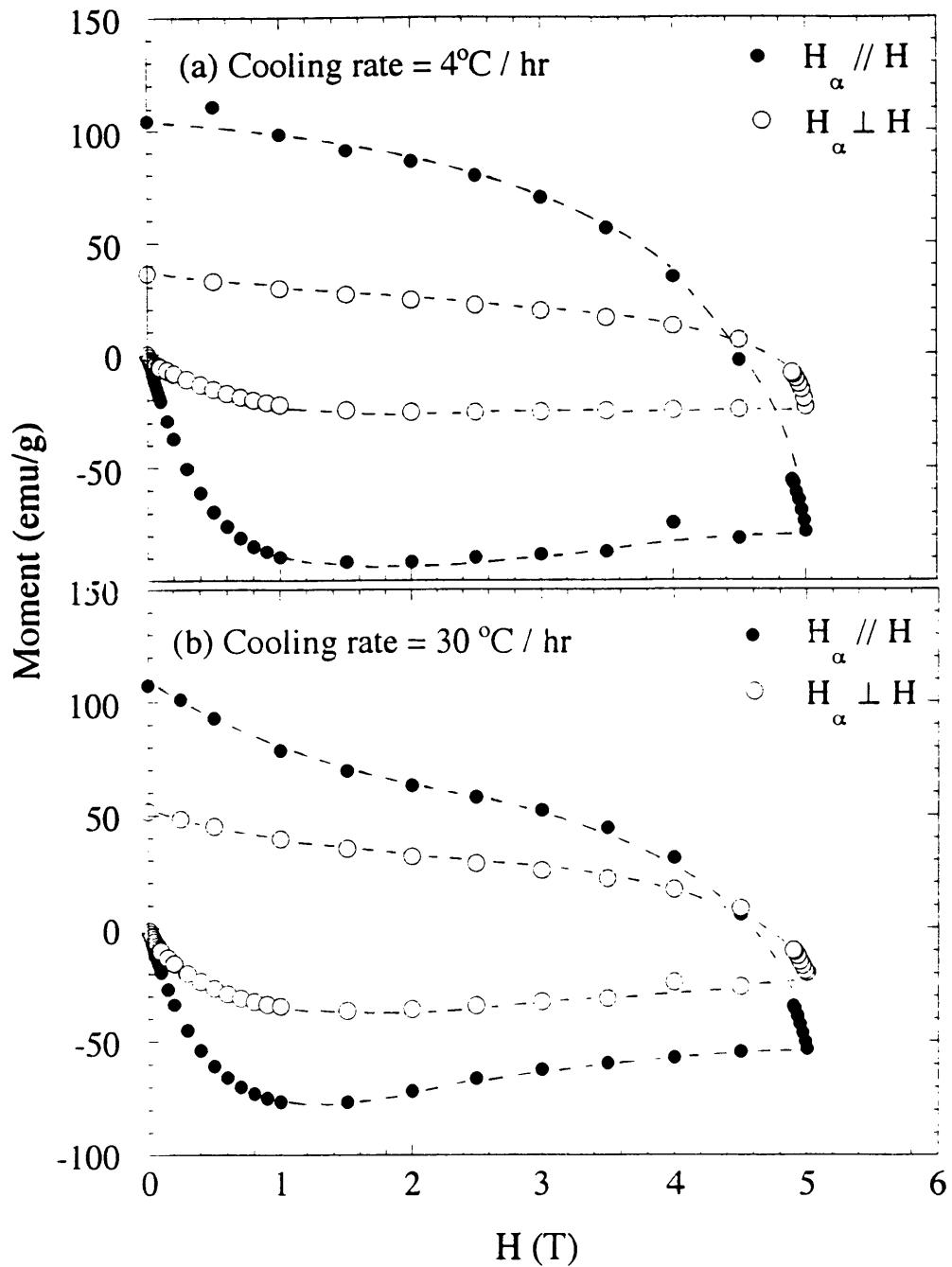
Fig. 5-2-6:   Magnetic hysteresis at 4.2 K of $YBa_2Cu_3O_7$ with T_m =
1075°C and H_α = 10 T were measured in two directions, i.e.
H_α // H and $H_\alpha \perp$ H. H_α is the processing field and H is the
measuring field.   (a) $\mathcal{R}$ = 4°C / hr and (b) $\mathcal{R}$ = 30°C / hr.
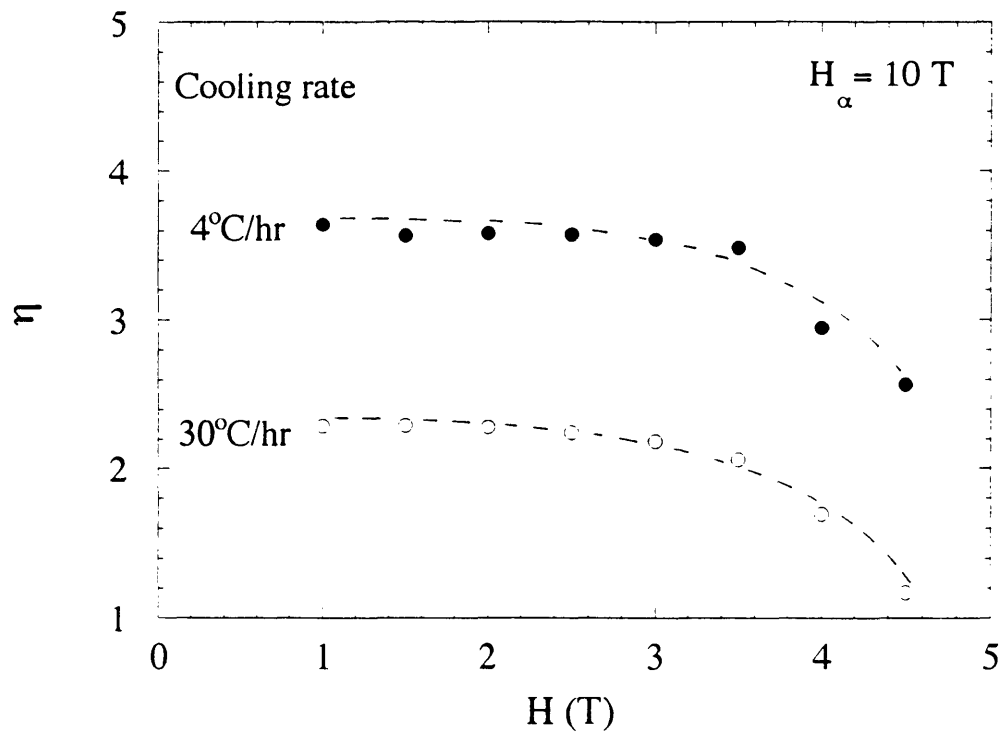
Fig. 5-2-7: Magnetic anisotropy factor $\eta = \Delta M(H_\alpha /\!/ H) / \Delta M(H_\alpha \perp H)$

dependence of measurement magnetic field H for $\mathcal{R} = 4^oC$

/ hr and 30^oC / hr.
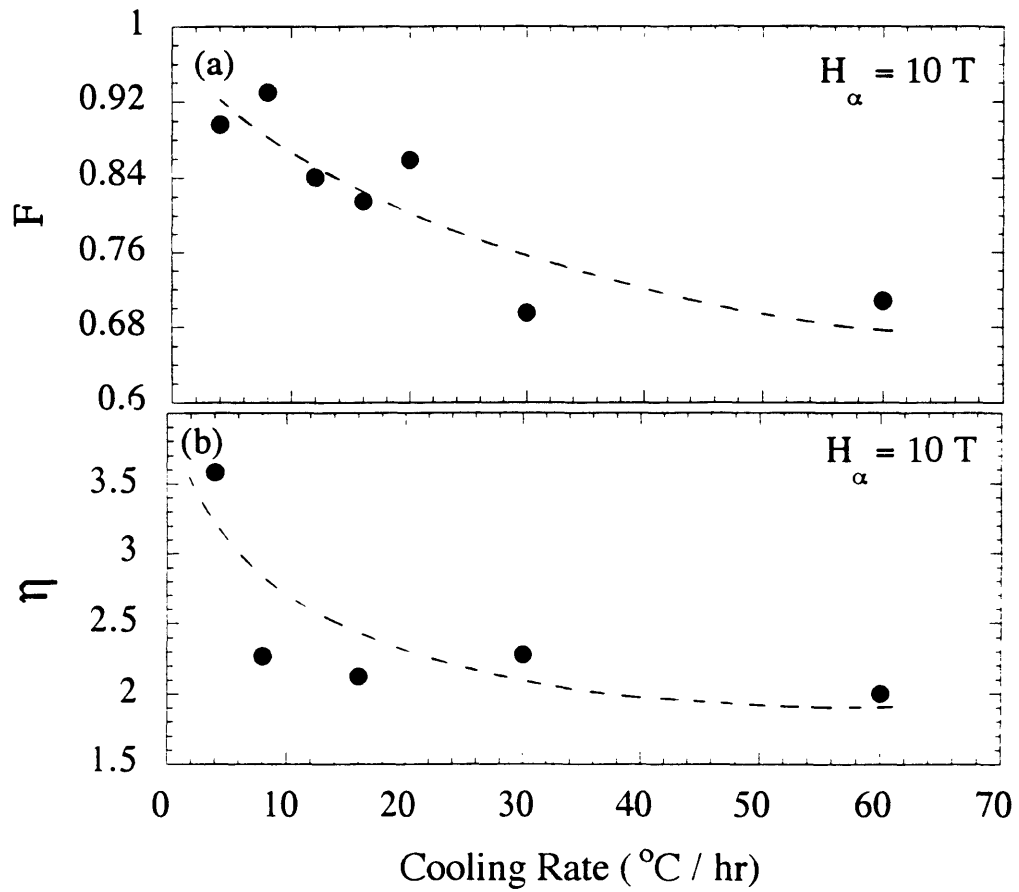
Fig. 5-2-8: (a) F factor and (b) $\eta = \Delta M(H_\alpha \mathbin{/\!/} H) / \Delta M(H_\alpha \perp H)$ dependence of cooling rate of $YBa_2Cu_3O_7$ with $T_m = 1075^\circ C$ and $H_\alpha = 10$ T.

5.2.4: Texture development dependence on the magnetic field H_α.

Before discussing texture development, let us first investigate the way in which a high magnetic field influences the microstructure inside domains. SEM images of the microstructure of samples processed under a 0 T and 10 T magnetic field are shown in Figs. 5-2-9(a) and (b). Clearly, from the microstructural point of view, there is not much difference between these two samples, and the superconducting transition temperature T_C are also the same for both samples (see Fig. 5-2-12). Even without the measurement of the transport properties for those two domains, the magnetic hysteresis of the powder at 4.2 K for these two samples did not show much difference. Thus it could be concluded that the influence of a 10 T magnetic field on the microstructure inside the domains is much less important than the influence of texture development between domains.

X - ray diffraction patterns of the samples grown under a 0 T , 1.5 T and 10 T magnetic field are shown in Figs. 5-2-10(a), (b) and (c). Under a 0 T magnetic field, the X - ray diffraction pattern of the cross section is similar to the powder diffraction pattern, and the F factor is very small. When the magnetic field increases to 1.5 T, the intensity of the (00ℓ) peaks increases and the F factor reaches 0.52. At a 10 T magnetic field, there are very strong (00ℓ) peaks and only weak (103) and (110) peaks remain, and the F factor increases to 0.82. The texture development processes can be clearly seen in Figs. 5-2-11(a), (b), (c) and (d), when the magnetic field increases from 0 T to 10 T. When $H_\alpha = 0$ T, the domains are randomly oriented. When the magnetic field increases from 0 T to 0.5T, 2.5 T and 10 T, the c - axis of the domains

155

moves gradually to the H_α direction, and finally parallel to H_α at 10 T. F

factors are plotted as a function of magnetic field in Fig. 5-2-15(a).

The temperature dependence of the weak field (30 Oe) diamagnetic susceptibility of the samples which were processed under a 0 T and 10 T magnetic field are shown in Fig. 5-2-12. The samples were placed in the SQUID with H_α // H, and the sample with H_α = 10 T shows a larger diamagnetic susceptibility due to the texture of the domains. The T_c for both samples are 90 K, demonstrating that the magnetic field does not influence the intrinsic superconducting properties of the superconductor Y - 123. The hysteresis of the samples under H_α = 0 T and 10 T with H_α // H and $H_\alpha \perp$ H are shown in Figs. 5-2-13 (a) and (b). For H_α = 0 T, there is a very small difference when the sample was placed in the two directions. This small difference may be due to some minor factors, such as sample shape or insufficient number of domains in the measured sample. When H_α = 10 T, the big difference between the curves can be seen when the sample was placed in the two directions, i.e. H_α // H and $H_\alpha \perp$ H. The magnetic anisotropy factors (η = $\Delta M(H_\alpha$ // H) / $\Delta M(H_\alpha \perp$ H)) were plotted as a function of the measurement magnetic field H for the samples processed under different magnetic fields in Fig. 5-2-14. Clearly, the magnetic anisotropy factor η increases with increasing magnetic field for different measurement fields, H. We choose the η value at H = 2 T and plot η(H = 2T) as a function of the magnetic field H_α in Fig. 5-2-15.

From Fig. 5-2-15, we can see that both structural anisotropy factor F and the magnetic anisotropy factor η increase with increasing magnetic field H_α. When H_α reaches around 2 T, both F and η begin to reach the saturation point. From the previous discussion on the texture development dependence of the cooling rate, we know that the degree of texture increases

with decreasing cooling rate under the same magnetic field. Thus if we decrease the cooling rate, the F and η vs H_α curves will shift to the upper left direction. This means that the saturation annealing magnetic field H_α can be reduced by lowering the cooling rate $\mathcal{R}$. There is a trade off between the annealing magnetic field and the cooling rate. In other words, to obtain the same degree of texture, we can use either higher magnetic fields and higher cooling rates, or use lower magnetic fields and lower cooling rates. From a fabrication point of view, it is desirable to obtain larger samples with larger domains. Thus, samples with large textured domains could be produced by lowering the cooling rate and reducing the magnetic field below 1 T. This lower magnetic field can be obtained with larger space in the magnet bore, and a larger furnace could be placed in a lower magnetic field to produce larger volumes of textured bulk material.
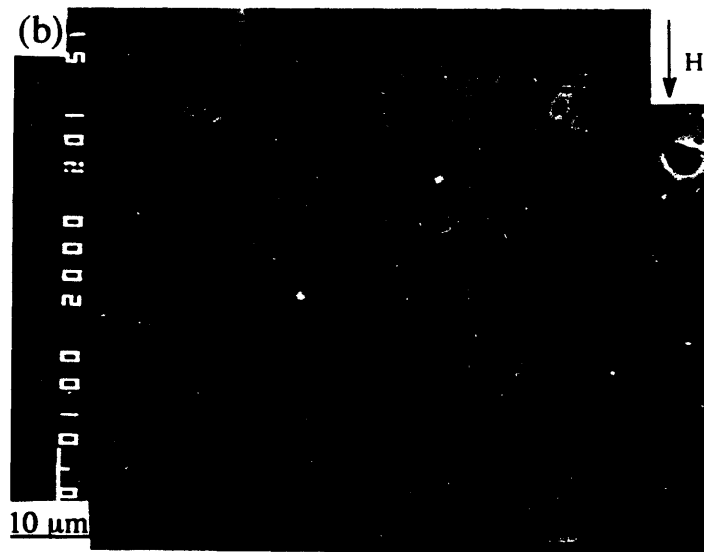
Fig. 5-2-9:   SEM images of polished cross section of inside domain of
YBa$_2$Cu$_3$O$_7$ with $\mathcal{R} = 4^oC$ / hr and T$_m$ = 1075°C.   (a) H$_\alpha$ = 0
T and (b) H$_\alpha$ = 10 T.
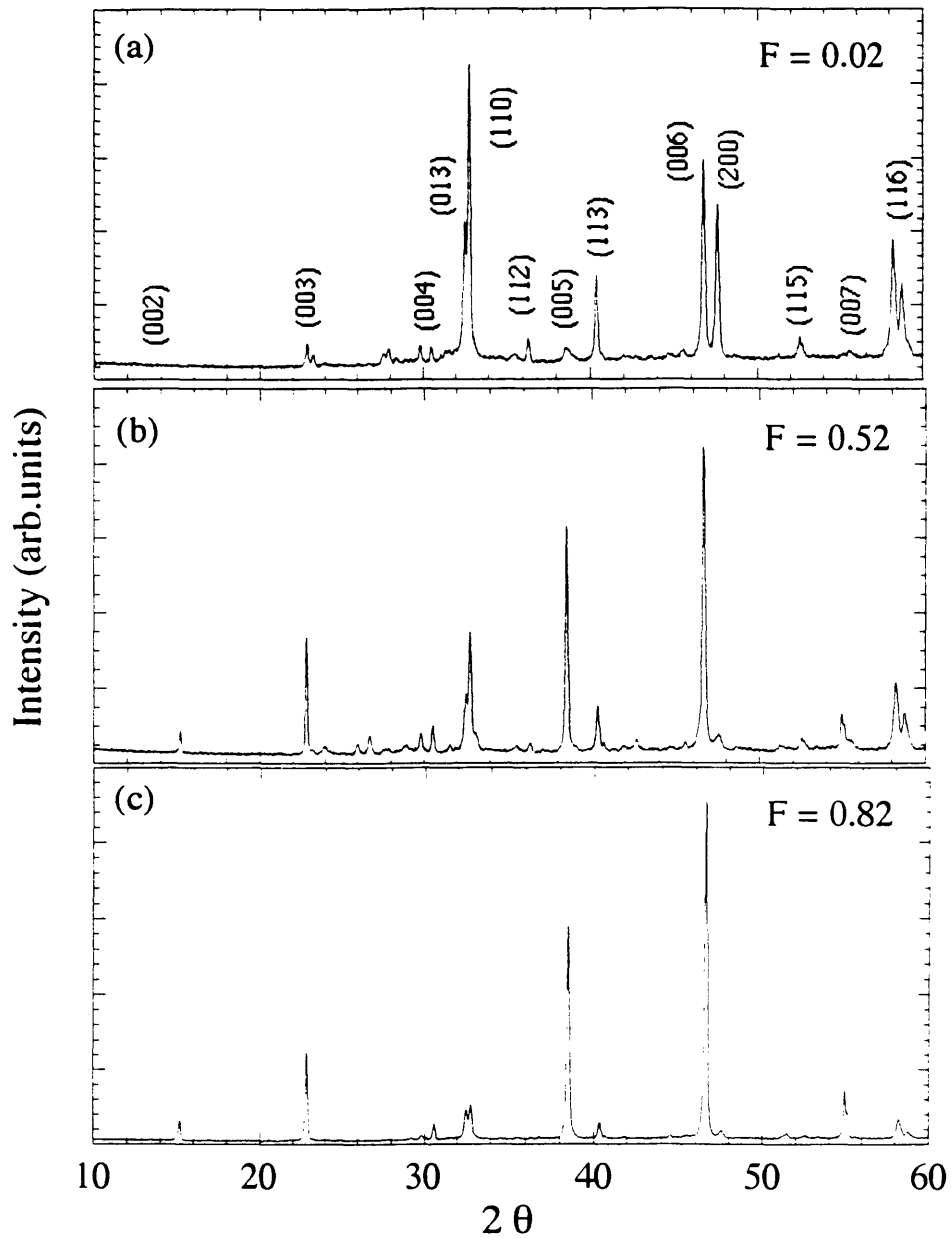
Fig. 5-2-10: X - ray diffraction patterns of $YBa_2Cu_3O_7$ polished along

transverse direction of magnetic field, with $T_m = 1075^oC$ and

$\mathcal{R} = 16^oC$ / hr. (a) $H_\alpha = 0$ T, (b) $H_\alpha = 1.5$ T and (c) $H_\alpha = 10$ T.

Fig. 5-2-11:   SEM images of polished cross section of $YBa_2Cu_3O_7$ with

$R = 16^{\circ}C$ / hr and $T_m = 1075^{\circ}C$. (a) $H_\alpha = 0$ T, (b) $H_\alpha = 2.5$ T.
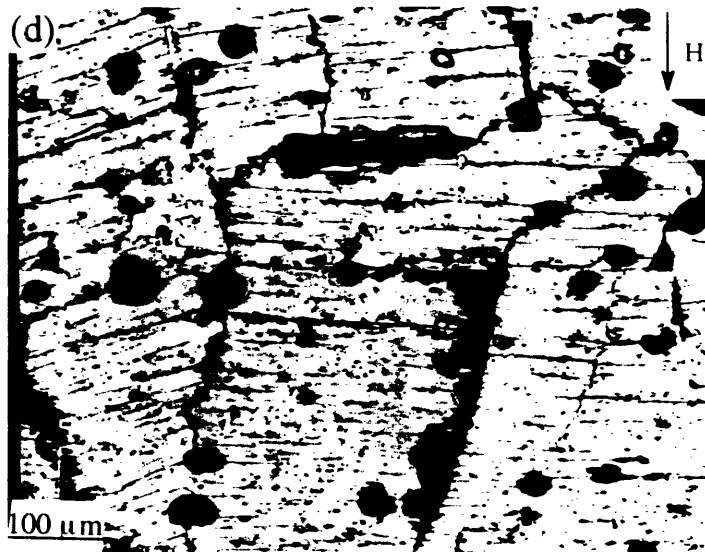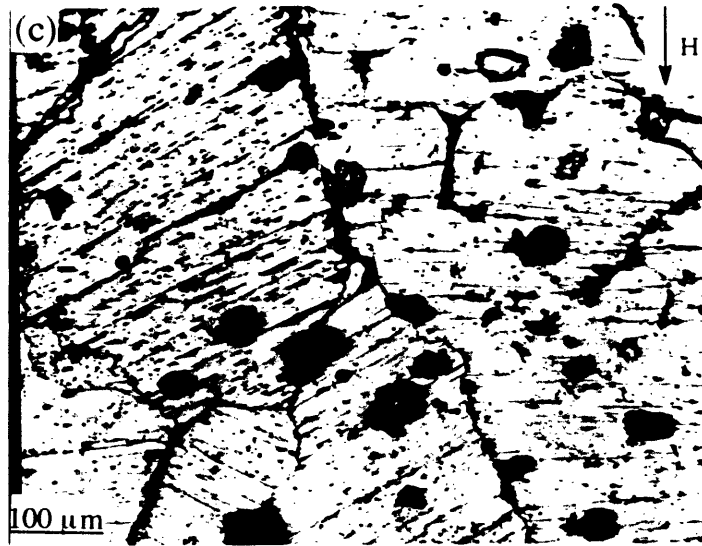
Fig. 5-2-11: SEM images of polished cross section of $YBa_2Cu_3O_7$ with

$\mathcal{R}$ = 16°C / hr and T_m = 1075°C. (c) H_α = 5 T and (d) H_α = 10 T.
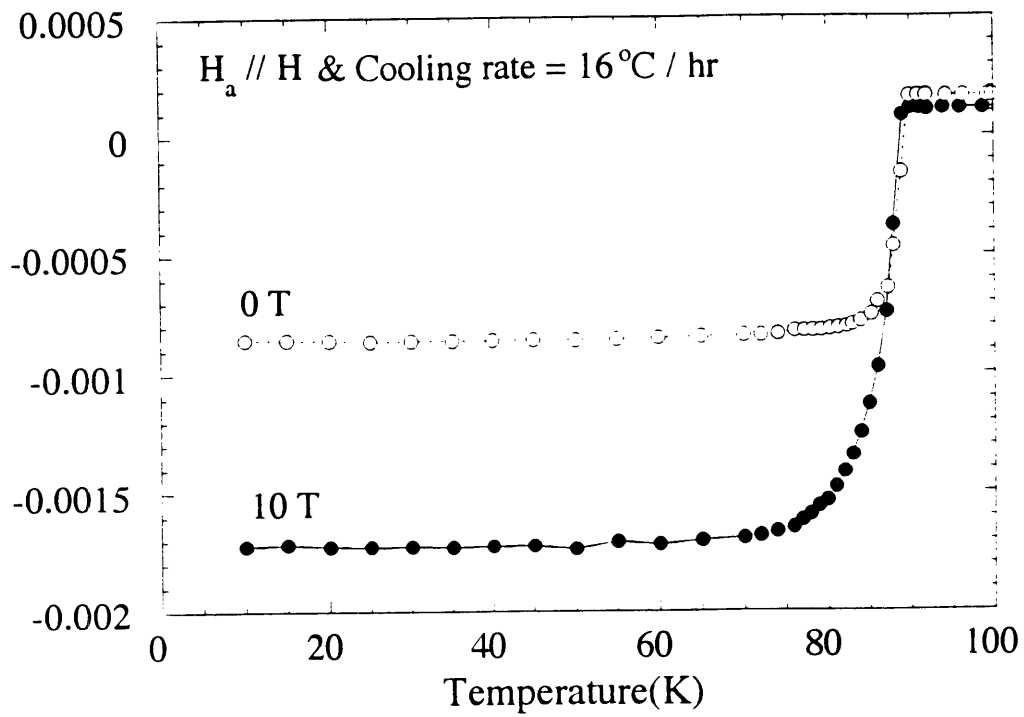
Fig. 5-2-12: Temperature dependence of diamagnetic susceptibility of

YBa2Cu3O7 with T_m = 1075°C, $\mathcal{R}$ = 16°C / hr for H_α = 0 T

and H_α = 10 T. The sample was placed in H_α // H direction.
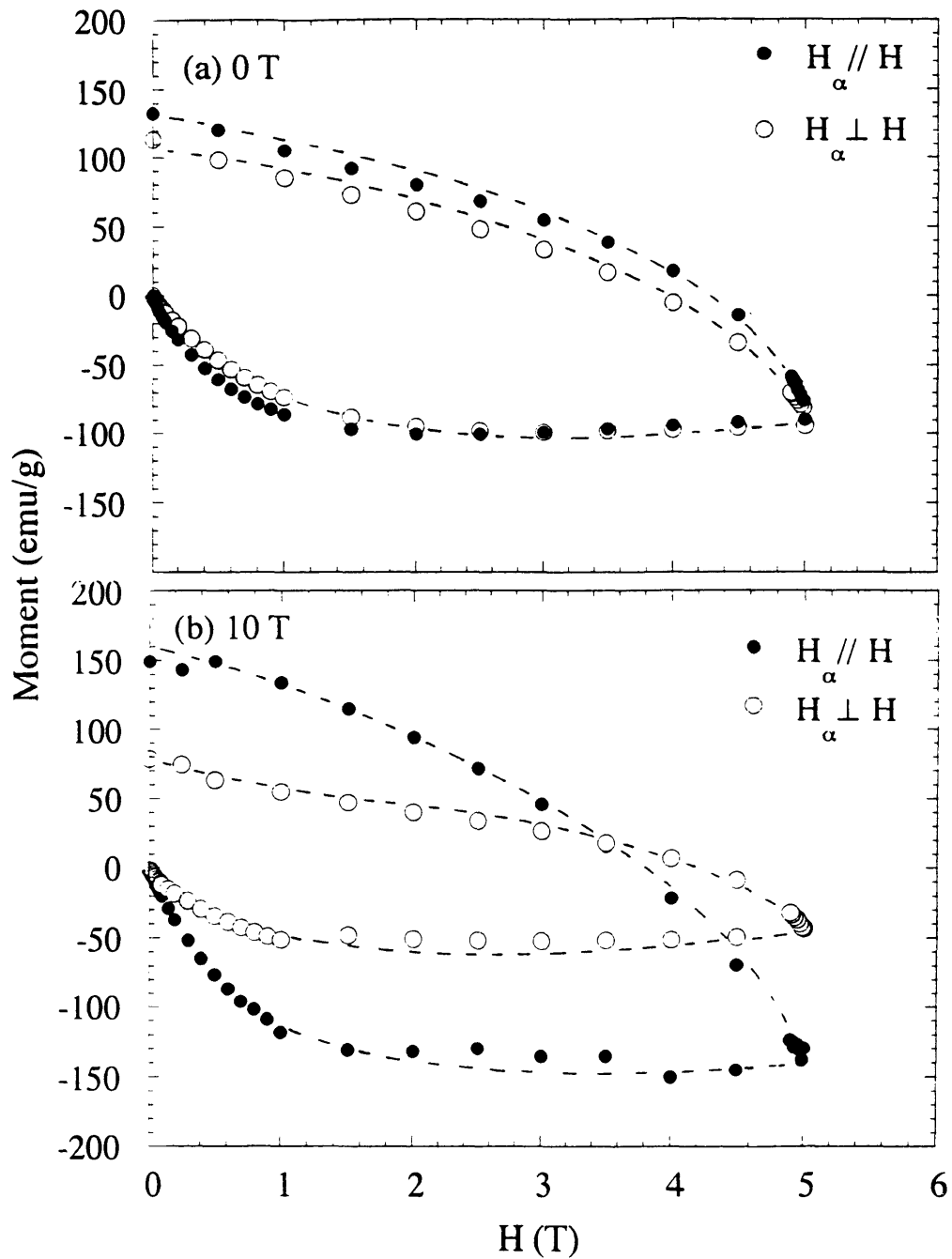
Fig. 5-2-13: Magnetic hysteresis at 4.2 K of $YBa_2Cu_3O_7$ with T_m = 1075°C and $\mathcal{R}$ = 16°C / hr were measured in two directions, i.e. H_α // H and $H_\alpha \perp$ H. H_α is the processing field and H is the measuring field. (a) H_α = 0 T and (b) H_α = 10 T.
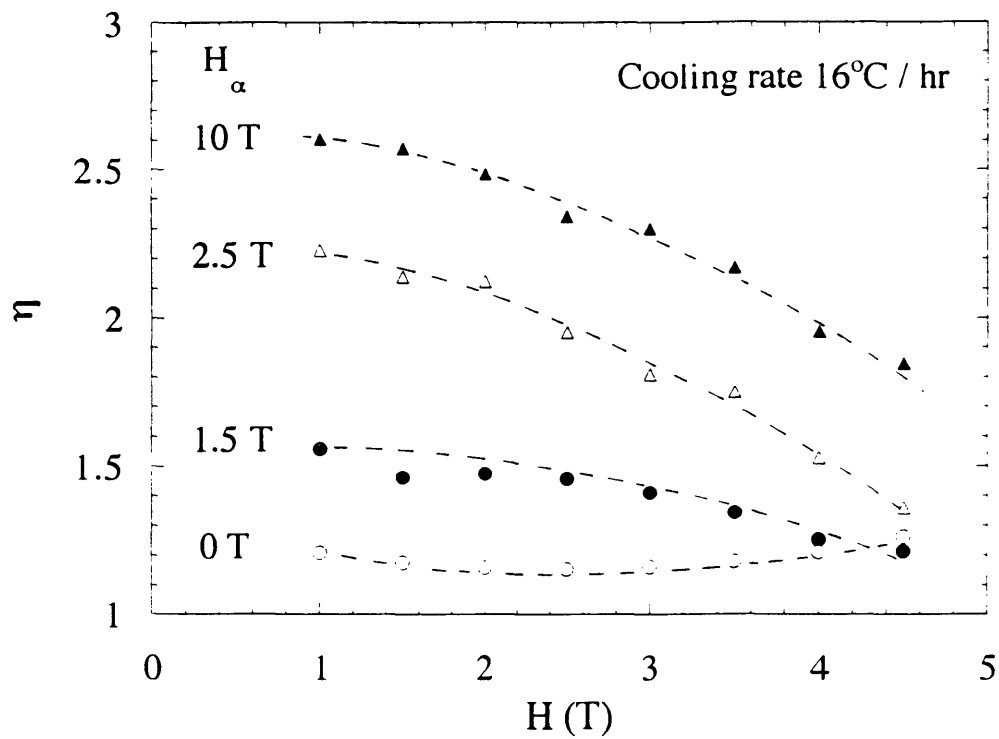
Fig. 5-2-14: Magnetic anisotropy factor $\eta = \Delta M(H_\alpha /\!/ H) / \Delta M(H_\alpha \perp H)$

dependence of measurement magnetic field H for $H_\alpha = 0$

T, 1.5 T, 2.5 T and 10 T.
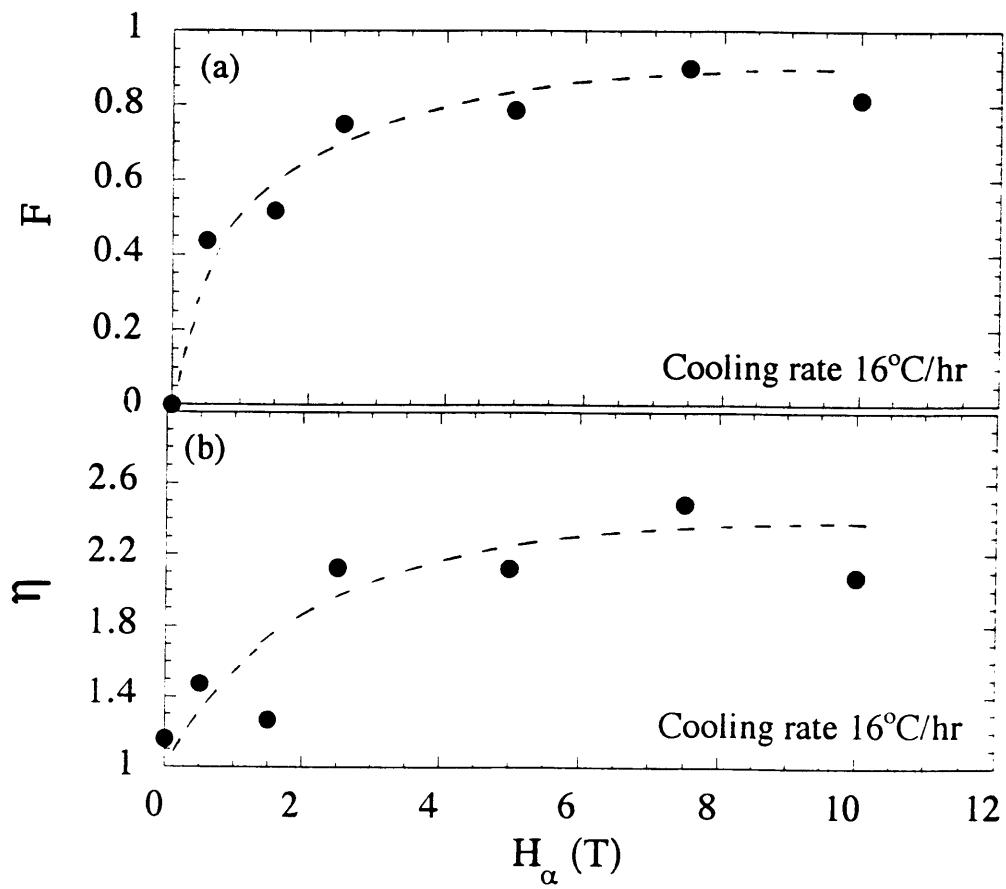
Fig. 5-2-15: (a) F factor and (b) $\eta = \Delta M(H_\alpha \mathbin{/\!/} H) / \Delta M(H_\alpha \perp H)$ dependence of

magnetic field of $YBa_2Cu_3O_7$ with $T_m = 1075^\circ C$ and $\mathcal{R} = 16^\circ C$ / hr.

5.2.5: Maximizing the diamagnetic moment

For magnetic levitation applications, the levitation force f can be written as [26]

$$f = m \, dH/dx$$

m is the diamagnetic moment of the superconductor and dH/dx is a field gradient produced by the magnet. Thus in order to increase the levitation force, the diamagnetic moment and the size of the superconductor must be increased. For levitation applications, the size of the superconductor required is very large. It is impossible to grow single domain superconductors for this kind of application, because the domain growth rate is very low leading to very long growth times. If a superconductor bulk material contains many domains which are misoriented, the diamagnetic moment will be reduced because of the anisotropic property of the superconductor. This effect can be seen clearly in Fig. 5-2-16, in which the magnetic anisotropy factor η was plotted as a function of structure anisotropy factor F. η increases with increasing F. If a bulk superconductor with many domains was textured, along the c - axis direction, the diamagnetic moment will be maximized, and the levitation force will be maximized. Thus we can decrease the cooling rate to increase the domain size in a low magnetic field to increase the diamagnetic moment.

After the domains are textured, the next problem is to introduce pinning centers. There are many papers published in this field. The pinning can be increased either by neutron irradiation [27] or by 211 phase addition during melt - growth [26].
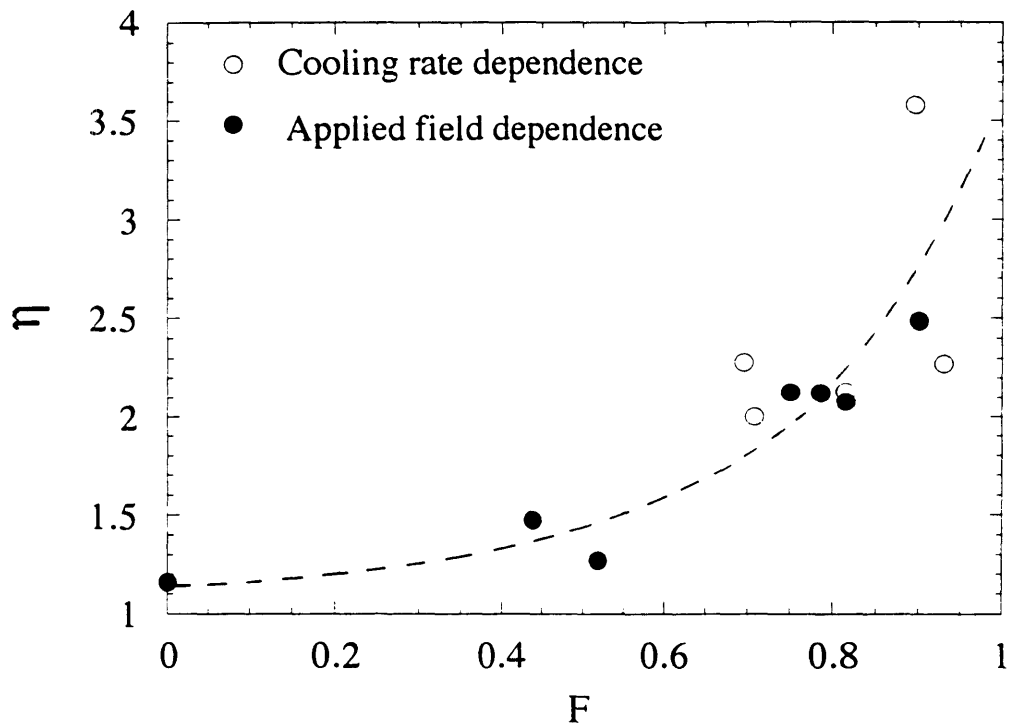
Fig. 5-2-16:   Magnetic anisotropy factor $\eta = \Delta M(H_\alpha // H) / \Delta M(H_\alpha \perp H)$

as a function of F factor. Open circle: data comes form

cooling rate dependence, and filled circle: data comes from

magnetic field dependence.
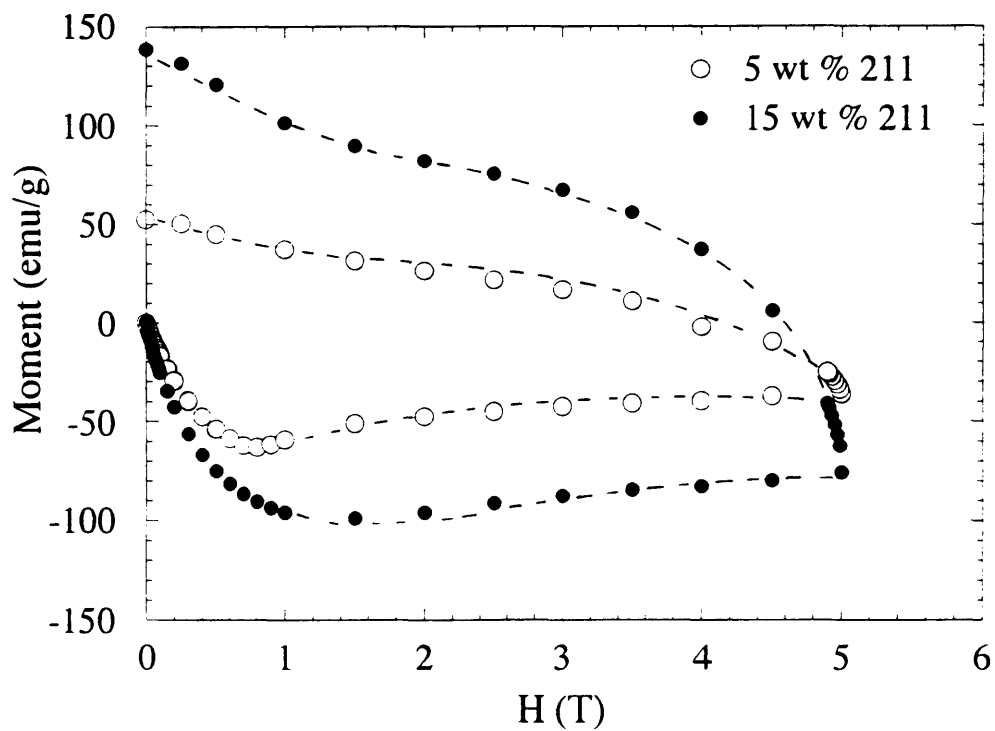
Fig. 5-2-17: Magnetic hysteresis at 4.2 K of powder $YBa_2Cu_3O_7$ added
with 211 phase under $T_m = 1075^oC$, $H_\alpha = 10\,T$ and $\mathcal{R} = 16^oC$
/ hr.

A small amount of Ag addition also can increase the diamagnetic moment [26]. More details about pinning will not be discussed here.

In summary, the levitation force could be maximized by melt - growth of Y - 123 + 211 under a magnetic field. A combination of a low cooling rate and a low magnetic field could be used to fabricate large, bulk Y - 123 materials in a useful size.

5.2.6: Grain growth direction of $RBa_2Cu_3O_7$ under a 10 T magnetic field.

The domain orientation of R - 123 depends on the rare earth elements when the materials were processed under a 10 T annealing magnetic field. This effect can be seen in Figs. 5-2-18(a), (b), (c) and (d).   When the samples were melt - grown under a 10 T magnetic field with cooling rate $\mathcal{R} = 16^{\circ}C$ / hr, the c - axis of the domains is parallel to the magnetic field direction and a-b planes are mis-oriented for R = Ho and Gd, and the a - b planes of the domains are almost parallel to the magnetic field and c - axes are mis-oriented for R = Er.

For $Y_1Ba_2Cu_3O_7$, there are no magnetic elements in the compound. The magnetic alignment of $Y_1Ba_2Cu_3O_7$ should result from anisotropy in the paramagnetic susceptibility associated with the Cu - O conducting planes [7]. Since the susceptibility parallel to the c - axis is higher than that perpendicular to the c - axis, the compound should align with the c - axis parallel to the applied field direction. For $R_1Ba_2Cu_3O_7$ with R = rare earth elements, the paramagnetic susceptibility is dominated by the R^{3+} ion, and the source of anisotropy is single - ion anisotropy associated with crystal fields at the rare - earth site. For $R_1Ba_2Cu_3O_7$ it was observed that for R = Gd and Ho the particles align with c // H but the opposite way (c ⊥ H) for R = Er [18] while

curing in epoxy at room temperature. From the grain orientation point of view, this is consistent with our results. But there is a key difference, i.e. in our work the liquid is created by melting the materials and in reference [18] the liquid is organic solvent. When the grains were textured by a high magnetic field in organic solvent, only a limited increase in J_c has been obtained since during heat treatment the organic species reacted with the Y - 123 phase producing secondary phases at the grain boundaries [17]. When the materials were textured by a high magnetic field during melt - growth, not only the textured larger domain structure can be obtained, but also textured small grains with better connection between the grains can be achieved by liquid phase binding during high temperature processing under a high magnetic field.
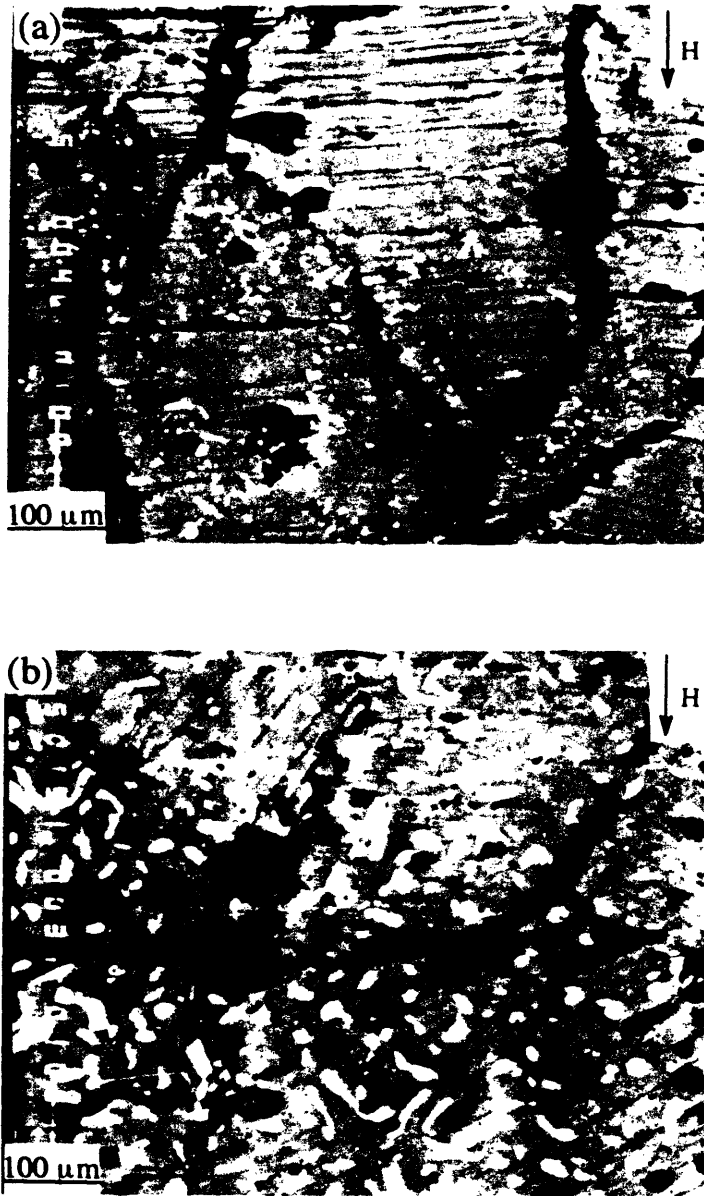
Fig. 5-2-18: SEM images of polished cross section of $RBa_2Cu_3O_7$ with

$\mathcal{R} = 16^\circ C$ / hr $H_\alpha = 10$ T and $T_m = 1075^\circ C$. (a) R = Ho, (b) R = Gd.

(c)

⊙ H

100 um

(d)

H

100 um

Fig. 5-2-18: SEM images of polished cross section of $RBa_2Cu_3O_7$ with

$R = 16^oC$ / hr $H_\alpha = 10$ T and $T_m = 1075^oC$. (c) and (d) R = Er.

5.2.7: Conclusion

Bulk $R_1Ba_2Cu_3O_7$ superconductors were melt - grown under an elevated magnetic field (0 ~ 10 T). Under a 10 T magnetic field, the degree of texture increases with increasing T_m. The domain alignment depends on the cooling rate and magnetic field strength, the higher the cooling rate, the larger the magnetic field required to produce a certain degree of texture. There is a trade off between the cooling rate and the magnetic field. We can use either a higher magnetic field and higher cooling rate, or use a lower magnetic field and lower cooling rate to obtain the same degree of the texture. The domain orientation under a high magnetic field is determined by the ionic moment orientation of the rare earth element in $RBa_2Cu_3O_7$ (R = Ho, Gd and Er).

Chapter 6. Processing Bi - 2212 / Ag Thick Films and Tapes Under A High Magnetic Field

Section 6.1. Overcoming the Bi -2212 / Ag interface effect via application of a magnetic field

The grain orientation of Bi - 2212 / Ag thick films can be controlled by application of a 10 T magnetic field during high temperature annealing. With a liquid phase present, the grains can be rotated by a 10 T magnetic field. The c - axis of the grains produced are parallel to the applied magnetic field H_α, i.e. the c - axis of the grains can be perpendicular or parallel to the silver substrate depending upon the magnetic field orientation. A 10 T magnetic field can overcome the Bi - 2212 / Ag interface effect and dominate the Bi - 2212 grain orientation and texture development when a liquid phase is present.

6.1.1. Thick film preparation and processing

The starting materials were first prepared by solid state reaction. Highly pure Bi_2O_3, $SrCO_3$, $CaCO_3$, PbO and CuO are weighed according to the normal composition $Bi_{1.6}Pb_{0.4}Sr_2CaCu_2O_x$. The mixed powders were first reacted at 800°C for 12 hours in air. The samples were then ground in an agate mortar and pestle, then pressed into pellets and sintered at 860°C for 24 hours. The samples were finally ground into fine particles and the particles were deposited on silver foil in isopropanol. The thick films were dried at 100°C for several hours and heated to 920°C for 5 minutes, and then quenched to room temperature in air. The quenched amorphous Bi - 2212 thick films were processed at 820°C - 840°C under a 10 T magnetic field. The high

temperature furnace is placed in the room temperature bore of a superconducting magnet. Magnetic fields of up to 10 T are oriented parallel to the long axis of the furnace throughout the processing cycle. The field was increased to 10 T, then the temperature was raised above 820°C - 840°C and held for 10 hours. After the process, the temperature was decreased to room temperature, then the magnetic field was reduced to zero. We placed samples in the field in two orientations. In one case, the surface of the film is perpendicular to the magnetic field and in the other case the surface of the film is parallel to the magnetic field.

6.1.2. Results and discussion

The SEM images of the surface and polished cross section of a sample which was annealed at 830°C ~ 840°C under a 10 T magnetic field is shown in Figs. 6-1-1(a) and 1(b). It is clear that the grains were textured both near the surface and under the surface, when the field was applied perpendicular to the surface of the film. Thus, the c - axis of the grains is parallel to the applied magnetic field. Surface X - ray diffraction patterns of the sample show strong (00ℓ) peaks and very weak (103), (105), (107) and (110) peaks. For this film, since the thickness is around 20 - 30 μm, we can not ignore the Bi - 2212 / Ag interface effect which enhances texture development near the interface. It is known that the Bi - 2212 / Ag interface plays an important role in texture development of the Bi - 2212 grains for Bi -2212 thick films and tapes [28]. The c - axis of Bi - 2212 grains is always perpendicular to the Bi - 2212 and silver interface [30]. The thinner the Bi - 2212 core, the greater the degree of texture obtained [29]. When the core thickness is about 20 μm, a well textured structure can be provided by the interface effect alone [28]. In our experimental condition, the temperature was controlled at around 830°C ~

840°C so that there is a liquid phase at the Bi - 2212 / Ag interface [31]. Thus, the interface effect will improve texture development. At the same time, surface nucleation and growth will also result in texture development of the other side of the film. When the field was applied perpendicular to the film surface, both the magnetic field and the Bi - 2212 / Ag interface have the same effect on the grain orientation of Bi - 2212, i.e. the c - axis of Bi - 2212 is perpendicular to the film surface. In this situation, we can not differentiate between these effects on the texture development in Bi - 2212.

In order to verify the magnetic field effect on the grain orientation, we processed an additional film with surface parallel to the magnetic field at the same processing temperature. The SEM images of the surface and polished cross sections of the sample processed under a 10 T magnetic field for 10 hours are shown in Figs. 6-1-1(c) and (d). For this case, the c - axis of most grains is parallel to the film surface. However, near the surface the c - axis of most grains is perpendicular to the Ag substrate. This effect can also be seen from the surface X - ray diffraction pattern (Fig. 6-1-2(b)). Although the SEM images of the polished cross sections show that the c - axis of the grains below the surface is parallel to the Ag substrate, X - ray diffraction patterns exhibit strong (00ℓ) diffraction peaks. It is known that X - rays only penetrate a few micrometers [32], therefore only the grains near the surface can be detected by X - ray diffraction and the grains deeper into the sample can not be analyzed. As we mentioned before, although the c - axis of most grains is parallel to the film surface when the magnetic field is parallel to the Ag substrate, the c - axis of some grains near the surface is still perpendicular to the Ag substrate. This effect can be seen from surface SEM images (Fig. 6-1-1(c)). However, the grains (c - axis $\perp$ surface) near the surface do not cover the entire surface of the

film (Fig. 6-1-1(c)), the intensity of the (103), (105), (107) and (110) diffraction peaks increases and the (200) peak appears in this case. The X - ray diffraction pattern and SEM images are therefore consistent.

The overall anisotropic effect of the grain growth is embodied in the measurement of the temperature dependence of the diamagnetic susceptibility (Fig. 6-1-3) and magnetic hysteresis at 4.2 K (Fig. 6-1-4). In the magnetic measurement, the magnetic field H was applied perpendicular to the film surface for both samples (the SEM images are shown in Fig. 6-1-1). Thus the sample with H // H_α (the c - axis of most grains is parallel to H) shows a large diamagnetic moment, and the sample with H $\perp$ H_α (the c - axis of most grains is perpendicular to the H) shows a small diamagnetic moment. This is consistent with the SEM and X - ray diffraction results. For both samples, superconducting transition temperature is the same, i.e. 76 K, but the ratio of the low temperature susceptibility for the samples is $\chi(H // H_\alpha)$ / $\chi(H \perp H_\alpha)$ = 3.5. Magnetic hysteresis at 4.2 K for both samples also shows the bulk anisotropic effect. This implies that a 10 T magnetic field does not affect the Bi - 2212 phase formation and superconductivity, it only affects the grain orientation of the Bi - 2212 superconductor.

Once the grain size of Bi - 2212 has grown larger than the critical volume V_c during the processing, the magnetic field will tend to rotate the grains by mechanical interaction between the grains. This effect is unlikely to happen in the solid state. If there are liquid phases present between the grains, the grains will be more easily rotated by the magnetic field. It is known that the melting point of Bi - 2212 doped with Pb in air is around 870°C and it also can be reduced more than 30 K [32] by Ag additions. In our experiment, it is clear that there is a liquid phase at the interface and Bi - 2212

remains solid away from the interface. When the magnetic field is parallel to the film surface, if a grain with $V > V_c$ contacts with Ag, i.e. it contacts with a liquid phase at the interface, the grain will be easily rotated by a 10 T magnetic field. This rotation effect leads to the c - axis of most grains which contact Ag being parallel to the film surface (Figs. 6-1-1(d) and (e)), i.e. the c - axis is parallel to the magnetic field, H_α. For the grains near the film surface where there is no liquid phase, the mechanical force acting on the grains is insufficient to rotate the grains in the solid state. Thus, near the surface grains do not contact Ag (the grains do not contact with liquid phase) and can not be rotated by the magnetic field. The grain orientation is controlled by surface nucleation and growth. If the processing temperature was decreased below 820°C, there is no apparent grain orientation under the same magnetic field. This is similar to the bulk Bi - 2212 material case where it was observed that bulk Bi - 2212 processed under a 10 T magnetic field below its melting point, there was no apparent grain orientation observed [29].

Evidence which supports the rotation process is that, when the film surface is parallel to the magnetic field direction, the Bi - 2212 / Ag interface no longer remains flat as is the case for melt - growth Bi - 2212 thick film or tape. The liquid phase has moved into the Bi - 2212 material due to grain rotation (Figs. 6-1-1(d) and (e)). It can be clearly seen that the Ag inserts itself between the Bi - 2212 grains when the magnetic field was parallel to the film surface (Figs. 6-1-1(d) and (e)). If the Bi - 2212 / Ag interface effect still dominates the texture development when a 10 T magnetic field is parallel to the thick film surface during the annealing, the c - axis of the grains would be perpendicular to the Bi - 2212 / Ag interface. But since this is not the case, a 10 T magnetic field is strong enough to overcome the interface effect and rotate

the c- axis of the grains to be parallel to the magnetic field H_α. It implies that if a 10 T magnetic field is applied perpendicular to the surface of the thick film or tape with a liquid phase, the magnetic field will dominate the texture development and enhance the degree of the texture through the whole body of the Bi - 2212 superconductor.

6.1.3. Conclusion

In conclusion, a 10 T magnetic field is strong enough to overcome the Bi - 2212 / Ag interface effect and dominate grain orientation with a liquid phase present. The c - axis of Bi - 2212 grains is always parallel to the magnetic field direction and do not depend on the Bi - 2212 / Ag interface orientation. A high magnetic field can be used in combination with a partial melting process to increase degree of the texture of the whole body of a Bi - 2212 superconductor in thick film or tape form.
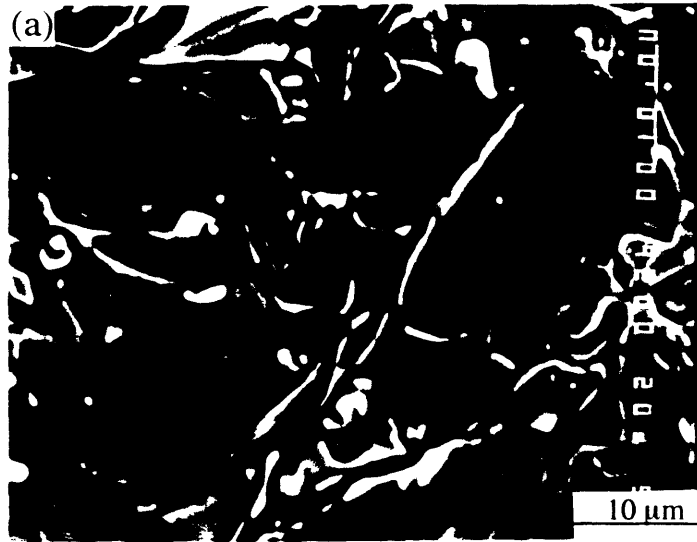
Fig. 6-1-1: SEM images of the samples processed under a 10 T

magnetic field for 10 hours. (a) surface image of the

sample processed with surface perpendicular to the

processing magnetic field H_α. (b) image of polished cross

section of the sample processed with surface perpendicular

to the processing magnetic field H_α.

(c)

10 μm

(d)   H_A

Ag

10 μm
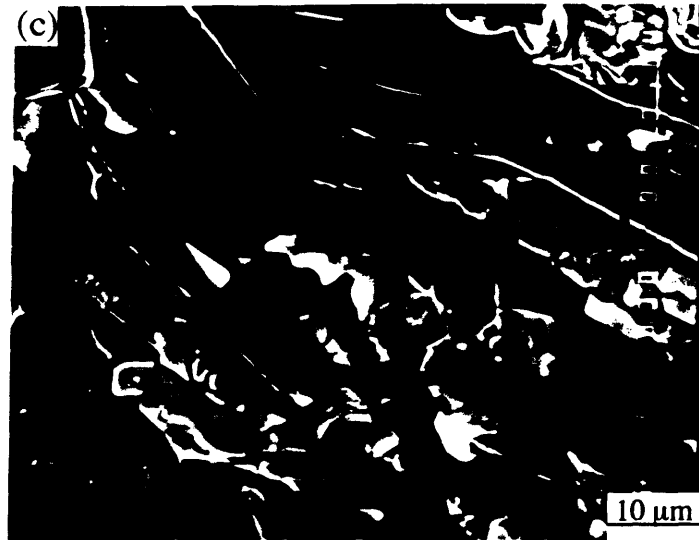
Fig. 6-1-1:   SEM images of the samples processed under a 10 T

magnetic field for 10 hours. (c) surface image of

the sample processed with surface parallel to the

processing magnetic field H_a, (d) image of polished cross

section of the sample processed with surface parallel to the

processing magnetic field H_a.   181
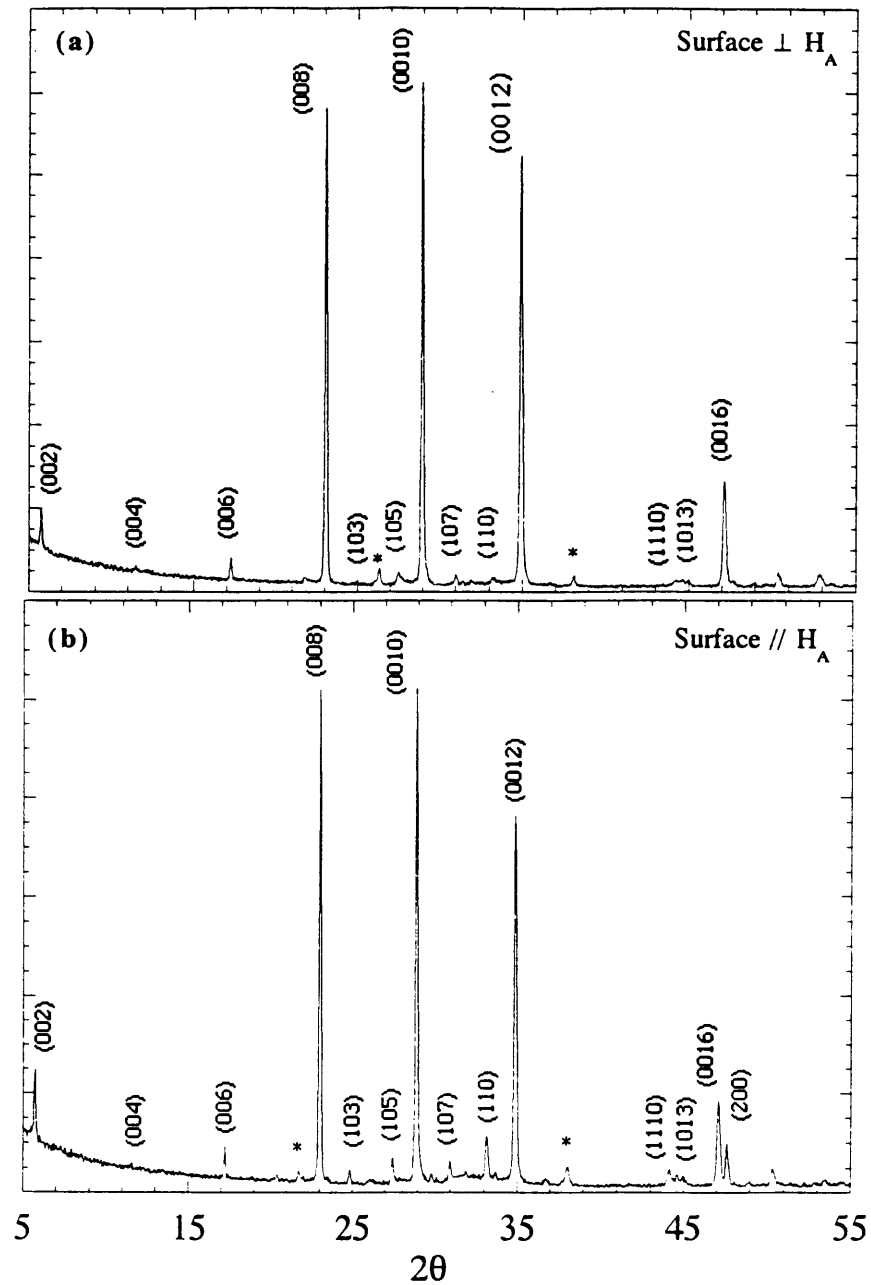
Fig. 6-1-2:   Surface X - ray diffraction of samples processed under a 10

T magnetic field. (a) sample processed with surface

perpendicular to the processing magnetic field H_α, (b)

sample processed with surface parallel to the processing

magnetic field H_α. * shows a small amount of impurity

phase.
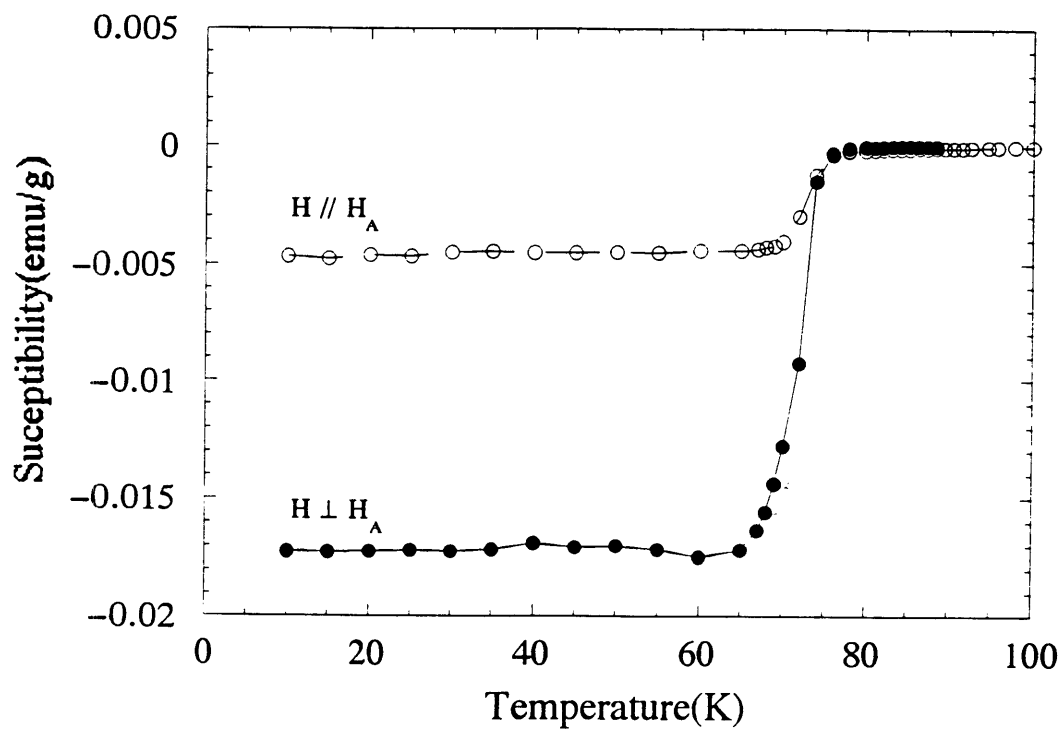
Fig. 6-1-3:   Temperature dependence of diamagnetic susceptibility of

samples processed under a 10 T magnetic field with surface

perpendicular to the processing magnetic field H_α and

with surface parallel to the processing magnetic field H_α.

Measurement field H is perpendicular to the thick film

surface for both samples.
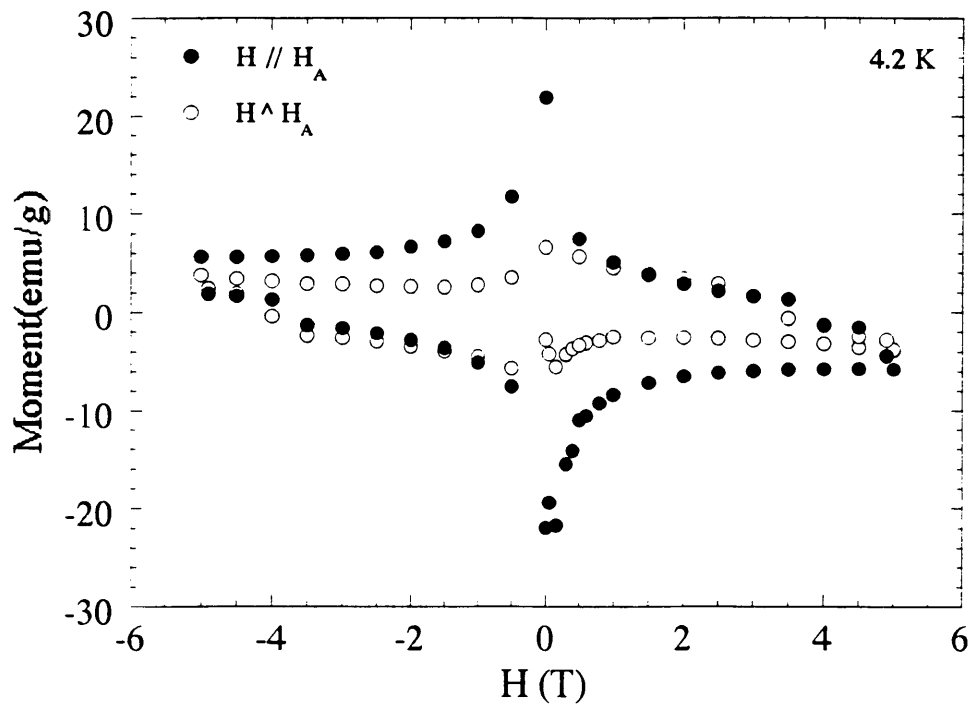
Fig. 6-1-4: Magnetic hysteresis at 4.2 K of samples processed under a
10 T magnetic field with surface perpendicular to the
processing magnetic field H_α and with surface parallel to the
processing magnetic field H_α. Measurement field H is
perpendicular to the thick film surface samples.

Section 6. 2: J_C enhancement of $Bi_2Sr_2CaCu_2O_8$/Ag thick films melt - growth under elevated magnetic fields (0 ~ 10 T)

Thick films with different thicknesses from 25 μm to 125 μm were melt - grown under an elevated magnetic field. The degree of texture and transport critical current, J_c, of thick films with different thickness were enhanced by application of the magnetic field. J_c increases with increasing magnetic field and the saturation magnetic field decreases with decreasing thickness of the film. This method leads to relatively rapid processing of highly textured Bi - 2212/Ag thick film or tape.

6. 2. 1: Experiment

The starting materials were first prepared by solid state reaction. Highly pure Bi_2O_3, $SrCO_3$, $CaCO_3$ and CuO are weighed according to the normal composition $Bi_2Sr_2CaCu_2O_8$. The mixed powders were first reacted at 800°C for 12 hours in air. The samples were then ground in an agate mortar and pestle, then pressed into pellets and sintered at 860°C for 24 hours. The samples were finally ground into fine particles and the particles were deposited on silver foil in isopropanol with different thicknesses. The thick films were dried at 100°C for several hours and heated to 885°C for 5 ~ 10 minutes, and then were cooled at 1°C/min to 840°C under an elevated magnetic field. The thick films were then cooled to room temperature by furnace cooling. The high temperature furnace is placed in the room temperature bore of a superconducting magnet. Magnetic fields of up to 10 T are parallel to the long axis of the furnace throughout the processing cycle. The magnetic field was increased, then the temperature was raised to 885°C

and finally the cooling processes followed. After the process, the temperature was decreased to room temperature, then the magnetic field was reduced to zero. The surface of the film is perpendicular to the magnetic field. After processing under a high magnetic field, the thick films were annealed in zero field at 800°C ~ 840°C for 24 hours. This low temperature annealing processing does not influence grain orientation.

6. 2. 2: Results and discussion

SEM images of polished cross sections of the thick films with different thickness are shown in Fig. 6-2-1 and Fig. 6-2-2. When the films were processed under a zero magnetic field, the degree of texture decreases with increasing thickness of the film (Fig. 6-2-1(a), (b), (c) and (d)). When the thickness of the film is below 40 μm (Fig. 6-2-1(a) and (b)), most of the grains grow with their ab planes parallel to the Ag surface. When the thickness of the films increases, grains of the thick film begin to grow randomly (Fig. 6-2-1(c) and (d)). In contrast to this, when the thick films were melt - grown under a 10 T magnetic field, the degree of texture of the films is unchanged when the thickness increases. The entire thickness of the Bi - 2212 material grows with the c - axis parallel to the magnetic field.

Transport critical current densities of the thick films at 4.2 K are plotted as a function of the thickness of the films which were processed under a zero magnetic field and under a 10 T magnetic field in Fig. 6-2-3. When the thickness of the film increases, the J_c (4.2K) decreases for both groups of films which were processed under a zero magnetic field and under a 10 T magnetic field. However, the J_c curves for the films processed under a 10 T magnetic field shifts upward. J_c of the films with different thickness was improved by

application of a 10 T magnetic field during the melt- growth. For the films processed under a zero magnetic field, the J_c decrease with increasing thickness can be understood as the degree of texture decreasing with increasing thickness. It is, therefore, difficult to increase J_c in thicker films due to random grain growth under a zero magnetic field. For films processed under a 10 T magnetic field, J_c also decreases with increasing thickness. However for this case, the decrease in the J_c is not a result of poor texture, but a result of imperfect grain contact. If the grain contact is improved by a proper thermal processing sequence, the J_c of the thicker film will approach that of thinner films. This is a potential way to fabricate thick films or tapes with large critical currents.

In Fig. 6-2-4, the J_c dependence on applied magnetic field for two types of films with thickness 25 μm and 125 μm is plotted. For both cases, J_c increases with increasing magnetic field. For d = 25 μm, the saturation magnetic field is around 2 T and further increasing the magnetic field does not effect the J_c improvement. For d = 125 μm, the saturation magnetic field increases to around 5 T. This suggests that for a thinner film the interface effect will aid the texture development process and the required magnetic field for texture development is reduced. The thinner the film, the lower the saturation magnetic field. We also know that when the cooling rate is decreased, the saturation magnetic field can be reduced. We can, therefore, choose a proper processing thermal sequence to reduce the magnetic field or the processing time. Future improvement in J_c for thicker films will be achieved by optimizing the thermal processing sequence under a magnetic field. We should also point out that under a high magnetic field, the texture development process can be finished during a short period of time· This will

provide a faster way to produce a large quantity of highly textured thick film or tape.

6. 2. 3: Conclusion

The degree of texture and transport critical current J_c of thick films with different thicknesses from 25 μm to 125 μm were enhanced by melt - growth under an elevated magnetic field. J_c increases with increasing magnetic field and the saturation magnetic field decreases with decreasing thickness of the film. Therefore, highly textured Bi - 2212 / Ag thick film or tape can be processed by application of a high magnetic field during melt - growth.

H

0 T

100 μm

Fig. 6-2-1: SEM images of polished cross section of the thick films with different thickness, which were melt - grown under a 0 T magnetic field.
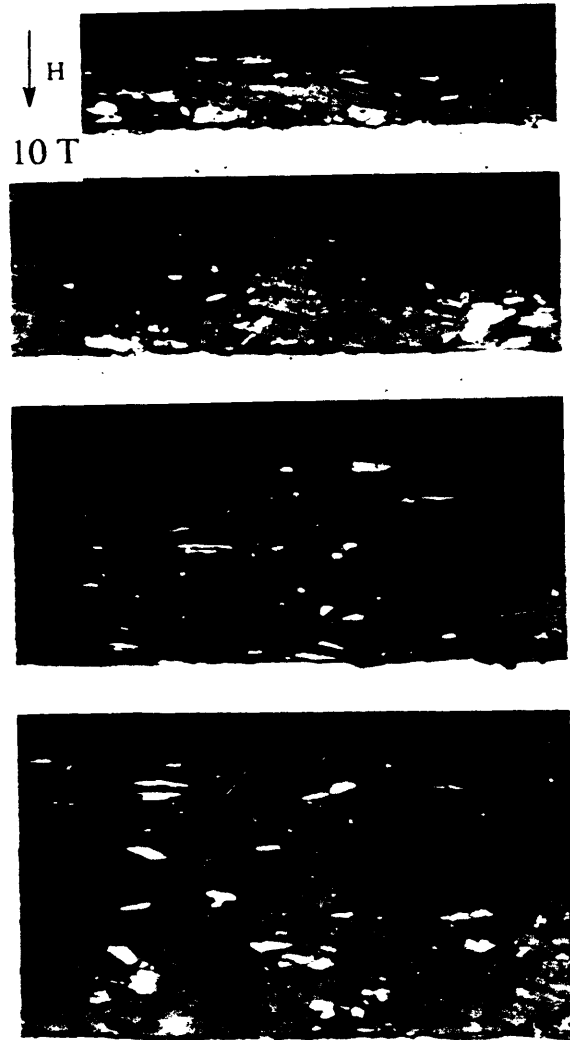
Fig. 6-2-2: SEM images of polished cross section of the thick films with different thickness, which were melt - grown under a 10 T magnetic field.
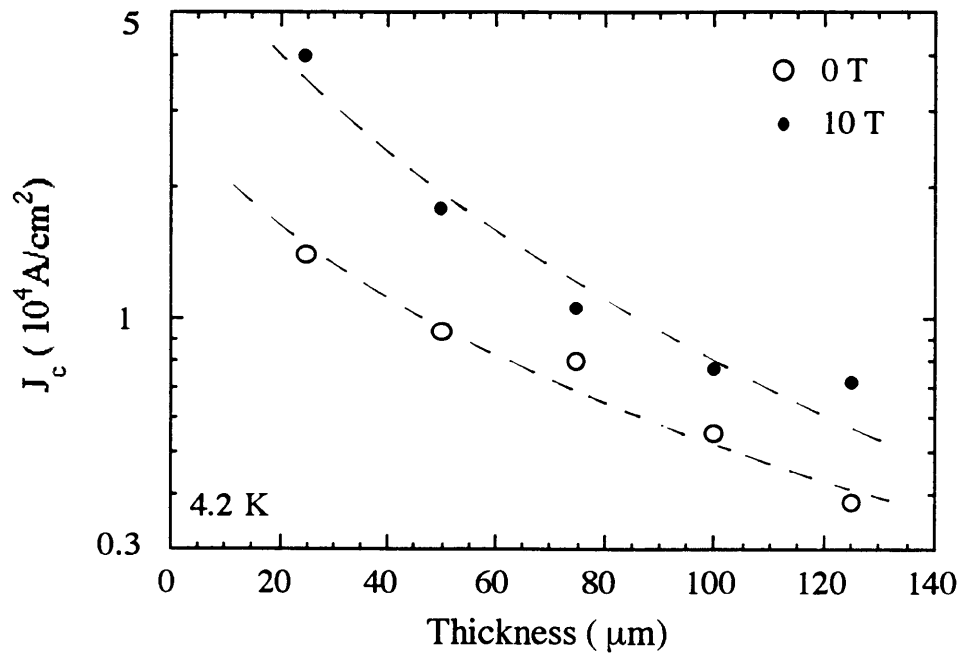
Fig. 6-2-3: Thickness dependence of transport J_c at 4.2 for the films processed
under 0 T and 10 T.
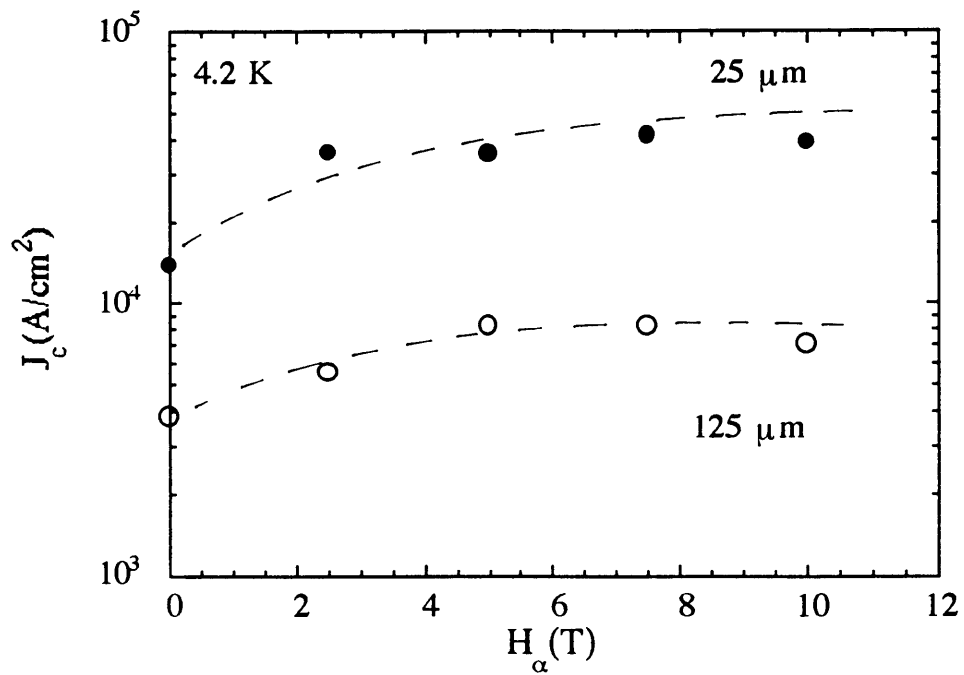
Fig. 6-2-4:   Magnetic field dependence of transport J_c at 4.2 for the films with
thickness 25 µm and 125 µm.

Section 6. 3: J_c Enhancement of $Bi_2Sr_2CaCu_2O_8$/Ag Tapes Melt - Growth under Elevated Magnetic Field (0 ~ 10 T)

Bi - 2212 / Ag tapes with thickness 30 μm were melt - grown under elevated magnetic fields following a new thermal sequence. The transport critical current density J_c dependence on maximum processing temperature, cooling rate, holding time and magnetic field was studied systematically. The impurity phase was reduced by reducing the holding time above the melting point of Bi - 2212 and increasing the cooling rate. The overall degree of texture of the tapes was increased by application of a high magnetic field during the melt - growth. Under the optimized thermal sequence, transport critical currents for Bi - 2212 tapes were enhanced by melt - growth under a high magnetic field. The highest J_c is about 8.3 x 10 ^{4} A/cm^2. It is demonstrated that a well textured structure and higher J_c can be achieved in thicker tapes. Therefore, both the critical current density J_c and the critical current I_c of the Bi -2212 / Ag tapes can be enhanced by application of a high magnetic field during melt - growth.

6.3.1: Experiment

The starting materials were first prepared by solid state reaction. Highly pure Bi_2O_3, $SrCO_3$, $CaCO_3$ and CuO are weighed according to the normal composition $Bi_2Sr_2CaCu_2O_8$. The mixed powders were first reacted at 800°C for 12 hours in air. The samples were then ground in an agate mortar and pestle, then pressed into pellets and sintered at 860°C for 24 hours. The samples were finally ground into powder with fine particles. The tapes were fabricated by standard powder - in - tube method. Then the tapes were melt - grown under an elevated magnetic field (0 ~ 10 T) following different thermal

sequences as shown in Fig. 6-3-1(a), (b) and (c). The tapes were then cooled to room temperature by furnace cooling. The high temperature furnace is placed in the room temperature bore of a superconducting magnet. Magnetic fields of up to 10 T are parallel to the long axis of the furnace throughout the processing cycle. The magnetic field was increased, then the temperature was raised to the maximum processing temperature T_m and finally the cooling processes following. After the process, the temperature was decreased to room temperature, then the magnetic field was reduced to zero. The surface of the tape is perpendicular to the magnetic field. After processing under a high magnetic field, the tapes were annealed in zero field at 840°C for 48 hours. This low temperature annealing processing does not influence grain orientation [5]. Critical current was measured at 4.2 K in zero field by a standard four - probe method. The J_c was determined from I - V curves using a criterion of 1 μV/cm.

6.3.2: Results and Discussions

SEM images of polished cross sections of the tapes are shown in Fig. 6-3-2(a) and (b). When the tapes were processed under a zero magnetic field, most of the grains near the Bi-2212 / Ag interface grow with their ab planes parallel to the Ag surface and the grains in the middle of the core grow randomly. Thus the overall degree of texture is low for the tapes processed under a zero magnetic field. In contrast to this, when the tapes were melt - grown under a 10 T magnetic field, all grains grow with their ab planes parallel to the Bi - 2212 / Ag surface. Thus the entire thickness of the Bi - 2212 material grows with the c - axis parallel to the magnetic field and ab plane parallel to the Bi - 2212 / Ag interface. Therefore, the overall degree of texture of the tape is enhanced by application of a 10 T magnetic field.

194

Transport critical current densities of the tapes which were processed following the thermal sequence (I) and (II) are plotted as a function of the maximum processing temperature T_m in Fig. 6-3-3. When the tapes were processed following the thermal sequence (I), the standard thermal sequence for melt - growth of Bi - 2212 / Ag tapes under a zero magnetic field, the J_c decreases slightly with T_m increase for both groups of tapes which were processed under a zero magnetic field and under a 10 T magnetic field. However, there is no significant difference in J_c between the two groups of tapes. However, the J_c curves shift upward when the tapes were processed under a 10 T magnetic field following the thermal sequence (II). When we reduce the holding time t (from 10 min to 5 min) and increase the cooling rate R (from 10°C / hour to 60°C / hour), the J_c of the tapes with different maximum processing temperature T_m was enhanced by application of a 10 T magnetic field during the melt- growth. When the holding time was reduced to zero, the J_c curve shifts upward again and the highest J_c is around 8.3 x 10^4 A/cm^2. If the tapes were processed under a zero magnetic field even following thermal sequence (II), the J_c values are around 4.5 x 10 ^{4} A/ cm^2 which are close to the J_c vs T_m curves of sequence (I). This can be seen clearly in the J_c dependence on magnetic field presented in a following section. Thus magnetic field is responsible for the J_c enhancement.

We have known that there are three key factors which limit J_c improvement, namely the presence of impurity phases, the degree of texture and grain connectivity. There is a trade - off between texture development and impurity phase formation. A higher T_m and slow cooling rate is required to form a well textured structure, and a lower T_m and a fast cooling rate is required to reduce the impurity phase. In thermal sequence (II), a fast cooling

rate (1°C/min) was chosen during the melt - growth stage to reduce the impurity phase formation, and the texture development process was accelerated by application of a high magnetic field.

When the tapes were processed following thermal sequence (I) (the standard thermal sequence with the tapes processed above the melting point for a longer period of time.), the Bi - 2212 materials were in liquid phase and the textured structure was provided by the Bi-2212 / Ag interface. However, more liquid phase will create more impurity phases during solidification, which will limit the J_c. Thus although application of a 10 T magnetic field increases the degree of texture, it does not improve the J_c for thermal sequence (I) in which the J_c is controlled by the impurity phases. When the tapes were processed following thermal sequence (II), especially when t = 0, there is less liquid phase present due to the short processing time above the melting point and the texture development process was dominated by the grain rotation under a high magnetic field. Thus, for thermal sequence (II), the lower liquid phase content will create less impurity phase during solidification and the J_c will be controlled by the degree of texture. For sequence (II), when the magnetic field was zero and even with less impurity phase, the grains grow randomly and J_c can not be improved. However, when a 10 T magnetic field is applied during thermal sequence (II), the grains will be rotated by the magnetic field, the degree of texture increases and J_cs are enhanced as seen in the Fig. 6-3-3. Therefore, application of a high magnetic field during the melt - growth could let us improve the degree of texture and reduce the impurity phase at the same time. Thus the J_cs were almost doubled when the tapes were processed following the thermal sequence (II)

196

under a 10 T magnetic field. In order to obtain the highest J_c, the third factor -- grain connectivity should be improved, leading to thermal sequence (III).

In thermal sequence (III), the tapes were held at T_m - 10°C for a period of time to reduce the liquid nucleation rate and improve the grain connectivity. The J_c vs T_m curves for different holding times at cooling rate R = 1°C/min are shown in Fig. 6-3-4. Even through there is scatter, it still can be seen that J_c was enhanced by holding at T_m -10°C for one hour, and the highest $J_c = 8.3 \times 10^4 A/cm^2$ was obtained for this case. We believe that holding at just below the melting point for a short period of time will improve grain to grain connection with liquid phase present at grain boundaries. At just below the melting point the liquid nucleation rate is low, thus the undercooled liquid phase will react at the grain boundaries and improve the bonding between the grains. It will improve the connectivity of grains and J_c will be enhanced as seen in Fig. 6-3-4. When the tapes were held for a longer period of time, such as 3 hours, there are no further J_c increases due to the limited liquid phase created in thermal sequence (III).

J_c vs T_m curves for different cooling rate are shown in Fig. 6-3-5. When the cooling rate R = 0.5°C/min and 1.0°C/min at t = 1 hour, the J_cs are the same order of magnitude. However, when the cooling rate was increased to 1.5°C/min, the J_c vs T_m curve shifts downward. We have known that the liquid content and the cooling are critical to texture development under a high magnetic field; less liquid phase content and a fast cooling rate will reduce the degree of texture under a high magnetic field. For the case R = 1.5°C/min, less liquid phase was created due to the short period for the holding time above the melting point of Bi - 2212. Thus both the degree of texture and J_c decrease. This means that the cooling rate can not be increased

197

further and also the cooling rate can not be reduced to below 0.5°C/min. In this study the cooling rate was optimized around 1.0°C/min.

J_c vs T_m curves of tapes processed under a 0 and 10 T magnetic field following thermal sequence (III) with R = 1°C/min and t = 1 hour are shown in Fig. 6-3-6. For the different maximum processing temperatures, J_cs of the tapes processed under a 10 T magnetic field are higher than that of the tapes processed under a 0 T magnetic field. The highest J_c which we obtained by application of a 10 T magnetic field is around 8.3×10^4 A/cm^2, i.e. $I_c = 45$ A. The J_c dependence of magnetic field for three different maximum processing temperatures is shown in Fig. 6-3-7. It is clear that J_c increases with increasing magnetic field and saturates at a higher magnetic field. This result is consistent with thick film and bulk material results.

6.3.3: Conclusions

Bi - 2212 / Ag tapes with thickness 30 μm were melt - grown under elevated magnetic fields following three different thermal sequences. The impurity phase was reduced by reducing the holding time above the melting point of Bi - 2212 and by increasing the cooling rate. The degree of texture was increased by application of a high magnetic field. Under the optimized thermal sequence, transport critical current of Bi - 2212 tapes were enhanced by melt - growth under a 10 T magnetic field. The highest J_c is about 8.3×10^4 A/cm^2. Therefore, highly textured Bi - 2212 / Ag thicker tape can be processed by application of a high magnetic field during melt - growth, and both the critical current density J_c and the critical current I_c can be enhanced following thermal sequence (III) under a high magnetic field.

(a) Sequence (I)

t

$10^{o}C$ / hour

(b) Sequence (II)

t

$1^{o}C$ / min

$10^{o}C$ / hour

(c) Sequence (III)

R

t

10° / hour
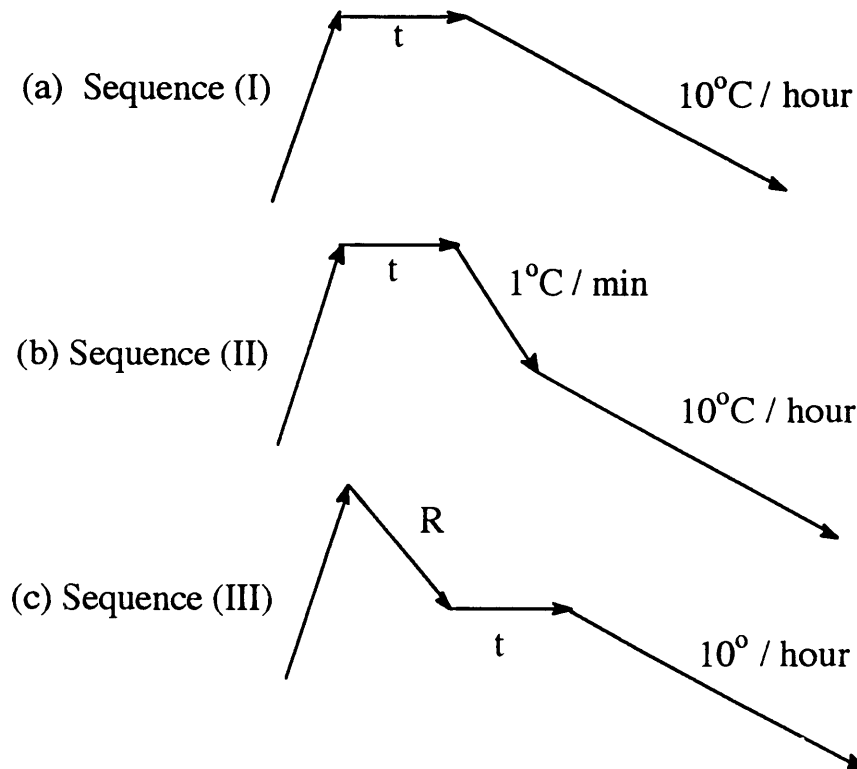
Fig. 6-3-1:   Three thermal sequences of melt - grown Bi - 2212 / Ag tapes

under an elevated magnetic field. (a) Standard thermal sequence

of melt - grown Bi - 2212 / Ag tapes. (b) Modified thermal

sequence of melt - grown Bi - 2212 / Ag tapes. (c) A new thermal

sequence of melt - grown Bi - 2212 / Ag tapes under a high

magnetic field. t is holding time, $\mathcal{R}$ is cooling rate.

199
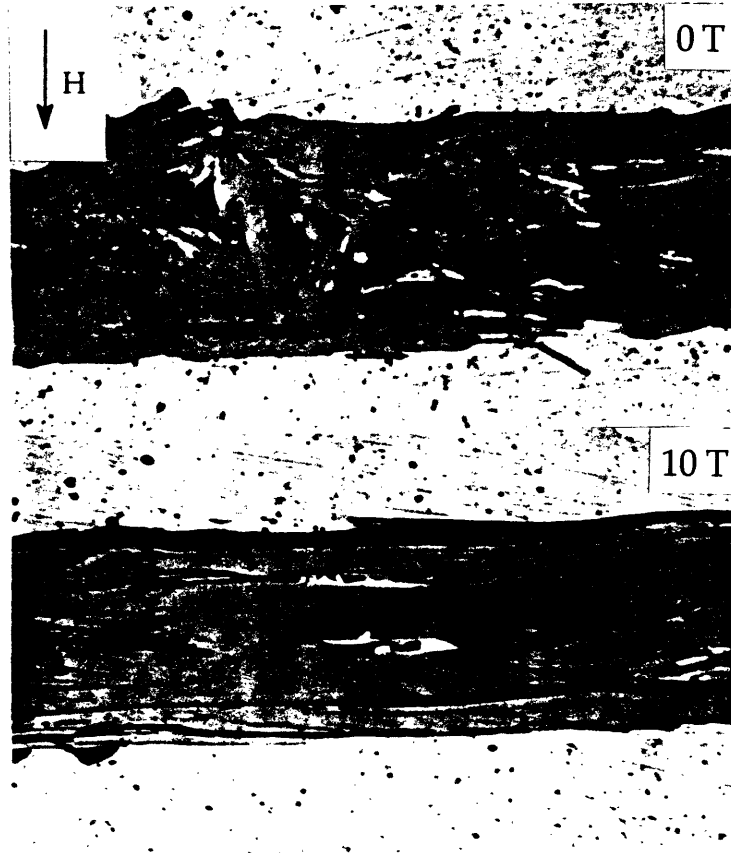
Fig. 6-3-2: SEM images of polished cross sections of the tapes which were melt - grown under a 0 T and 10 T magnetic field following the thermal sequence (III) with $T_m = 850^{\circ}C$, $t = 1$ hour and $R = 1.0^{\circ}C/min$.
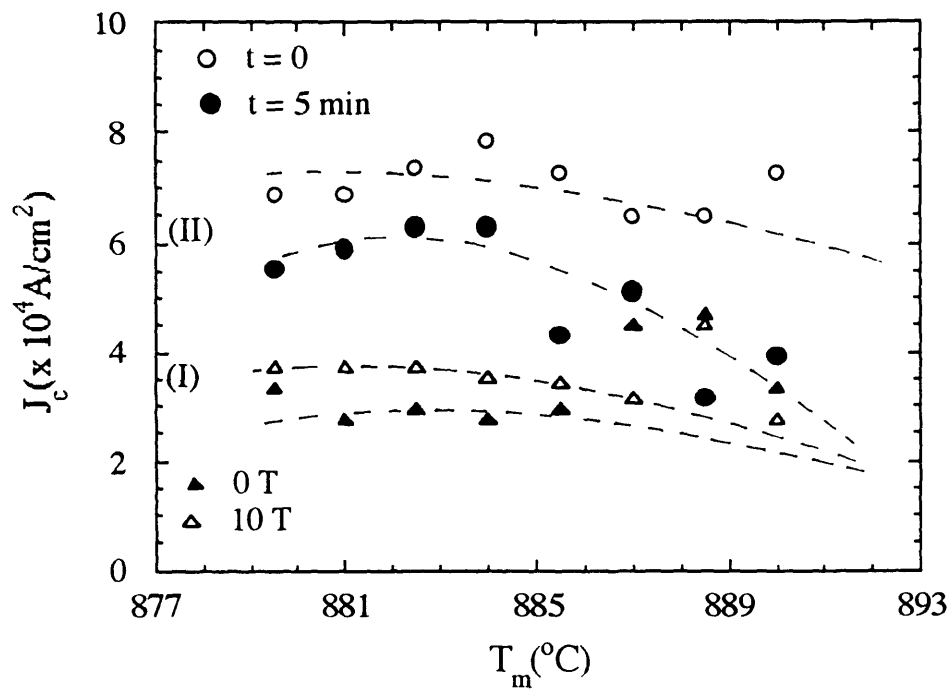
Fig. 6-3-3: J_c dependence on maximum processing temperature T_m at 4.2 K for the tapes processed following the thermal sequence (I) and (II).
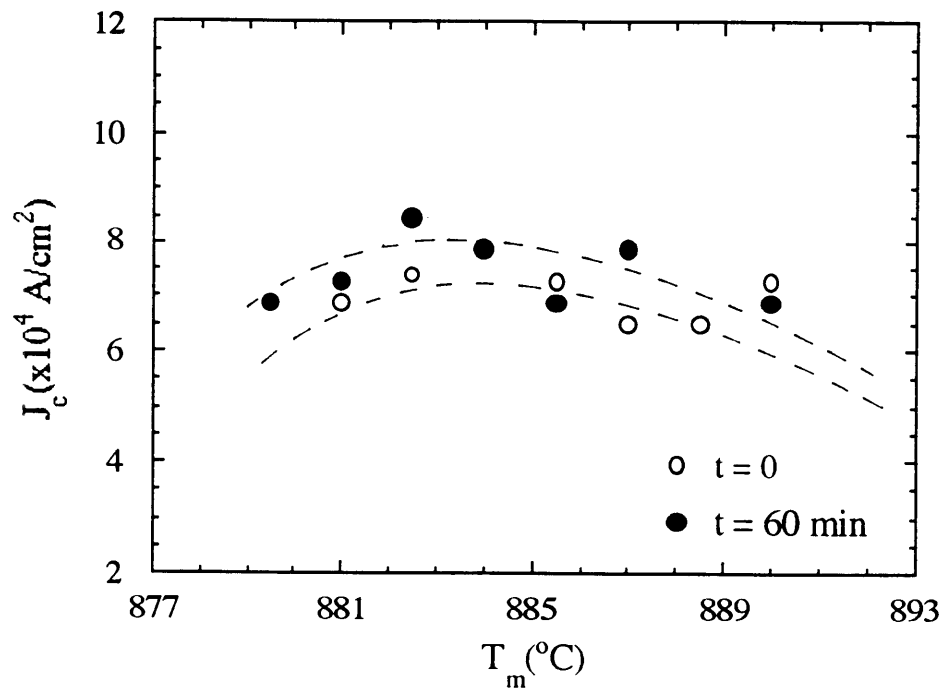
Fig. 6-3-4: J_c dependence on maximum processing temperature T_m at
4.2 K for the tapes processed following the thermal sequence
(III) under a 10 T magnetic field for t = 0 min and 60 min.
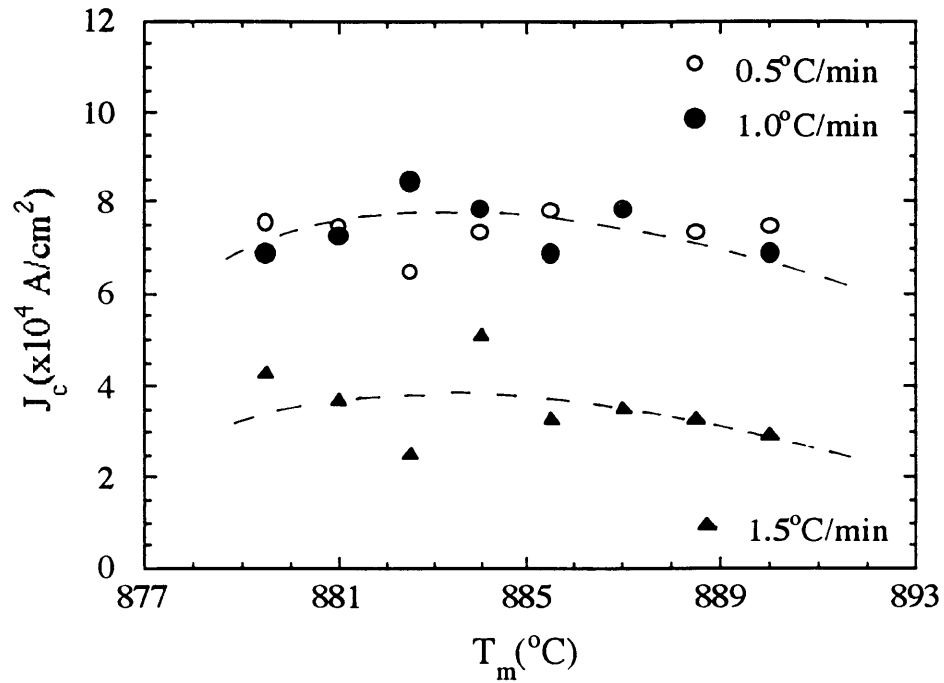
Fig. 6-3-5: J_c dependence on maximum processing temperature T_m at 4.2 K for the tapes processed following the thermal sequence (III) under a 10 T magnetic field for R = 0.5°C/min, 1.0°C/min and 1.5°C/min.
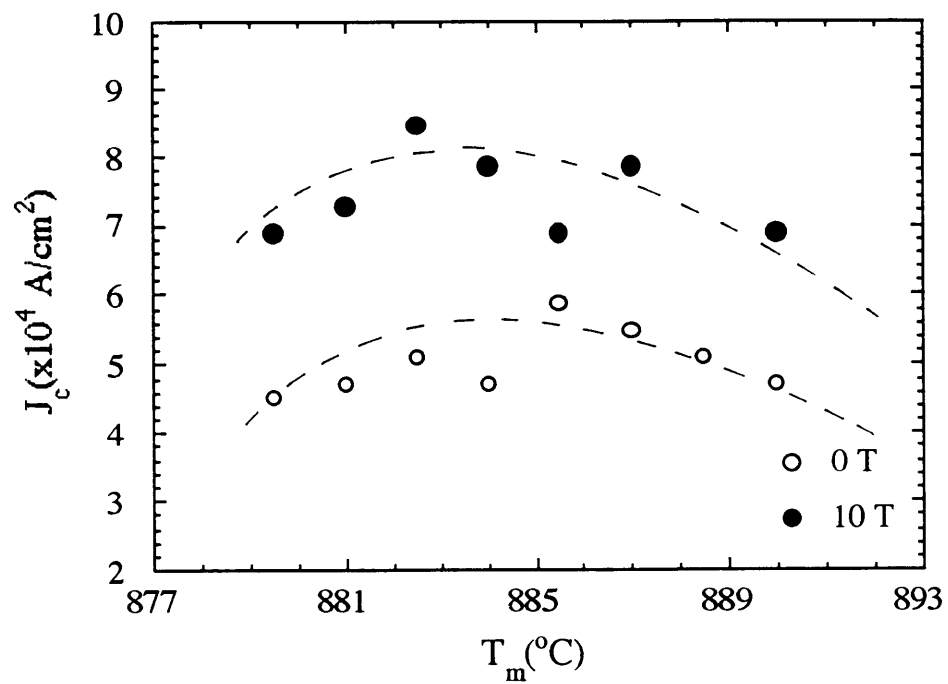
Fig. 6-3-6: J_c dependence on maximum processing temperature T_m at

4.2 K for the tapes processed following the thermal sequence

(III) for H = 0 T and 10 T for R = 1.0°C and t = 1 hour.

$J_c (\times 10^4 \ A/cm^2)$

H (T)

O 890°C
• 884°C
▲ 881°C
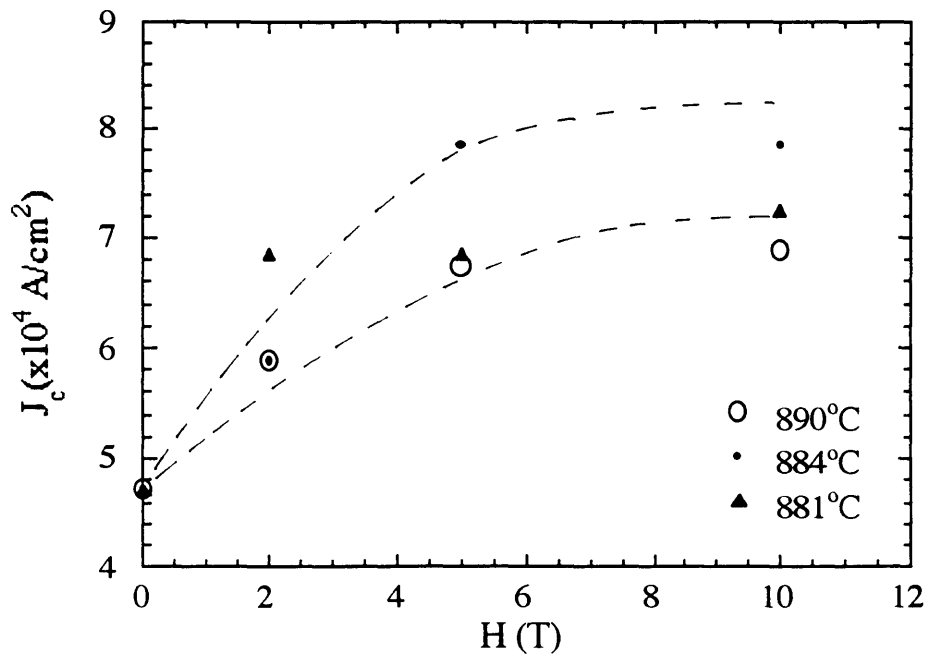
Fig. 6-3-7: Magnetic field dependence of J_c at 4.2 K for the tapes processed

following the thermal sequence (III) with R = 1.0°C/ min and

t = 1 hour for different maximum processing temperature T_m.

Chapter 7: Comparison Between Theory and Experiment.

In chapter 2, a theoretical model has been developed to describe the texture development of high - T_c superconductors under a high magnetic field. A factor describing texture, F, has been expressed as a function of $\beta(T, H, V) = \dfrac{[\Delta\chi VH^2/2 - K(T, x)]}{kT}$; $\Delta\chi$ is the anisotropic susceptibility, V is grain volume, H is magnetic field and $K(T, x)$ is the interaction energy. For the interaction energy $K(T, x) = 0$ case, the F factor depends on magnetic field, grain size and temperature. F always increases with increasing magnetic field and grain size, and F decreases with increasing temperature. For the interaction energy $K(T, x) \neq 0$ case, the F factor not only depends on magnetic field, temperature and grain size, but also depends on the interaction constant and liquid phase content, x. For constant magnetic field and grain size, F increases with decreasing interaction constant and increasing liquid phase content. When H -> ∞, F -> 1. These results from the modeling effort are compared to experiments as follows.

In a real system, such as melt - growth of the R - 123 and the Bi - 2212 case, there is always an interaction between the grains. Thus, for different materials and grain sizes, we can adjust the interaction energy constant $K(T, x)$ to fit the experimental F vs H curve. A comparsion of the theoretical and experimental curves for Y - 123, which were melt - grown under an elevated magnetic field, are plotted in Fig. 7-1. During the melting growth process for Y - 123 there is considerable liquid phase present and the interaction between the grains is small, thus we choose a small interaction constant. It is clear that the traces of the curves are qualitatively consistent with each other.

206
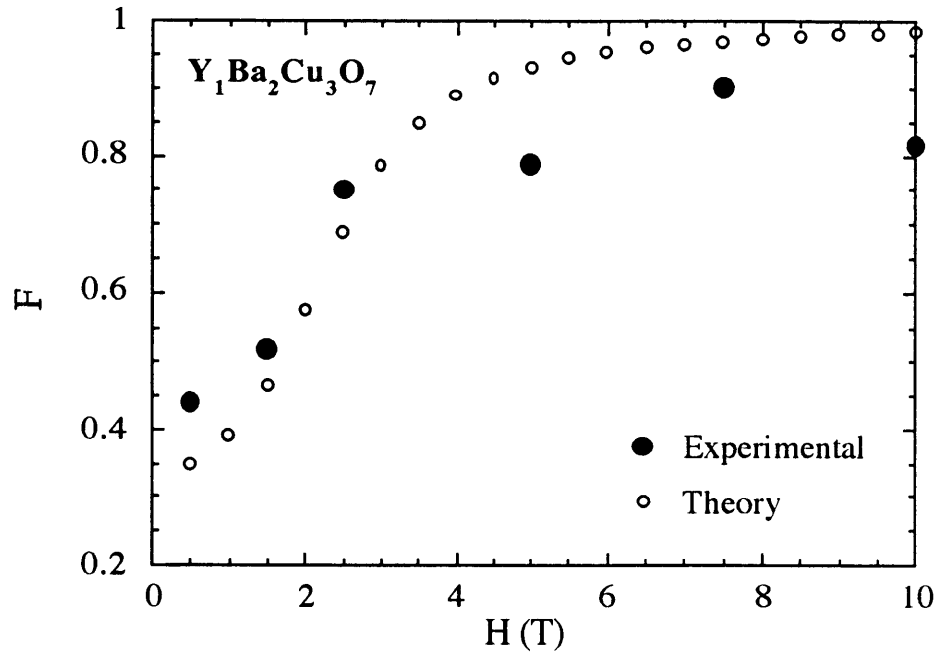
Fig. 7-1: Comparison between experimental data with theory for Y-123.

For the Bi-Ho-2212 case, the highest processing temperature is only slightly higher than the melting point, thus the interaction between the grains is high and we choose $\alpha = 50$ (Fig. 7-2). It is clear that the experimental data and theory are qualitatively consistent with each other. The experimental data could be fit more accurately by adjusting the interaction energy constant $K(T, x)$.

That the superconductor powders can be textured in organic solvent under a high magnetic field is known [16]. For this system, the interaction energy constant $K(T, x)$ should be zero; the degree of texture will increase with increasing magnetic field. Unfortunately, there are not systematic data

available to compare with the theory. However, the theory could be used to guide the experiments for such a study.
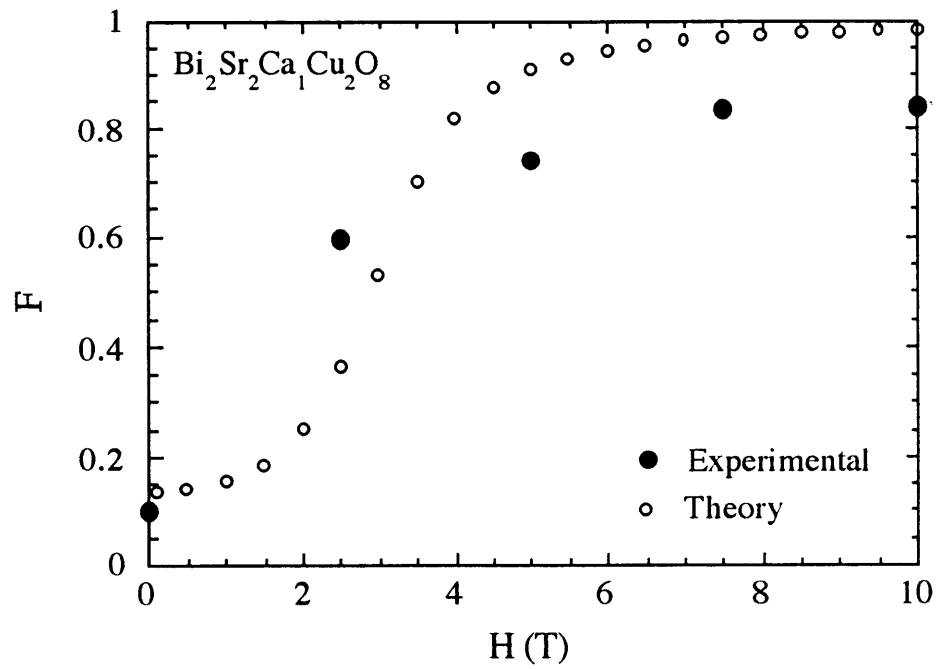
Fig. 7-2: Comparison of experimental data with theory for Bi - 2212.

Chapter 8: Suggestions for Future Work

Section 8.1: Processing long Bi-2212/Ag tapes under a high magnetic field.

J_c enhancement of Bi-2212/Ag tapes of 30 μm thickness under an elevated magnetic field has been systematically studied. It was found that the texture development in Bi - 2212 could be completed in a very short period of time by application of a high magnetic field. In other words, well textured Bi-2212 tape with higher J_c could be produced with a very fast cooling rate, i.e. 1°C/min above the melting point. Based on these results, more detailed experiments on Bi - 2212/Ag tape should be carried out.

(1) Thickness dependence of J_c in Bi-2212/Ag tapes:

Bi-2212/Ag tapes with thicknesses in the range of 10 ~ 100 μm should be processed under an elevated magnetic field based on the understanding of texture development of Bi-2212/Ag under a high magnetic field. The purpose of the experiment is to produce thicker tape with a high I_c. For applications, the overall critical current I_c is very important.

(2) Minimizing the processing time under the high magnetic field.

In these experiments, the shortest necessary processing time under a high magnetic field should be investigated. Because processing under a high magnetic field is difficult and expensive, reducing the magnetic field time will reduce the processing complexity and reduce the cost of processing. Thus, reducing the processing time will allow for mass fabrication of Bi-2212/Ag tape.

(3) Designing and building apparatus for processing long lengths of Bi-2212/Ag tape.

An apparatus for continuous processing of long lengths of Bi-2212/Ag tape under a high magnetic field should be built. In this apparatus the furnace should be placed horizontally in a vertical magnetic field, with the hot zone of the furnace located in the magnetic field and the lower temperature zone placed outside the magnetic field. The tape can be continually pulled through the hot zone under a high magnetic field, thus the tape will be melt - grown under the magnetic field with completion of phase formation in the low temperature zone in zero field. By this process a well textured long tape with higher J_c could be formed continuously.

Section 8. 2: Processing Bi-Ho -2212/Ag tape under a high magnetic field.

Bi-Ho-2212/Ag tape with composition $(Bi_2Sr_2Ca_{0.9}Ho_{0.1}Cu_2O_8)_{0.9}$ $(Bi_2Sr_2CaCu_2O_8)_{0.1}$ will be processed under an elevated magnetic field at temperatures between 880 - 910°C. We have shown that the texture development of $Bi_2Sr_2Ca_{0.9}Ho_{0.1}Cu_2O_8$ under a high magnetic field is a fast process, i.e. requiring 0.5 hour, thus the J_c of Bi-Ho-2212/Ag tape could be enhanced with short processing time under a high magnetic field. The fastest processing period and the lowest magnetic field should be investigated for Bi-Ho-2212/Ag tape.

(1) J_c enhancement of Bi-Ho-2212/Ag tape under an elevated magnetic field.

Bi-Ho-2212/Ag tape with different thicknesses between 10 ~ 100 μm will be processed under an elevated magnetic field. The J_c dependence on the

magnetic field and thickness will be studied systematically. We hope to produce high J_c and I_c tape in the shortest processing time.

(2) Mechanical deformation after grain rotation induced by application of a high magnetic field.

After a short time annealing under a high magnetic field, the density of Bi-Ho-2212/Ag tape may be not very high. Thus a mechanical deformation processes will be introduced to increase the density of the superconducting material. Following this, the tape will be annealed under zero field at lower temperature for a long time. This magnetic rotation and mechanical deformation combination will both increase the degree of texture and connectivity of the grains, thus a high J_c tape should be produced.

(3) Continuous processing of long Bi-Ho-2212/Ag tape under a high magnetic field.

Due to the relatively rapid texture development of Bi-Ho-2212 superconductor under a high magnetic field, the tape could be pulled through the hot zone under a magnetic field at a rapid rate, using the apparatus built above to produce the long Bi-Ho-2212/Ag tape under a high magnetic field. Thus a long tape could be produced very fast and this process will allow for mass fabrication. The long tape also could be rolled once again to increase the connectivity, i.e. increase the J_c.

Section 8. 3: Processing long Bi-2223 superconductor under a high magnetic field.

It is very well known that the T_c of the Bi-2223 superconductor is 108 K, thus it is a superconductor which could be used at liquid N_2 temperature.

211

After successful application of a high magnetic field during the processing for Bi-2212 and R-123, it is necessary to apply high magnetic field technology to the Bi-2223 material.

(1) Processing Bi-2223 bulk material under an elevated magnetic field.

The $Bi_{1.4}Pb_{0.4}Sr_2Ca_2Cu_3O_{10}$ material will be processed under an elevated magnetic field. It is known that during 2223 phase formation, it is necessary to sinter the 2223 material close to its melting point and create some liquid phase. The liquid phase will enhance the 2223 phase formation. We have demonstrated that grains can be rotated by a high magnetic field with a liquid phase present. Thus the existence of the liquid phase would enhance both the 2223 phase formation and texture development under a high magnetic field. It is reasonable that a high degree of texture in the Bi - 2223 phase could be introduced by application of a high magnetic field.

(2) Processing Sb-doped Bi-2223 superconductor under an elevated magnetic field.

It is known that doping Sb in Bi-2223 will create more liquid phase below the melting point of Bi-2223 and reduce the Bi-2223 phase formation time, thus Sb-doped Bi-2223 could be a potentially important candidate for magnetic field processing.

(3) Combination of hot pressing and magnetic field annealing.

If there is a liquid phase present, the grains could be easily rotated by application of a high magnetic field, and hot pressing will increase the density of the sample, i.e. increase the connectivity and J_c. When applying the magnetic field alone, the density of a sample is low due to the low amount of

liquid phase present. When hot pressing alone, the pressure should be very high and the apparatus becomes complicated. Thus it is difficult to continuously fabricate long lengths of superconductor. The combination of magnetic field annealing and hot pressing could be a potential method to fabricate long and well textured superconductor.

(4) Processing Bi-2223 or Sb-doped Bi-2223 /Ag tape under an elevated magnetic field.

After the systematic study of texture development in bulk Bi-2223 material under an elevated magnetic field described above, Bi-2223 or Sb-doped Bi-2223 /Ag tape will be processed under an elevated magnetic field. The J_c dependence on the magnetic field, thickness and other processing parameters will be studied. After processing under a high magnetic field, the tape will also be rolled to increase the grain - to - grain connectivity and to increase J_c. Finally we will use the resulting optimized processing condition and the apparatus built as described above to process long lengths of Bi-2223 tape in a continuous fashion. A hot rolling process could be combined with magnetic field processing to produce highly textured Bi-2223/Ag tape with high J_c.

Chapter 9. Conclusions

(1) The F factor has been expressed as a function of β, and a critical point and a saturation point are defined. From the critical point, we introduce critical grain size d_c, critical magnetic field H_c, critical anisotropic susceptibility $\Delta\chi_c$ and critical temperature T_c. From the saturation point, we introduce saturation grain size d_s, saturation magnetic field H_s, saturation anisotropy susceptibility $\Delta\chi_s$ and saturation temperature T_s. For the interaction energy $K(T, x) = 0$ case, the F factor depends on the magnetic field, grain size and temperature. F always increases with increasing magnetic field and grain size and F decreases with increasing temperature. For the interaction energy $K(T, x) \neq 0$ case, the F factor not only depends on magnetic field, temperature and grain size, but also depends on the interaction constant and liquid phase content x. For constant magnetic field and grain size, F increases with decreasing interaction constant and increasing liquid phase content. When $H \rightarrow \infty$, $F \rightarrow 1$. These results are consistent with the experimental results.

(2) Bi - 2212 superconductors were processed under a 10 T magnetic field at 870°C ~ 940°C. A high magnetic field can not introduce anisotropic nucleation and anisotropic growth during early stages of growth. A liquid phase is important for texture development by application of a high magnetic field. Substitution of a small amount of Ca by Ho in Bi - 2212 increases the degree of texture in Bi - 2212 by application of a 10 T magnetic field during partial melt - growth.

(3) $Bi_2Sr_2Ca_{0.9}Ho_{0.1}Cu_2O_8$ superconductor was textured by rotating the grains by elevated annealing magnetic field with exiting a liquid phase. Texture development depends on annealing temperature T_a, annealing magnetic

field H_α, processing time t and content of the liquid phase. The F factor increases with increasing annealing magnetic field and the curve saturates at 2 - 5 T for different content x. By increasing T_a, the degree of texture increases under a high annealing magnetic field for a fixed annealing time. For the same liquid phase content x, the F factor also increases with increasing annealing time, but for same annealing time the F factor depends on the liquid phase content x. The transport critical current density increases with increasing degree of texture. Processing Bi - based materials under a high annealing magnetic field provides a potential pre - texturing method for powder - in - tube technology.

(4) $Bi_2Sr_2Ca_{0.9}R_{0.1}Cu_2O_8$ with R = Y, Ho and Gd materials were melt - grown under elevated magnetic fields. Texture development depends upon the cooling rate, the maximum processing temperature T_m, and the magnetic field applied during processing. By increasing T_m, a textured structure can be introduced in a very short period of time, i.e. the processing time is reduced by a factor of 10 by increasing T_m from 950°C to 970°C under a 10 T magnetic field. There is a trade-off between the cooling rate and the magnetic field. We can introduce a highly textured structure with a faster cooling rate under a stronger magnetic field, or with a lower cooling rate under a weaker magnetic field. The transport critical current density can be increased dramatically by improving both texture and connection between the grains under a high annealing magnetic field. Processing Bi - based materials under a high magnetic field provides a potential way to increase the transport critical current density.

(5) Bulk $R_1Ba_2Cu_3O_7$ Superconductors were melt - grown under an elevated magnetic field (0 ~ 10 T). Under a 10 T annealing magnetic field, the degree of texture increases with increasing T_m. The domain alignment depends on the

cooling rate and magnetic field strength, the higher the cooling rate, the larger the magnetic field required to produce a certain degree of texture. There is a trade off between the cooling rate and the magnetic field. We can use either a higher annealing magnetic field and higher cooling rate, or use a lower magnetic field and lower cooling rate to obtain the same degree of the texture. The domain orientation under a high magnetic field is determined by the ionic moment orientation of the rare earth element in $RBa_2Cu_3O_7$ (R = Ho, Gd and Er).

(6) A 10 T magnetic field is strong enough to overcome the Bi - 2212 / Ag interface effect and dominate grain orientation with a liquid phase present. The c - axis of Bi - 2212 grains is always parallel to the magnetic field direction and do not depend on the Bi - 2212 / Ag interface orientation. A high magnetic field can be used in combination with a partial melting process to increase degree of the texture of the whole body of a Bi - 2212 superconductor in thick film or tape form.

(7) The degree of texture and transport critical current J_c of thick films with different thicknesses from 25 μm to 125 μm were enhanced by melt - growth under an elevated magnetic field. J_c increases with increasing magnetic field and the saturation magnetic field decreases with decreasing thickness of the film. Therefore, highly textured Bi - 2212 / Ag thick film or tape can be processed by application of a high magnetic field during melt - growth.

(8) Bi-2212/Ag tapes with thickness 30 μm were melt -grown under an elevated magnetic field. A new thermal processing sequence is introduced to produce high J_c tapes under a high magnetic field. The J_c reaches almost 8 x 10^4 A/cm^2 the tape processed under a 10 T magnetic field.

Reference:

[1] M. K. Wu, J. R. Ashburn, C. J. Torng, P. H. Hor, R. L. Meng, L. Gao, Z. J. Huang, Y. Q. Wang and C. W. Chu, Phys. Rev. Lett., 58 (1987) 908.

[2] H. Maeda, Y. Tanaka, M. Fukutomi and T. Asano, Jpn. J. App.Phys., 27 (1988) L 209.

[3] Z. Z. Sheng and A. M. Herman, Nature, 332 (1988) 55.

[4] D. W. Murphy, D. W. Jonson, Jr, S. Jin and R. E. Howard, Science, 241 (1988) 922.

[5] S. Jin and J. E. Graebner, Materials Science and Engineering, B7 (1991) 243.

[6] K. Heine, J. Teubriuk and M. Thouer, Appl. Phys. Lett., 55 (1989) 2441.

[7] J. Kase, K. Togano, H. Kumakura, D. R. Rietdereich, N. Irisawa, T. Morimoto and H. Maeda, Jpn. J. Appl. Phys. 29 (1990) L1096.

[8] S. Jin, T. H. Tiefel, R. C. Sherwood, R. B. van Dover, M. E. Davis, G. W. Kammlott, R. A. Fastnacht, and H. D. Keith, Phys. Rev. B 37 (1988) 7850.

[9] S. Jin, T. H. Tiefel, R. C. Sherwood, M. E. Davis, R. B. van Dover, G. W. Kammlott, R. A. Fastnacht, and H. D. Keith, Appl. Phy. Lett. 52 (1988) 2074.

[10] J. Kase, T. Morimoto, K. Togano, H. Kumakura, D. R. Dietderich and H. Maeda, IEEE Trans. Magn. 27 (1991) 1254.

[11] H. Kumakura, K. Togano, D. R. Dietderich, H. Maeda, J. Kase and T. Morimoto, Supercond. Sci. Technol. 4 (1991) S157.

[12] R. Flukiger, T. Graf. M. Decroux, C. Groth and Y. Yamada, IEEE Trans. Magn. 27 (1991) 1258.

[13] F. Mehran, T. R. McGuire and G. V. Chandrashekhar, Phys. Rev. B. 41 (1990) 11583.

[14] D. C. Johnston and J. H. Cho, Phys. Rev. B 42 (1990) 8710.

[15] J. D. Livingston, H. R. Hart, Jr. and W. P. Wolf, J. Appl. Phys. 64, (1988) 5806.

[16] D. E. Farrell, B. S. Chandrasekhar, M. R. DeGuire, M. M. Fang, V. G. Kogan, J. R. Clem, and D. K. Finnemore, Phys. Rev. B 36 (1987) 4025.

[17] C. P. Ostertag, R. D. Shull, M. D. Vaudin, J. E. Blendell, L. C. Sterns, and E. R. Fuller, Jr., in Ceramic Superconductors II, edited by M. F. Yan (The American Ceramic Society, Weaterville, OH, 1988) 332.

[18] F. Chen, R. S. Markiewicz and B. C. Giessen, Mat. Res. Soc. Symp. Pro. Vol 169 (1990) 413.

[19] A. Holloway, R. W. McCallum, and S. R. Arrasmith, J. Mater. Res., 8 (1993) 727.

[20] P. Sarkar, and P. S. Nicholson, Appl. Phys. Lett. 61 (1992) 492.

[21] P. de Rango, M. Lees, P. Lejay, A. Sulpice, R. Tournier, M. Ingold, P. Germi and M. Pernet, Nature 349 (1991) 770.

[22] F. K. Lotgering, J. Inorg. Nucl. Chem. 9 (1959) 113.

[23] C.P.Bean, Rev. Mod. Phys. 36, (1964) 31.

[24] S. Jin, T. H. Tiefel, R. C. Sherwood, M. E. Davis, R. B. van Dover, G. W. Kammlott, R. A. Fastnacht, and H. D. Keith, Appl. Phys. Lett., 52 (1988) 2074.

[25] K. Salama, V. Selvamanickam, L. Gao, and K. Sun, Appli. Phys. Lett., 54 (1989) 2352.

[26] M. Murakami, T. Oyama, H. Fujimoto, T. Taguchi, S. Gotoh, Y. Shiohara, N. Koshizuka, and S. Tanaka, Jpn. J. Appl. Phys., 29 (1990) 1991.

[27] R. B. van Dover, E. M. Gyorgy, L. F. Schneemeyer, J. W. Mitchell, K. V. Rao, R. Puzniak, and J. V. Waszczak, Nature 342 (1989) 55.

[28]T. D. Aksenova, P. V. Rratukhin, S. V. Shavkin, V. L. Melnikov, E. V. Antipova, N. E. Khlebova and A. K. Shikov, Physica C 205 (1993) 271.

[29] J. Kase, T. Morimoto, K. Togano, H. Kumakura, D. R. Dietderich and H. Maeda, IEEE Trans. Magn. 27 (1991) 1254.

[30] W. Zhang and E. E. Hellstrom, Physica C 218 (1993) 141.

[31] J. Polonka, M. Xu, Q. Li, A. I. Goldman and D. K. Finnemore, Appl. Phys. Lett. 59 (1991) 3640.

[32] J. Polonka, M. Xu, Q. Li, A. I. Goldman and D. K. Finnemore, Appl. Phys. Lett. 59 (1991) 3640.

Biographical Note

Hongbao Liu grew up in the north of China where he attended high school. He did his undergraduate and graduate studies at University of Science and Technology of China (USTC) in physics. While at USTC, he served as captain and assistant coach for the university soccer team. As a visiting scientist, he worked at National Aviation Research Institute at Wichita, Lawrence Berkeley Laboratory at Berkeley and Morris Research Inc. from 1989 to 1992. He began his graduate work in Professor J. B. Vander Sande's group at MIT in 1992 and took his general exams in the field of Electronic Materials. He is a member of MRS. He loves soccer, foot ball, tennis, skating and swimming.